

COMBUSTION CONTROL AND PERFORMANCE ANALYSIS OF CI MODIFIED HCCI ENGINE USING LEAN COMBUSTION TECHNOLOGY

Thesis

Submitted in partial fulfillment of the requirements for the Degree of

DOCTOR OF PHILOSOPHY

by

SUMANLAL M R



**DEPARTMENT OF MECHANICAL ENGINEERING
NATIONAL INSTITUTE OF TECHNOLOGY KARNATAKA,
SURATHKAL, MANGALORE – 575025**

October, 2017

DECLARATION

I hereby declare that the Research Thesis entitled “**COMBUSTION CONTROL AND PERFORMNACE ANLAYSIS OF CI MODIFIED HCCI ENGINE USING LEAN COMBUSTION TECHNOLOGY**” which is being submitted to the **National Institute of Technology Karnataka, Surathkal** in partial fulfillment of the requirements for the award of the Degree of **Doctor of Philosophy in Mechanical Engineering** is a *bonafide report of the research work carried out by me*. The material contained in this Research Thesis has not been submitted to any other Universities or Institutes for the award of any degree.

Register Number: **102018ME10P07**

Name of the Research Scholar: **SUMANLAL M R**

Signature of the Research Scholar:

Department of Mechanical Engineering

Place: NITK-Surathkal

Date:

CERTIFICATE

This is to certify that the Research Thesis entitled “**COMBUSTION CONTROL AND PERFORMANCE ANALYSIS OF CI MODIFIED HCCI ENGINE USING LEAN COMBUSTION TECHNOLOGY**” submitted by **Mr. SUMANLAL M R (Register Number: 102018ME10P07)** as the record of the research work carried out by him, *is accepted as the Research Thesis submission* in partial fulfillment of the requirements for the award of the Degree of **Doctor of Philosophy**.

Prof. P. Mohanan

Research Guide

Date:

Chairman-DRPC

Date:

ACKNOWLEDGEMENTS

Having a Doctoral degree was a kind of dream to me. But finally the dream became true. Every success needs support and the contentment that accomplishes the successful achievement of any chore would be incomplete without the expression of gratitude and appreciation to the people who made it possible.

With a deep sense of gratitude, first and foremost I wish to express my sincere thanks to my dear guide Prof. P. Mohanan, former Head, Department of Mechanical Engineering, for his excellence and support throughout the research work. Being my M.Tech. guide I know Prof. P. Mohanan since 2005 as an enthusiastic, hard working, dedicated and honest person. I cannot imagine this work without his technical input right from the beginning till day. Because of his practical approach and helping nature, it is my pleasure to work under him with gratitude. As a teacher I have observed and learned his way of handling students with respect and enthusiasm. Besides being a guide, he is also a mentor to me.

I am thankful to Dr. Narendranath S., Professor and Head, Department of Mechanical Engineering for his help and wholehearted support. I would also like to thank Dr. K.V. Gangadharan, Dr. Prasad Krishna and Dr. G.C. Mohan Kumar, Professors and former Heads, Department of Mechanical Engineering.

I am thankful to Dr. A Vittal Hegde, Professor, Department of Applied Mechanics and Dr. Kumar G.N., Assistant Professor, Department of Mechanical Engineering for being the members of the Research Progress Assessment Committee and offering their valuable comments and suggestions during this work.

I am very much thankful to Mr. Sreebhash S Kutty for timely help and valuable suggestions in the area of my work. I am also obliged to Dr. Ansal Valappil, Associate Professor, NITTE, Karkala for his valuable contributions for completing this work.

I am deeply indebted to Dr. Vighnesh V. Nayak, Assistant Professor, Moodbidri Institute of Technology, Managlore for his valuable suggestions and help for the completion of this work.

I am also grateful to Dr. Shankar K. S, Dr. Dinesh P, Dr. Manoj kumar A. P, Dr. B. S Sonage and Dr. Arun P Parameshwaran, my senior research scholars for their support in completing this work.

I am thankful to Mr. Jithin Gopinath, Mr. Nikhil V V, Mr. Aqueel Nazim, Mr. Bhaskara, Mr. Sreeram Nandakumar and Mr. Arun Augustin for their contributions in completing this work.

I wish to remember the help extended to me by Mr. Chandrashekar, I.C. Engine lab in-charge, Mr. Jayantha, Mr. Raviraj, Mr. Yathish and Mr. Vinayraj, Fuel and I. C. Engine lab instructors.

I wish to remember my colleagues and friends Mr. Dileep G, Dr. Sajeev John, Dr. Jose Cherian, Mr. Jithin Babu, Mr. Sajan S, Mr. Chinmaya Krishna, Mr. Srijith Rajeev, Mrs. Devi Parvathy, Dr. Archanana R and Mr. Renjith R for the support they provided to complete this work.

And foremost, I would like to express my deepest gratitude to my parents, guardian, wife and my kids for always being there with me.

Finally, I would like to thank all those who have helped directly or indirectly in completing this work.

Place: NITK

Date:

SUMANLAL M. R.

ABSTRACT

Amongst the numerous research papers published over the last decade, the homogenous charge compression ignition (HCCI) has often been considered as a new combustion process in reciprocating internal combustion engines. With increasingly stringent emission legislation and demand for significant reduction in CO₂ emission, research and development of cleaner and more efficient combustion engines has been intensified. HCCI combustion has emerged as an effective and viable technology that has the potential of simultaneously reducing pollutant emissions and fuel consumption from internal combustion engines.

The investigation focuses on the effect of diesel vapour induction on the engine performance and to try and achieve Homogeneous Charge Compression Ignition (HCCI) mode of combustion in the engine. An existing direct injection CI engine is modified to work as an HCCI engine by using a shell and tube heat exchanger which aids in the production of diesel vapour by utilising heat content of exhaust gases. The external mixture formation is adopted for the preparation of homogenous charge. The diesel vapour coming out of the heat exchanger is mixed with air near the intake manifold. The experimental set up is modified so that the flow of exhaust gas to the heat exchanger and the flow of diesel vapour to the engine can be controlled. A separate fuel tank is provided to measure the amount of diesel vapour utilized. Vapour utilization studies were carried out. It is found that a maximum utilization was limited to 60 percentage at different load conditions. After that knocking occurs and engine stops working. The loading of HCCI mode was limited from 50 to 100 % due to poor vapour quality at lower loads. The performance and emission characteristics of HCCI engine is studied at different injection pressures and injection timings and is compared with conventional engine. It is found that a higher injection pressure of 200 bar and advancing the injection timing to 31.5° bTDC improved the brake thermal efficiency of the engine and reduced NO_x emissions with increase in Hydrocarbon and Carbon Monoxide emissions. A maximum of 20.54 % increase in brake thermal efficiency is obtained at 75 % load condition. NO_x emissions

are reduced upto a maximum of around 50% at 31.5 deg. bTDC, 200 bar injection pressure and in vapour induction by 37% whereas CO emissions are increased around 31% and HC emissions are increased by 47%.

Normally Research engines are fitted with piezoelectric pressure transducer for the measurement of in cylinder pressure. But strong ion concentration is formed in the cylinder by the combustion process. If the ion concentration is detected, it can be used as a combustion diagnosis tool. Here a standard spark plug is converted to work as the ion sensor. It is carefully mounted over the cylinder head without affecting the passage of cooling water. An electrical circuit is designed to measure the ion voltage produced during the combustion process. Then a correlation between ion voltage and cylinder pressure is developed from the measured data so that ion voltage is calibrated in to in cylinder pressure. The results show that there is only 10% difference between the pressure given by the pressure sensor and ion sensor. Therefore the expensive pressure transducer is replaced by cheap and reliable ion sensor for combustion monitoring.

Extending the operation range in HCCI mode is a very important factor. For every load condition the amount vapour inducted to the engine is limited. Preheating of intake charge reduces the possibility of condensation of diesel vapour near intake manifold. Therefore the effect of preheating was also studied by heating the inlet air by using a heating coil. Preheating always improved the percentage vapour utilization. A percentage increase of 5.91 %, 7.93 % and 7.3 % in percentage vapour utilization is found for 50 %, 75 % and 100 % load conditions respectively. Preheating improved the brake thermal efficiency and brought down CO and HC emissions however it slightly increased NO_x emissions. The maximum efficiency is 33.5% seen at 75% load condition for preheating temperature of 65 °C and at percentage vapour utilization of 37.95 %. A maximum percentage reduction of 78.33 %, 45.15 % and 57.14 % in CO emissions was attained by preheating of air at 50, 75 and 100 % load conditions respectively. A maximum percentage decrease of 48.3 %, 50 % and 44.82 % in Unburned Hydrocarbon emissions was attained by preheating for 50, 75 and 100 % load conditions respectively. NO_x emissions are increased by almost 5% for different load conditions by preheating of the

intake air. Preheating of vapour was limited to 65 °C due to continuous increase in NO_x emissions. Thus the most suitable operating condition for HCCI mode can be identified as 75 % load coupled with 65 °C preheating.

The increase in vapor mass fraction increased the performance of the engine. This was mainly because the HCCI mode of combustion was approached. At the same time the start of combustion was still governed by the injection of vapor fuel. This gave a method of control of combustion which is normally difficult in HCCI engines.

Key words: HCCI, Combustion, Diesel Vapour Induction, Performance, Emissions, Air preheating.

CONTENTS

TITLE	Page No.
<i>ACKNOWLEDGENTS</i>	
<i>ABSTRACT</i>	
<i>CONTENTS</i>	i - iii
<i>LIST OF FIGURES</i>	iv - viii
<i>LIST OF TABLES</i>	ix
<i>NOMENCLATURE</i>	x
CHAPTER 1	INTRODUCTION
1.1	INTRODUCTION TO HCCI TECHNOLOGY
1.2	ADVANTAGES OF HCCI ENGINE
1.3	CHALLENGES IN HCCI TECHNOLOGY
1.3.1	Controlling Ignition Timing over a Range of Speeds and Loads
1.3.2	Cold Start Capability
1.3.3	Hydrocarbon and Carbon Monoxide Emissions
1.3.4	Extending the Operating Range to High Loads
1.4	INTRODUCTION TO ION SENSING
1.5	EFFECT OF AIR PREHEATING
1.6	INTRODUCTION TO EXTERNAL CHARGE FORMATION
1.7	PRESENT WORK
1.8	ORGANIZATION OF THESIS
CHAPTER 2	LITERATURE REVIEW
2.1	HCCI TECHNOLOGY
2.2	ION SENSOR TECHNOLOGY
2.3	RESEARCH GAP
2.4	OBJECTIVES OF THE RESEARCH
CHAPTER 3	ION SENSOR TECHNOLOGY
3.1	MODIFICATIONS FOR ION SENSOR
3.2	P- θ DIGRAM FOR CONVENTIONAL DIESEL ENGINE WITH ALL LOADS
3.3	ION VOLTAGE vsPRESSURE
CHAPTER 4	EXPERIMENTAL SETUP AND METHADODOLOGY
4.1	EXPERIMENTAL SETUP

4.2	MODIFICATIONS FOR HCCI MODE	50
4.3	METHODOLOGY	55
4.4	OBSERVATIONS	59
4.4.1	Sample Calculations	58
CHAPTER 5	RESULTS AND DISCUSSION	63 - 131
5.1	EFFECT OF INJECTION PRESSURE AND INJECTION TIMING ON THE PERFORMANCE AND EMISSION CHARACTERISTICS	63
5.1.1	Performance Parameters	63
5.1.1.1	Effect of vapour induction on Brake Thermal Efficiency	64
5.1.1.2	Brake Specific Fuel Consumption	73
5.1.1.3	Exhaust Gas Temperature	76
5.1.2	Emission Parameters	78
5.1.2.1	Unburned Hydrocarbons	79
5.1.2.2	Carbon Dioxide	82
5.1.2.3	Carbon Monoxide	85
5.1.2.4	Nitrogen Oxides	89
5.1.2.5	Smoke Opacity	97
5.1.3	Net Heat Release rate	100
5.1.4	Cumulative Heat Release Rate	102
5.2	EFFECT OF PREHEATING OF AIR ON THE PERFORMANCE AND EMISSION CHARACTERISTICS	105
5.2.1	Performance Parameters	105
5.2.1.1	Effect of preheating on Brake Thermal Efficiency at different load conditions	106
5.2.1.2	Effect of preheating on Brake Specific Fuel Consumption at different load conditions	108
5.2.1.3	Effect of preheating on Exhaust Gas Temperature at different load conditions	111
5.2.1.4	Effect of preheating on % Vapour Utilization at different load conditions	114
5.2.2	Emission Parameters	117
5.2.2.1	Effect of preheating on Carbon Monoxide Emissions (CO)	117
5.2.2.2	Unburned Hydrocarbons	121
5.2.2.3	Effect of preheating on NO _x emissions	123

5.2.2.4	Effect of Preheating on smoke opacity	126
5.2.3	Net Heat Release rate	128
5.2.4	Cumulative Heat Release rate	130
CHAPTER 6	CONCLUSIONS AND SCOPE FOR FUTURE WORK	133 - 136
6.1	SCOPE FOR FUTURE WORK	135
	REFERENCES	137
	Appendix I – Design Calculations of Heat Exchanger	147 - 152
	Appendix II – Correlation between Ion Voltage and Cylinder Pressure	153 - 155
	LIST OF PUBLICATIONS BASED ON RESEARCH WORK	
	BIO - DATA	

LIST OF FIGURES

Fig. No.	Title	Page No.
Fig. 1.1	Diagram of CIDI, HCCI, SIDI Engines.	2
Fig.3.1	Spark Plug.	38
Fig.3.2	Electrical circuit of the ion sensor in an HCCI Engine.	38
Fig.3.3	View of Spark Plug ion sensor fitted on the cylinder Head.	39
Fig.3.4	Pressure (Bar) vs crank angle (deg) for conventional diesel engine with all load at 180 bar Injection pressure and Injection timing 27.5 deg, bTDC.	41
Fig.3.5	Ion voltage (mV) vs Time (sec) for conventional diesel engine at 0%, 25%, 50%,75% and 100% Load and at 180 bar Injection pressure with Injection timing 27.5 deg. bTDC.	43
Fig. 3.6	Pressure (bar) vs crank angle (deg) for conventional diesel engine at 50% Load based on Ion voltage value and 180 bar Injection pressure with Injection timing 27.5 deg. bTDC.	43
Fig.3.7	Pressure (bar) vs crank angle (deg) for conventional diesel engine at 75% Load based on Ion voltage value and 180 bar Injection pressure with Injection timing 27.5 deg. bTDC.	44
Fig.3.8	Pressure (bar) vs crank angle (deg) for conventional diesel engine at 100% Load based on Ion voltage value and 180 bar Injection pressure with Injection timing 27.5 deg. bTDC.	45
Fig.3.9	Comparison between actual pressure and pressure based on Ion voltage at 50% Load	45
Fig.3.10	Comparison between actual pressure and pressure based on Ion voltage at 75% Load	46
Fig.3.11	Comparison between actual pressure and pressure based on Ion voltage at 100% Load	46
Fig.4.1	Experimental Setup for Vapour Induction	50
Fig.4.2	Fuel tank and flow measurement for diesel vapour production	51
Fig.4.3	Shell and Tube Heat Exchanger – front and sectional side view	52
Fig.4.4	Shell and Tube Heat Exchanger Inner and Outer Assembly	53
Fig.4.5	Heat Exchanger Connections	53
Fig.4.6	Three way valve for vapour quality checking and connection to inlet manifold	54
Fig.4.7	Schematic Diagram of the Experimental Setup.	55
Fig.5.1	Effect of diesel vapour induction on BTE for various injection timings at 50% load and 180 bar injection pressure.	64
Fig.5.2	Effect of diesel vapour induction on BTE for various injection timings at 75% load and 180 bar injection pressure.	65
Fig.5.3	Effect of diesel vapour induction on BTE for various injection timings at 100% load and 180 bar injection pressure	65

Fig.5.4	Effect of diesel vapour induction on BTE for various injection timings at 50% load and 200 bar injection pressure	66
Fig.5.5	Effect of diesel vapour induction on BTE for various injection timings at 75% load and 200 bar injection pressure	66
Fig.5.6	Effect of diesel vapour induction on BTE for various injection timings at 100% load and 200 bar injection pressure	67
Fig.5.7	Effect of diesel vapour induction on BTE for various injection timings at 50% load and 220 bar injection pressure	67
Fig.5.8	Effect of diesel vapour induction on BTE for various injection timings at 75% load and 220 bar injection pressure	68
Fig.5.9	Effect of diesel vapour induction on BTE for various injection timings at 100% load and 220 bar injection pressure	68
Fig.5.10	Effect of vapour induction on BTE at different injection timings and 180 bar injection pressure	72
Fig.5.11	Effect of vapour induction on BTE at different injection timings and 200 bar injection pressure	72
Fig.5.12	Effect of vapour induction on BTE at different injection timings and 220 bar injection pressure	73
Fig. 5.13	Effect of vapour induction on BSFC at different injection timings and 180 bar injection pressure	74
Fig. 5.14	Effect of vapour induction on BSFC at different injection timings and 200 bar injection pressure	74
Fig. 5.15	Effect of vapour induction on BSFC at different injection timings and 220 bar injection pressure	75
Fig. 5.16	BSFC with direct diesel injection at old rated condition (27.5 deg. bTDC and 180 bar) and vapour induction at new rated condition(31.5 deg. bTDC and 200 bar)	76
Fig. 5.17	Effect of vapour induction on exhaust gas temperature at different load conditions at 31.5 deg. bTDC and 200 bar injection pressure	77
Fig. 5.18	Effect of vapour induction on exhaust gas temperature at different loads at 27.5 deg. bTDC and 180 bar injection pressure	77
Fig.5.19	Exhaust Gas Temperatures with new (HCCI mode at 31.5 deg. bTDC and 200 bar) and old (Conventional diesel injection at 27.5 deg. bTDC and 180 bar) rating conditions.	78
Fig. 5.20	UBHC emissions for conventional and vapour induction mode at different injection timings at 180 bar	80
Fig.5.21	UBHC emissions for conventional and vapour induction mode at different injection timings at 200 bar	80
Fig.5.22	UBHC emissions for conventional and vapour induction mode at different injection timings at 220 bar	81
Fig.5.23	UBHC emissions at optimized vapour induction mode and conventional diesel injection mode at different loads	82
Fig.5.24	CO ₂ emissions for conventional and vapour induction mode at different injection timings at 180 bar	83

Fig.5.25	CO ₂ emissions for conventional and vapour induction mode at different injection timings at 200 bar	83
Fig.5.26	CO ₂ emissions for conventional and vapour induction mode at different injection timings at 220 bar	84
Fig.5.27	CO ₂ emissions at optimized vapour induction mode and conventional diesel injection mode at different loads	84
Fig.5.28	Effect of vapour induction on CO Emissions at 27.5 deg. bTDC and 200 bar injection pressure	85
Fig.5.29	Effect of vapour induction on CO Emissions at 29.5 deg. bTDC and 200 bar injection pressure	86
Fig.5.30	Effect of vapour induction on CO Emissions at 31.5 deg. bTDC and 200 bar injection pressure	86
Fig.5.31	CO emissions for conventional and vapour induction mode at different injection timings at 180 bar	87
Fig.5.32	CO emissions for conventional and vapour induction mode at different injection timings at 200 bar	87
Fig.5.33	CO emissions for conventional and vapour induction mode at different injection timings at 220 bar	88
Fig.5.34	CO emissions at optimized vapour induction mode and conventional diesel injection mode at different loads	88
Fig.5.35	NO _x variation with vapour induction at 27.5 deg. bTDC and 180 bar injection pressure.	91
Fig.5.36	NO _x variation with vapour induction at 29.5 deg. bTDC and 180 bar injection pressure.	92
Fig.5.37	NO _x variation with vapour induction at 31.5 deg. bTDC and 180 bar injection pressure.	92
Fig.5.38	NO _x variation with vapour induction at 27.5 deg. bTDC and 200 bar injection pressure.	93
Fig.5.39	NO _x variation with vapour induction at 29.5 deg. bTDC and 200 bar injection pressure.	93
Fig.5.40	NO _x variation with vapour induction at 31.5 deg. bTDC and 200 bar injection pressure.	94
Fig.5.41	NO _x variation with vapour induction at 27.5 deg. bTDC and 220 bar injection pressure	94
Fig.5.42	NO _x variation with vapour induction at 29.5 deg. bTDC and 220 bar injection pressure	95
Fig.5.43	NO _x variation with vapour induction at 31.5 deg. bTDC and 220 bar injection pressure	95
Fig.5.44	NO _x emissions for conventional and vapour induction mode at different injection timings at 180 bar	96
Fig.5.45	NO _x emissions for conventional and vapour induction mode at different injection timings at 200 bar	96
Fig.5.46	NO _x emissions for conventional and vapour induction mode at different injection timings at 200 bar	97
Fig.5.47	NO _x emissions at optimized vapour induction mode and conventional diesel injection mode at different loads	97

Fig.5.48	Smoke Opacity for conventional and vapour induction mode at different injection timings at 180 bar	98
Fig.5.49	Smoke Opacity for conventional and vapour induction mode at different injection timings at 200 bar	99
Fig.5.50	Smoke Opacity for conventional and vapour induction mode at different injection timings at 220 bar	99
Fig.5.51	NO _x emissions at optimized vapour induction mode and conventional diesel injection mode at different loads	100
Fig.5.52	Effect of vapour induction on NHRR at 50% load condition	101
Fig.5.53	Effect of vapour induction on NHRR at 75% load condition	101
Fig.5.54	Effect of vapour induction on NHRR at 100% load condition	102
Fig.5.55	Effect of vapour induction on CHRR at 50% load condition	103
Fig.5.56	Effect of vapour induction on CHRR at 75% load condition	103
Fig.5.57	Effect of vapour induction on CHRR at 100% load condition	104
Fig.5.58	Brake thermal Efficiency vs Preheating temperature for different % vapor induction at 50 % load	106
Fig.5.59	Brake thermal Efficiency vs Preheating temperature for different % vapor induction at 75 % load	108
Fig.5.60	Brake thermal Efficiency vs Preheating temperature for different % vapor induction at 100 % load	108
Fig.5.61	Brake Specific Fuel Consumption vs Preheating temperature for different % vapor induction at 50 % load	110
Fig.5.62	Brake Specific Fuel Consumption vs Preheating temperature for different % vapor induction at 75 % load	110
Fig.5.63	Brake Specific Fuel Consumption vs Preheating temperature for different vapour induction at 100 % load	111
Fig.5.64	Exhaust Gas Temperature vs Preheating temperature for different vapour induction at 50 % load	112
Fig.5.65	Exhaust Gas Temperature vs Preheating temperature for different vapour induction at 75 % load	113
Fig.5.66	Exhaust Gas Temperature vs Preheating temperature for different vapour induction at 100 % load	113
Fig.5.67	Percentage vapour Utilization vs Preheating Temperature for different % vapour induction at 50 % load	114
Fig.5.68	Percentage vapour Utilization vs Preheating Temperature for different % vapour induction at 75% load	115
Fig.5.69	Percentage vapour Utilization vs Preheating Temperature for different % vapour induction at 100 % load	116
Fig.5.70	Carbon monoxide v/s Preheating Temperature for different % vapor induction at 50 % load	118
Fig.5.71	Carbon monoxide vs Preheating Temperature for different vapor induction at 75 % load	119

Fig.5.72	Carbon monoxide vs Preheating Temperature for different % vapor induction at 100 % load	120
Fig.5.73	Unburned Hydrocarbons vs Preheating Temperature for different vapor induction for 50 % load	121
Fig. 5.74	Unburned Hydrocarbons vs Preheating Temperature for different %vapor induction for 75 % load	122
Fig. 5.75	Unburned Hydrocarbons vs Preheating Temperature for different %vapor induction for 100 % load	123
Fig. 5.76	NO _x vs Preheating temperature for 50 % load at different % vapor induction	124
Fig. 5.77	NO _x vs Pre-heating temperature for 75 % load at different %vapor induction	125
Fig. 5.78	NO _x vs Preheating temperature for 100 % load at different %vapor induction	125
Fig. 5.79	Smoke opacity vs preheating temperature for 50 % load for different %vapor induction	126
Fig. 5.80	Smoke opacity vs preheating temperature for 75 % load for different vapor induction	127
Fig. 5.81	Smoke opacity vs preheating temperature for 100 % load for different % vapor induction	127
Fig. 5.82	Net Heat Release rate at 50% load and different preheating temperatures	128
Fig. 5.83	Net Heat Release rate at 75% load and different preheating temperatures.	129
Fig. 5.84	Net Heat Release rate at 100% load and different preheating temperatures	129
Fig. 5.85	Cumulative Heat Release Rate at 50% load and different preheating temperatures	130
Fig. 5.86	Cumulative Heat Release Rate at 75% load and different preheating temperatures.	131
Fig. 5.87	Cumulative Heat Release Rate at 100% load and different preheating temperatures	131

LIST OF TABLES

Table No.	Title	Page No.
Table.3.1	Performance Characteristics of Diesel Engine after modification	40
Table 4.1	Specifications of the Diesel engine test rig	49
Table 4.2	Specification of Heat Exchanger	52
Table 4.3	Scheme of Experiments of the Research Work	56
Table 4.4	50% load readings at 31.5 deg. bTDC and 200 bar injection pressure	57
Table 4.5	75% load readings at 31.5 deg. bTDC and 200 bar injection pressure	58
Table 4.6	100% load readings at 31.5 deg. bTDC and 200 bar injection pressure	58
Table 4.7	Emissions at 50% load -31.5 deg. bTDC and 200 bar injection pressure	58
Table 4.8	Emissions at 75% load - 31.5 deg. bTDC and 200 bar injection pressure	59
Table 4.9	Emissions at 100 % load - 31.5 deg. bTDC and 200 bar injection pressure	59
Table 5.1	Maximum brake thermal efficiency obtained by vapour induction at different operating conditions.	69
Table 5.2	Maximum increase in BTE at different loads in vapour induction mode at 200 bar injection pressure and injection timing of 31.5 ⁰ btDC	71
Table 5.3	Maximum efficiency at different loads	109
Table 5.4	Maximum percentage vapour possible for different loads	117
Table 5.5	Maximum reduction in CO for 50 % load	118
Table 5.6	Maximum reduction in CO for 75 % load	119
Table 5.7	Maximum reduction in CO for 100 % load	120
Table 5.8	Operating conditions for minimum UBHC for each loads	123
Table 5.9	Preheating employed for minimum NO _x condition	124

NOMENCLATURE

BSFC	Brake specific fuel consumption (kg/kW-hr)
bTDC	Before Top Dead Centre
BTE	Brake thermal efficiency (%)
CA	Crank angle (deg.)
CHRR	Cumulative Heat Release rate (kJ/deg.)
CI	Compression Ignition
DI	Direct Injection
ECU	Electronic control unit
EGR	Exhaust gas recirculation
EMF	Electromotive force (V)
HCCI	Homogenous Charge Compression Ignition
I.C	Internal combustion
NHRR	Net Heat Release rate (J/deg.)
NO _x	Oxides of Nitrogen
PHT	Preheating Temperature (°C)
ppm	Parts per million
PVI	Percentage Vapour Induction (%)
RPM	Revolutions per minute

CHAPTER 1

INTRODUCTION

Internal combustion engines have been developed extensively over the last decades. The main objectives of all these research is to meet the increasing demand of output power and fuel mileage while decreasing the poisonous emissions which are serious threat to life in nature. On the other hand authorities are doing their best to commercialize alternate fuels, to eventually replace gasoline and diesel which will be limited in supply in the future. Therefore the future demands a combustion technology which can adopt gasoline, diesel or any alternate fuel with increased efficiency and reduced emissions (Gajendra et al. 2014). Homogenous Charge Compression Ignition (HCCI) is a new combustion technology which has the potential of becoming the engine technology for next generation passenger vehicles (Onishi et al. 1979).

1.1 INTRODUCTION TO HCCI TECHNOLOGY

HCCI is a combustion process rather than an engine type and it combines the advantages of SI and CI engines. The HCCI engines breaths premixed charge which is formed either by external mixture formation or very early direct injection so that fuel and air has got time to mix. During the compression pressure and temperature is increased so that auto ignition occurs. The charge is ignited at several locations simultaneously in the combustion chamber where the temperature is highest or mixture is richest so that chemical reaction occurs.

HCCI engine has higher efficiency when compared to SI engines and better emission than CI engines. It can provide efficiencies as high as compression-ignition, direct-injection (CIDI) engines (an advanced version of the commonly known diesel engine) while, unlike CIDI engines, producing ultra- low oxides of nitrogen (NO_x) and particulate matter (PM) emissions (Haruyuki et. al.1997). HCCI engines operate on the principle of having a dilute, premixed charge that reacts and burns volumetrically throughout the cylinder as it is compressed by the piston. In some regards, HCCI incorporates the best features of both spark ignition (SI) and compression ignition (CI), as shown in Fig. 1.1.

As in an SI engine, the charge is well mixed, which minimizes particulate emissions, and as in a CIDI engine, the charge is compression ignited and has no throttling losses, which leads to high efficiency (Khandala et al. 2017). However, unlike either of these conventional engines, the combustion occurs simultaneously throughout the volume rather than in a flame front. This important attribute of HCCI allows combustion to occur at much lower temperatures, dramatically reducing engine-out emissions of NO_x (Morteza et al. 2010). Most engines employing HCCI to date have dual mode combustion systems in which traditional SI or CI combustion is used for operating conditions where HCCI operation is more difficult (Mingfa et al. 2009 and Morteza et al. 2017). Typically, the engine is cold-started as an SI or CIDI engine, then switched to HCCI mode for idle and low to mid-load operation to obtain the benefits of HCCI in this regime, which comprises a large portion of typical automotive driving cycles (Annarita and Vinicio 2012). For high-load operation, the engine would again be switched to SI or CIDI operation (Mathivanan et al. 2016).

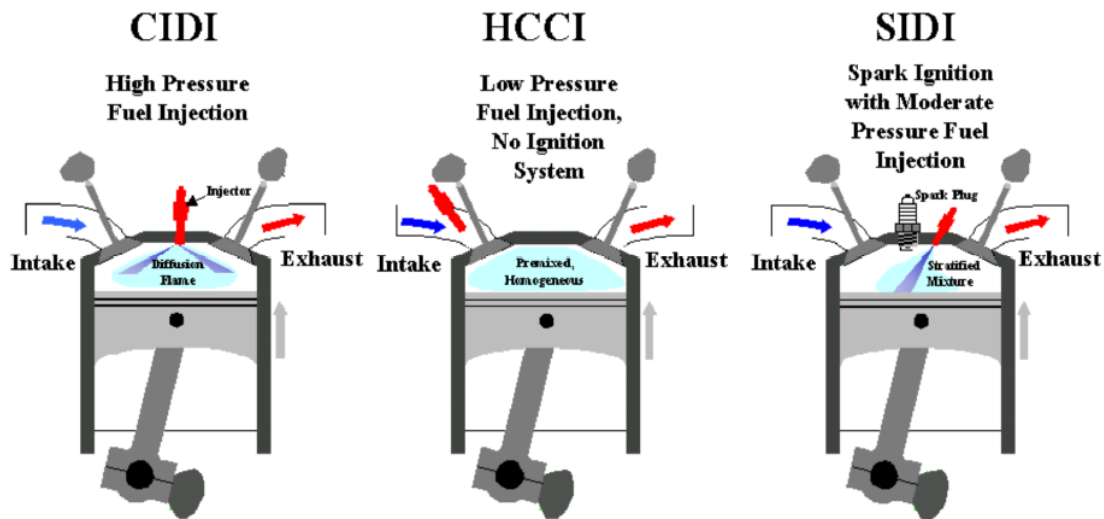


Fig 1.1 Diagrams of CIDI, HCCI, SIDI Engines.

1.2 ADVANTAGES OF HCCI ENGINE

The advantages of HCCI are numerous and depend on the combustion system to which it is compared. Relative to SI gasoline engines, HCCI engines are more efficient, approaching the efficiency of a CIDI engine (Mathivanan et al. 2017). This improved efficiency results from three sources: the elimination of throttling losses, the use of high compression ratios (similar to a CIDI engine), and a shorter combustion duration (since it is not necessary for a flame to propagate across the cylinder). HCCI engines also have lower engine-out NO_x than SI engines (Wang et al. 2009). Although three-way catalysts are adequate for removing NO_x from current-technology SI engine exhaust, low NO_x is an important advantage relative to spark-ignition, direct-injection (SIDI) technology, which is being considered for future SI engines. Relative to CIDI engines, HCCI engines have substantially lower emissions of PM and NO_x (Mustafa 2007). Emissions of PM and NO_x are the major impediments to CIDI engines meeting future emissions standards and are the focus of extensive current research (Mustafa 2012).

The low emissions of PM and NO_x in HCCI engines are a result of the dilute homogeneous air and fuel mixture in addition to low combustion temperatures. The charge in an HCCI engine may be made dilute by being very lean, by stratification, by using exhaust gas recirculation (EGR), or some combination of these (Hatim et al. 2008 and Ivan et al. 2012). Because flame propagation is not required, dilution levels can be much higher than the levels tolerated by either SI or CIDI engines. Combustion is induced throughout the charge volume by compression heating due to the piston motion, and it will occur in almost any fuel/air/exhaust-gas mixture once the 800 to 1100 K ignition temperature (depending on the type of fuel) is reached (Megaritis et al. 2006 and Miguel et al. 2011). In contrast, in typical CI engines, minimum flame temperatures are 1900 to 2100 K, high enough to make unacceptable levels of NO_x . Additionally, the combustion duration in HCCI engines is much shorter than in CIDI engines since it is not limited by the rate of fuel/air mixing (Stuart et al. 2007). This shorter combustion duration gives the HCCI engine an efficiency advantage (Zhu et al. 2006 and Qiang et al.

2012). Finally, HCCI engines may be lower cost than CIDI engines since they would likely use lower-pressure fuel-injection equipment (Myung and Chang 2007).

Another advantage of HCCI combustion is its fuel-flexibility (Xingcai et al. 2006), Abdul et al. 2011 and Bang et.al. 2015). HCCI operation has been shown using a wide range of fuels (Magnus and Bengt 2011). Gasoline is particularly well suited for HCCI operation. Highly efficient CIDI engines, on the other hand, cannot run on gasoline due to its low cetane number (Junjun et al. 2008 and Wang et al. 2015). With successful R&D, HCCI engines might be commercialized in light-duty passenger vehicles by 2010, and by 2015 as much as a half-million barrels of oil per day may be saved (Sjoberg and John 2006).

Tests have also shown that under optimized conditions HCCI combustion can be very repeatable, resulting in smooth engine operation (Haifeng et al. 2010). The emission control systems for HCCI engines have the potential to be less costly and less dependent on scarce precious metals than either SI or CIDI engines (Suyin et al. 2011). HCCI is potentially applicable to both automobile and heavy truck engines (Xingcai et al. 2011). In fact, it could be scaled to virtually every size- class of transportation engines from small motorcycle to large ship engines. HCCI is also applicable to piston engines used outside the transportation sector such as those used for electrical power generation and pipeline pumping (Wang et al. 2010).

1.3 CHALLENGES IN HCCI TECHNOLOGY

HCCI combustion is achieved by controlling the temperature, pressure and composition of the air/fuel mixture so that it auto ignites near top dead center (TDC) as it is compressed by the piston. This mode of ignition is fundamentally more challenging than using a direct control mechanism such as a spark plug or fuel injector to dictate ignition timing as in SI and CIDI engines, respectively (Miguel et.al. 2009 and Mahrous et al. 2009). While HCCI has been known for some twenty years, it is only with the recent advent of electronic engine controls that HCCI combustion can be considered for application to commercial engines (Hyung et al. 2011 and Ming et al. 2011). Even so, several technical barriers must be overcome before HCCI engines will be viable for high-

volume production and application to a wide range of vehicles. The following describes the more significant challenges for developing practical HCCI engines for transportation.

1.3.1 Controlling Ignition Timing over a Range of Speeds and Loads

Changing the power output of an HCCI engine requires a change in the fueling rate and, hence, the charge mixture. As a result, the temperature history must be adjusted to maintain proper combustion timing (Toshio et al. 2009). Similarly, changing the engine speed changes the amount of time for the autoignition chemistry to occur relative to the piston motion (Xing-Cai et al. 2005). Again, the temperature history of the mixture must be adjusted to compensate. These control issues become particularly challenging during rapid transients (Starck et al. 2010 and Rakesh and Avinash 2011).

1.3.2 Cold-Start Capability

At cold start, the compressed-gas temperature in an HCCI engine will be reduced because the charge receives no preheating from the intake manifold and the compressed charge is rapidly cooled by heat transferred to the cold combustion chamber walls (Zhaolei and Mingfa 2009). Without some compensating mechanism, the low compressed-charge temperatures could prevent an HCCI engine from firing (Shuaiqing et al. 2011).

1.3.3 Hydrocarbon and Carbon Monoxide Emissions

HCCI engines have inherently low emissions of NO_x and PM, but relatively high emissions of hydrocarbons (HC) and carbon monoxide (CO). Some potential exists to mitigate these emissions at light load by using direct in-cylinder fuel injection to achieve appropriate partial-charge stratification. However, in most cases, controlling HC and CO emissions from HCCI engines will require exhaust emission control devices (Amit et al. 2007 and Wen and Maozhao 2008). However, HC and CO emission control devices are simpler, more durable, and less dependent on scarce, expensive precious metals than are NO_x and PM emission control devices (Cinar et al. 2009 and Yaopeng et al. 2013).

1.3.4 Extending the Operating Range to High Loads

Although HCCI engines have been demonstrated to operate well at low-to-medium loads, difficulties have been encountered at high-loads (Javad et al. 2015). Combustion

can become very rapid and intense, causing unacceptable noise, potential engine damage, and eventually unacceptable levels of NO_x emissions (Komninos 2009 and Cinar et al. 2015). Preliminary research indicates the operating range can be extended significantly by partially stratifying the charge (temperature and mixture stratification) at high loads to stretch out the heat-release event (Lijima et al. 2007). Several potential mechanisms exist for achieving partial charge stratification, including varying in-cylinder fuel injection, injecting water, varying the intake and in-cylinder mixing processes to obtain non-uniform fuel/air/residual mixtures, and altering cylinder flows to vary heat transfer (Suet al.2004 and Jacek 2014). Because of the difficulty of high-load operation, most initial concepts involve switching to traditional SI or CI combustion for operating conditions where HCCI operation is more difficult (Qian et al. 2006 and Tao et al. 2014). This dual mode operation provides the benefits of HCCI over a significant portion of the driving cycle but adds to the complexity by switching the engine between operating modes (Anthony et al. 2007 and Kyeonghyeon et al. 2015).

1.4 INTRODUCTION TO ION SENSING

The fact that ions are produced in flames has been known for many years (Petter et al. 2003). The basic principle of ion current sensing is that a voltage applied over an electrode gap placed into the combustion chamber. In a non reacting charge, no ion current through the gap will be present where as in a reacting charge a small electric current will be present(Saxena et al. 2009). Thus the ion current produced reflects the ambience in the combustion chamber.

HCCI is a lean and low temperature combustion event, which leads to small quantities of ions being produced during the combustion event (Gregory et al. 2009). Ion sensors using standard spark plugs are inexpensive sensors which are ideal for production engines. Currently combustion event in HCCI engines is measured using expensive pressure transducers which are impractical for production engines and thus making ion sensors a more likely candidate; however, the ion signal measured using ion sensors (spark plugs) is localized where the pressure signal is a global measurement (Mehresha

et al. 2005). Although the ion sensors are local measurement of the combustion event, the potential for control of combustion phasing is still valid (Anders et al. 2004).

1.5 EFFECT OF AIR PREHEATING

HCCI mode is achieved by the combustion of the fuel by the compression process inside the engine cylinder. For this the intake charge should be at high temperature (Rakesh and Avinash 2010 and Zhang et al. 2011). Many methods can be employed for external mixture formation, but the temperature of incoming air always imparts a limitation for HCCI combustion. Therefore the air can be preheated to improve the operational range of HCCI Engines (Hui et al. 2014). This also reduces the possibility of condensation of fuel in the intake line. The preheating of air improves the brake thermal efficiency and % vapor induction, decreases CO and HC emission but increases NO_x emissions (Rakesh and Avinash 2016 and Chunhua et.al. 2016).

1.6 INTRODUCTION TO EXTERNAL CHARGE FORMATION

One of the main challenge is HCCI is the formation of homogenous mixture. The volatility of the diesel fuel is very less so that vaporization by injection is little difficult (Ganesh et al. 2008 and Ganesh and Nagarajan 2010). The flue gases coming out engine has high energy content which is normally wasted and in turn causes thermal pollution. Therefore some methods can be adopted for the recovery of heat from exhaust gases and this can be used for the vaporization of diesel. A shell and tube heat exchanger is suitable for the above purpose and this imparts much flexibility to the HCCI mode of combustion (Pandiyarajan et al. 2011 and Pravin and Rehman 2016).

1.7 PRESENT WORK

The present study deals with experimental investigations on the combustion, performance and emission characteristics of single cylinder DI diesel engine converted to HCCI mode of operation. For experimentation, 5.2 kW capacity Kirloskar engine has been made in to test rig with all necessary instrumentation for measuring combustion, performance and emission parameters. Engine test rig is modified to work in HCCI mode of operation (Wang et al. 2009). This is achieved by formation of homogenous mixture externally and for this purpose a shell and tube heat exchanger is designed and installed in the exhaust

line. This heat exchanger is used for vaporizing diesel by exchanging heat with exhaust of the engine. The incoming air and diesel vapour produced is mixed near the intake manifold and this mixture is sucked by the engine during suction stroke. This study proposes a method for monitoring the combustion characteristics by using a spark plug converted ion sensor. This sensor is used further monitoring of engine performance. The engine is coupled with an eddy current dynamometer for measuring the load on the engine. Sequence of experiments are carried out with engine operating parameters of load , injection pressures, injection timings and various percentage of vapour inducted(Pranab et al. 2015). Experimental results are compared with conventional diesel engine to get an optimum condition for HCCI mode.. Experiments are further carried out with preheating of incoming air to increase the % vapour utilization in HCCI mode. Finally this work proposes the optimum operating conditions for a DI converted HCCI engine which uses a comparably in expensive method (ion sensing) for engine diagnosis.

1.8 ORGANIZATION OF THESIS

The thesis has been organized in to 6 chapters starting with the introduction. This chapter gives the background of the problem definition and basic details. The second chapter deals with the in depth literature review covering mainly the various aspects related to HCCI combustion, ion sensing, effect of preheating the charge and waste heat recovery. Pervious experimental and analytical studies using different types of fuels in HCCI technology is detailed in this chapter. Based on the literature review, the objectives of the present work are also described in this chapter. The third chapter presents the experimental work, covering modification for ion sensor, instrumentation and measurements. The development of a co-relation between ion voltage and in cyinder pressure is explained in this chapter. This also contains the comparison between in cylinder pressure measured by the piezosensor and obtained through the co-relation. The experimental setup with modifications, done for HCCI mode and experimental methodology are described in chapter four. The details performance parameter calculations are also given in this chapter. In Fifth chapter the results obtained from the experiment are discussed in detail. The results of engine operation with different

injection pressures and different injection timings are detailed in the beginning and optimum values are selected for further experimentation. In the next part effect of air preheating on performance and combustion characteristics are detailed for the optimized value. The sixth chapter is devoted to bring out the important conclusions based on this work and the scope for future work.

[This Page is kept intentionally blank]

CHAPTER 2

LITERATURE REVIEW

Government policies have become more stringent due to the deterioration of environment; thus it is a challenging task to the automotive industry to develop an efficient and environment friendly technologies meet the norms. In this view, many researchers have been investigated several new technologies and the research is still being carried out all over the world. Homogeneous charge compression ignition (HCCI) technology is one of the efforts to achieve high efficiency, low emission automobile vehicles. In this context a review of literature on development of HCCI engines has been done in this chapter. And also evolution of ion sensors as a combustion diagnosis tool is also discussed through the studies done by various researchers.

2.1 HCCI TECHNOLOGY

Onishi et al. (1979): This study gives the development of first HCCI engine. They conducted the experiments on two stroke petrol engine. The simultaneous combustion process was named as “Active-Thermo Atmospheric Combustion” (ATAC), a different combustion process from gasoline and diesel engine. The research reported improved fuel consumption and exhaust emissions.

Haruyuki et al. (1997): A new concept of diesel combustion was investigated both theoretically and experimentally. The calculation results showed the combustion concept had possibilities for low NO_x emissions. This was proved right for a limited range of operating condition. The difference in theoretical and experimental results were attributed to lack of homogeneity of the pre mixture, the fuel that entered the crevices of the cylinder remained unburned and the auto ignition occurred well before the TDC. Combustion analysis and observation indicated that in 6 hole nozzle mixture formation of early injection was poor on the other hand micro hole nozzle proved better.

Su et al. (2004): In this investigation the engine was operated in HCCI mode by means of advanced high pressure fuel injection and diffusion lean burn combustion through BUMP combustion chamber. The experiment showed that the BUMP combustion chamber was effective in reducing NO_x and smoke emissions this is due to enhanced mixing in the combustion chamber staged fuel was employed here. The system had a good operating range covering low load and high load as well which was a great achievement.

Xing Cai Lu et al. (2005): In this study the influence of exhaust gas recirculation (EGR) rate, intake charge temperature, coolant temperature, and engine speed on the HCCI combustion characteristics and its emissions are evaluated. The experimental results indicate that the ignition timing of the first-stage combustion and second-stage combustion retard, and the combustion duration prolongs with the introduction of cooled EGR. Moreover, when the combustion phase advances, and the combustion duration shorten with the increase of intake charge temperature and the coolant out temperature, and the decrease of the engine speed. It is found that the intake charge temperature gives the most sensitive influence on the HCCI combustion characteristics.

Xing Cai Lu et al. (2005): This gives a further study on the basic combustion parameters including start of the ignition timing, burn duration, cycle-to-cycle variation, and carbon monoxide (CO), unburned hydrocarbon (UHC), and nitric oxide (NO_x) emissions of homogeneous charge compression ignition (HCCI) engines fueled with primary reference fuels (PRFs) and their mixtures. Two primary reference fuels, n-heptane and iso-octane, and their blends with RON25, RON50, RON75, and RON90 were evaluated. The experimental results show that, in the first-stage combustion, at the start of ignition retards, the maximum heat release rate decreases, the pressure rises and the temperature rises during the first-stage combustion decrease with the increase of the research octane number (RON). Furthermore, the cumulative heat release in the first-stage combustion is strongly dependent on the concentration of n-heptane in the mixture.

Lu et al. (2006): This article investigates the auto-ignition, combustion, and emission characteristics of homogeneous charge compression ignition combustion engines fuelled

with n-heptane and ethanol/n-heptane blend fuels. The results show that, with the introduction of ethanol in n-heptane, the maximum indicated mean effective pressure (IMEP) can be increased. It also gives the fact that the cycle-to-cycle variation of the maximum combustion pressure and its corresponding crank angle, and ignition timing deteriorated with the increase of ethanol addition.

Zhi et al. (2006): This analytical study deals with spray, combustion and pollution formation processes of compression ignition engine with high-octane fuel by coupling multi-dimensional computational fluid dynamic (CFD) code with detailed chemical kinetics. The model is validated by experimental data from HCCI engine with direct injection. The results show that the two – zone HCCI leads to sequential combustion, thus the ignition rate and combustion rate are controllable.

Sjoberg and John (2006): The characteristics of auto ignition after TDC for both single and two-stage ignition fuels was investigated in a homogeneous charge compression ignition (HCCI) engine. The single stage ignition fuel was iso-octane and the two-stage ignition fuel was PRF80 (80% iso-octane and 20% n-heptane). The heat-release rate and pressure-rise rate both decreased as the combustion is retarded later into the early expansion stroke for both fuel-types, cycle-to-cycle variations of the ignition and combustion phasing increase with combustion-phasing retard. Also, the cycle-to-cycle variations are higher for iso-octane compared to PRF80. These observations can be explained by considering the magnitude of random temperature fluctuation and the temperature-rise rate just prior to thermal run-away. Furthermore, too much combustion phasing retard leads to the appearance of partial-burn or misfire cycles, but the responses of the two fuels are quite different. The different behaviours can be explained by considering the thermal and chemical state of the residual exhaust gases that are recycled from one cycle to the next. The data indicate that a partial burn cycle with iso-octane produces residuals that increase the reactivity of the following cycle. However, for the already more reactive PRF80 fuel, the partial-burn products present in the residuals do not increase the reactivity enough to overcome the retarding effect of cool residual gases

Qian et al. (2006): This work investigates the effects of exhaust gas recirculation (EGR) and operation parameters including engine speed, equivalence ratio, coolant-out temperature, and intake charge temperature on the basic characteristics of a single-cylinder HCCI engine. The running range of iso-octane HCCI engine can be expanded to lower temperature and more load by adding di-tertiary butyl peroxide (DTBP) in the fuel. The combustion timing advances with the increase of DTBP concentrations, coolant temperature and equivalence ratio. The effects of EGR on the combustion and emissions are good when the EGR rate was higher than 25%, and the combustion phase is sharply postponed and the UHC and CO emissions decreased. The intake charge temperature has a small effect on combustion and emissions when it is lower than 35°C; but the combustion timing advances, the combustion duration shortens, and sometimes it leads to knock combustion when the intake charge temperature increases to above 35 °C.

Yap et al. (2006): It has been shown that the addition of hydrogen advances the start of combustion in the cylinder. This is a result of the lowering of the minimum intake temperature required for auto-ignition to occur during the compression stroke, resulting in advanced combustion for the same intake temperatures. This paper documents experimental results using closed loop exhaust gas fuel reforming for production of hydrogen. When this reformed gas is introduced into the engine, a decrease in intake air temperature requirement is observed for a range of engine loads.

Mustafa (2007): In this study, the effect of inlet air pressure on the performance and exhaust emissions of a DI-HCCI gasoline engine has been investigated after converting a heavy-duty diesel engine to a HCCI direct-injection gasoline engine. The experiments were performed at three different inlet air pressures while operating the engine at the same equivalence ratio and intake air temperature as in normally aspirated HCCI engine condition at different engine speeds. It was found that the combustion efficiency increased with engine speed for the three boost pressure. However, the combustion efficiency in the highest boost pressure remained relatively constant for the entire engine speed range.

Stuart et al. (2007): The objective of the study is to better understand the transition process in terms of characteristic changes to the combustion stability as indicated by patterns of cyclic variations. The transition was experimentally achieved by incrementally adjusting the level of internal exhaust gas recirculation (EGR) using variable exhaust valve actuation. The transition dynamics include complex regions of multi periodicity and deterministic chaos. The general similarity of the PF-HCCI transition to the lean-limit transition suggests that both processes are driven by nonlinear feedback through recirculated exhaust gas.

Myung and Chang (2007): This study investigates the effect of narrow fuel spray angle injection and dual injection strategy on the exhaust emissions of a common rail diesel engine. To achieve successful homogeneous charge compression ignition by an early timing injection, a narrowed spray cone angle injector and a reduced compression ratio are employed. The results showed that a dual injection strategy consisting of an early timing for the first injection for HCCI combustion and a late timing for the second injection was effective to reduce the NO_x emissions while it suppress the deterioration of the combustion efficiency caused by the HCCI combustion.

Amit et al. (2007): This work is an investigation of the factors influencing a reliable prediction of CO emissions in a homogeneous charge compression ignition (HCCI) engine using an improved probability density function (PDF)-based engine cycle model. The CO emissions were found to be influenced by fluid-wall interactions, mixing of hot and cold air-fuel particles, and the wall temperature. The work offered an explanation for the role of inhomogeneities introduced due to the aforementioned factors, in the formation of CO emissions. Particularly, the inhomogeneities occurring during compression stroke influenced the ignition timing of the stochastic particle, and in turn the rate of formation of CO. Furthermore, the inhomogeneities persisting in the expansion stroke dictated the level of CO emissions obtained at the exhaust.

Lijima et al. (2007): An investigation on the heat release rate in HCCI engines with fuels of varying octane number and varying rate of EGR was done. It was observed that with increasing octane number the low temperature heat release decreased and was completely

absent for gasoline like fuels it was also noticed that the peak of heat release curve shifted towards and after TDC with increase in octane number. As the EGR increased the low temperature heat release decreased and was negligible at around 20 % EGR. it was also noticed that the peak of heat release curve shifted towards and after TDC with increase in EGR. The heat release was also decreased because of the decrease in fuel concentration with increasing EGR.

Anthony et al. (2007): In this study, experiments were performed using a homogeneous charge compression ignition (HCCI) engine to characterize the effect of exhaust gas recirculation (EGR) rates (from 0% to 50%) with NO addition (from 0 to 500 ppm) on ignition delays at low and high temperatures for an equivalence ratio of 0.3 and a constant intake temperature of 350 K. Two surrogate automotive fuels (n-heptane/iso-octane, n-heptane/ toluene) were used and compared to the pure n-heptane case. Zero-dimensional single zone modeling was also performed using the detailed kinetic scheme and compared to the experimental results in terms of cool and principal flames ignition delays, phasing time and also the importance of the cool flame combustion heat release in comparison to the main one.

Hatim et al. (2007): EGR is one of the most important methods used in controlling of combustion phasing in HCCI engines. An investigation into thermal and diluting effects of EGR showed that CO, in the investigated domain, did not influence the ignition delays, while NO had two different effects. At concentrations up until 45 ppm, NO advanced the ignition delays for the PRF40 and at higher concentrations, the ignition delayed. The influence of NO on the auto ignition of n-heptane seemed to be insignificant, probably due to the higher burn rate of n-heptane. CH₂O seemed to delay the ignition

Wen and Maozhao (2008): In this study a method is proposed to reduce unburned hydrocarbon emissions from a homogeneous charge compression ignition engine by using in-cylinder catalysts. The study gives that the unburned hydrocarbons of the HCCI engine arise primarily from sources near the combustion chamber wall, such as flame quenching at the entrance of crevice volumes and at the combustion chamber wall. The

Platinum is used as the catalyst which is coated on piston crown and this reduces exhaust unburned hydrocarbon emissions by approximately 15%.

Hatim et al. (2008): This study is useful in order to gain more understanding in the emission reduction possibilities via HCCI combustion technology. The inlet temperature, the equivalence ratio and the compression ratio are changed, respectively, from 30 to 70 °C, 0.28 to 0.41 and 6 to 14. This study gives that an increase in the inlet temperature, the EGR temperature, the equivalence ratio and the compression ratio results into a decrease of the emissions of CO and the hydrocarbons of up to 75%. However the emission of CO₂ is increased by 50%.

Junjun et al. (2008): In this experimental study a port injected n-heptane homogeneous charge compression ignition in combination with in cylinder diesel fuel direct injection (DI) was conducted on a single cylinder diesel engine. By adjusting the quantities of premixed n-heptane as well as the direct injected diesel fuel, different premixed ratios were obtained over a wide range of load conditions while the test engine was kept at a constant speed. It is found that that the NO_x emissions decreased dramatically with partial premixing and the indicated thermal efficiency is improved at low to medium loads.

Ganesh et al. (2008): In this work homogeneous mixture, diesel fuel was inducted in vapour form by using a diesel fuel vaporizer. EGR was used to control the combustion phasing. It is found that, the ignition delay is reduced considerably for diesel vapour induction due to better mixture preparation and results in low emissions. A reduction of about 55% and 80% in NO_x emissions and 20% and 30% reduction in smoke emissions are obtained for diesel vapour induction without EGR and Diesel vapour induction with 10% EGR compared to conventional mode of operation.

Miguel et al. (2009): An experimental study of the performances of a modified diesel engine operating in homogeneous charge compression ignition (HCCI) combustion mode versus the original diesel combustion mode was carried out. The effects of EGR and operating conditions on HCCI combustion mode and NO_x HC soot emissions were studied. It showed that the ignition timing in HCCI combustion mode at large engine

loads can be delayed to an optimum timing by cold EGR. At the same time, smoother HCCI combustion will be obtained. The best crank angle for injection in the HCCI combustion 45 degrees BTDC.

Komninos (2009): A multi-zone model is used to investigate the importance of mass transfer on the formation of the most important HCCI engine emissions. The combustion mechanism is modeled using a reduced set of chemical reactions coupled with a chemical kinetics solver. The results indicate that mass transfer during combustion and expansion plays a significant role on the formation of both the unburned HC and the CO emissions and therefore must be taken into account for the closed part of the engine cycle, i.e. compression, combustion and expansion.

Hatim et al. (2009): This work deals with Influence of fuel type, dilution and equivalence ratio on the emission reduction from the auto-ignition in a Homogeneous Charge Compression Ignition engine. The dilution increases the emission of CO and hydrocarbons, while decreasing that of CO₂. This is because of the decreasing overall concentrations and kinetics that are caused by the dilution. The consequence is a decreased overall reactivity and especially a decreased peak temperature. The concentration of oxygen is also low, lowering the probability of a collision of oxygen with the fuel. Fewer hydrocarbons are then converted into CO₂ and H₂O and due to the lower temperature less CO is converted into CO₂. It seems that for the auto-ignition of gasoline, the dilution had a strong influence and should not be used as a parameter to control the emission it appears so that the auto-ignition of the diesel fuel results a lower hydrocarbon and CO emission than gasoline. Because of the easiness of diesel to auto-ignite contrary to gasoline. The results suggest that both gasoline and diesel can be used in an HCCI engine, having possibilities to control their emissions. The difficulty, however, is to choose which parameter is most suitable for this.

Can et al. (2009): Here the effects of premixed diethyl ether (DEE) on combustion and exhaust emissions in HCCI-DI diesel engine are examined. The work concludes that single stage ignition was found with the addition of premixed DEE fuel. Increasing and phasing in-cylinder pressure and heat release were observed in the premixed stage of the

combustion. Lower diffusion combustion was also occurred. Cycle-to cycle variations were very small with diesel fuel and 10% DEE premixed fuel ratio. Audible knocking occurred with 40% DEE premixed fuel ratio. NO_x and soot emissions decreased, while exhaust gas temperature decreased by On the other hand, CO and HC emissions increased.

Miguel et al. (2009): This study is an approach to characterize an engine that has been modified from the base diesel engine to work in HCCI combustion mode. It shows the experimental results for the modified diesel engine in HCCI combustion mode fueled with commercial diesel fuel compared to the diesel engine mode. The best crank angle for injection in the HCCI combustion mode for this modified engine has been established as 45⁰ BTDC. It also shows that an increase of inlet temperature at constant EGR rate has a large effect on the start of combustion in HCCI mode.

Toshio et al. (2009): This research investigates the basic characteristics of methanol reforming in a reactor tube with different catalysts with the aim to produce fuels for the HCCI combustion system. The study reveals that adjusting the proportion of dimethyl ether and hydrogen-containing methanol reformed gas can control the ignition timing in an HCCI combustion engine fueled with the two fuels. A very high overall thermal efficiency is achieved by combining the high engine efficiency with HCCI and the waste heat recovery.

Wang et al. (2009): In this study the HCCI-DI compound combustion concept is presented, which is a compromise to full HCCI in that only a portion of the fuel is premixed and a portion of combustion is still controlled by the direct injection timing. Engine experimental results showed that HCCI-DI combustion could extend the operating range with a comparatively high brake thermal efficiency in comparison to HCCI combustion. CO and HC emission for HCCI-DI were lower than those of HCCI engine. As for NO_x emissions for HCCI-DI operation, it is decreased remarkably at low loads with an increase in port DME aspiration quantity, while showed an increasing trend at high loads.

Zhaolei and Mingfa (2009): This investigation gives the engine experimental study and a fully coupled CFD and reduced chemical kinetics model with n-heptane as fuel to analyze the combustion processes of HCCI like charge stratification combustion aimed at diesel HCCI application. It is found that at larger injection ratio, the onset of the high temperature reaction advances and the maximum pressure rise rate decreases with the retarding of injection timing.

Mahrous et al. (2009): In this analytical study the auto-ignition in HCCI engine is facilitated by adjusting the timing of the exhaust-valve-closing and, to some extent, the timing of the intake-valve-opening so as to capture a proportion of the hot exhaust gases in the engine cylinder during the gas exchange process. The effects of variable valve timing strategy on the gas exchange process and performance of a 4-valve direct injection HCCI engine were computationally investigated using a 1D fluid-dynamic engine cycle simulation code. The results demonstrated the potential of the non-typical intake-valve strategy in achieving and maintaining the HCCI combustion at much lower loads within a wide range of valve timings.

Morteza et al. (2010): In this study, the first law heat release model which is widely used in engine combustion analysis was presented and the applicability of this model in HCCI engines was investigated. In addition to this, a new heat release model based on the first law of thermodynamics accompanying with a temperature solver was developed and assessed. The model was applied in four test conditions with different operating conditions and a variety of fuel compositions, including i-octane, n-heptane, pure NG, and at last, a dual fueled case of NG and n-heptane. Results of this work indicate that utilizing the modified first law heat release model together with a solver for temperature correction will guarantee obtaining a well-behaved and accurate apparent heat release trend and magnitude in HCCI combustion engines.

Starck et al. (2010): This study is to assess how the fuel, through its characteristics, could increase the maximum load achievable in HCCI condition. A set of fuels having different cetane numbers (from 33 to 40) and different chemical compositions (via the addition of reactive products which are olefinic and naphthenic compounds) have been

tested. The study conclude that a fuel having a low cetane number, a high volatility and an appropriate chemical composition could improve the HCCI operating range of more than 30% without a too large decrease of the performance under conventional Diesel combustion mode.

Rakesh and Avinash (2010): Here the effect of intake air temperature and air fuel ratio on cycle-to-cycle variations of HCCI combustion and performance parameters was examined. At lower intake air temperature it is possible to ignite the riche mixture in HCCI combustion mode. As intake air temperature increase, engine running on richer mixture tend to knock with very high rate of pressure rise. But at higher intake air temperature it is possible to ignite the leaner mixture in HCCI combustion mode. Coefficient of variation (COV) of Pmax increases with increasingly richer mixture and COV increases with increase in intake air temperature.

Haifeng et al. (2010): This work investigated the influence of piston bowl geometries. Results showed that combustion chamber geometry could play an important role in HCCI combustion. The auto ignition for the re-entrant bowl (Atype) combustion chamber always occurred at the centre of the combustion chamber even with different intake temperatures and coolant temperatures. However, the auto ignition for salient bowl (V-type) combustion chamber was more dispersive and closer to the chamber wall compared to A-type. For the V-type combustion chamber, the peak value of the heat release rate and the pressure rise rate was the highest and the combustion duration was the shortest among three cases, because of the piston bowl forming a lower turbulence intensity; while A-type combustion chamber induced a higher turbulence intensity, which enhanced the temperature in homogeneities in the piston bowl, leading to moderate pressure rise rate and heat release rate.

Wang et al. (2010): In this paper HCCI and PCCI combustion were studied in a four stroke, single cylinder, naturally aspirated, direct injection compression ignition engine. PCCI was achieved by the combination of part aspiration and part direct injection of DME in the experiments and in HCCI only a portion of the fuel was premixed and the portion of combustion was still controlled by the injection timing. The results show that

CO and HC emissions for the PCCI combustion operation were lower than those of the HCCI engine. In comparison to conventional DICl operation, NO_x emissions for the PCCI combustion operation decreased significantly. Experiments also indicated that the fuel injection timing had a great influence on the performance and emissions of a DME engine at a PCCI combustion mode.

Suyin et al. (2011): This study reviews the implementation of HCCI combustion in direct injection diesel engines using early, multiple and late injection strategies. The major factors in HCCI operation are injector characteristics, injection pressure, piston bowl geometry, compression ratio, intake charge temperature, exhaust gas recirculation (EGR) and supercharging or turbo charging. This study also investigates the effects of design and operating parameters on HCCI diesel emissions, particularly NO_x and soot.

Miguel et al. (2011): This study investigates the main parameters which are needed for modeling the heat release rate in HCCI mode of combustion. The influence of these parameters on fuel-air equivalence ratio, engine speed and EGR are examined. The analytical HRR law is validated over a wide range of conditions in HCCI combustion mode and found that the parameters are directly related to any load condition, engine speed, fuel flow rate and EGR. Thereby an analytical model for HCCI mode of combustion is obtained from this study.

Hyung et al. (2011): This paper describes the combustion and emission characteristics as well as engine performance according to the narrow spray angle and advanced injection timing for homogeneous charge compression ignition combustion in dimethyl ether fueled diesel engine. The injection timing ranging from BTDC 80° to BTDC 10° and two fuel masses were selected to evaluate the combustion, emission and engine performance. The calculated results were in good accordance with the experimental results of the combustion and emissions of the engine. Nitrogen oxide emissions at injection timing before BTDC 30° remarkably decreased, while hydrocarbon and carbon monoxide emissions at an injection timing of BTDC 70° showed high levels.

Rakesh et al. (2011): This study is focused on various aspect of signal processing like cycle averaging and smoothing of in cylinder pressure signal from a HCCI engine

acquired using a piezoelectric pressure sensor. The cylinder pressure history of 3000 consecutive engine cycles is acquired for analysis using piezoelectric pressure sensor. This study gives that the optimum number of engine cycles should be higher than 1000 cycles to get reasonably good pressure signals based on standard deviation of in cylinder pressure, rate of pressure rise and rate of heat release signals.

Gregory and Chen (2011): This study reveals the fact that the piston crevice and the quench zone, the area of fluid close to the cylinder walls, are responsible largely for emissions in Homogeneous Charge Compression Ignition engines. They developed an improved numerical model with three zones: the piston crevice zone, the quench zone close to the cylinder walls, and the cylinder zone comprising up of the rest of the cylinder. This model also provides a useful platform for development/validation of reduced chemistry for emissions.

Zhang et al. (2011): The effects of intake temperature and mixture concentration on HCCI combustion characteristics and emissions are analyzed in this study. The engine was fuelled with ethanol, methanol and gasoline with heating the intake air. The emissions of HC and CO both decrease and NO_x emission for gasoline slightly increases with the increase of intake temperature. Methanol has the minimum HC emission among the three fuels.

Xingcai et al. (2011): This gives a review of concepts and methods of fuel design and management and provides the effects of these strategies on ignition, combustion, and emissions for HCCI, LTC, and SCCI engines etc. Strategies based on the fuel design concept including fuel additives, fuel blending, and dual-fuel technology are discussed for primary reference fuels, alternative fuels, and practical gasoline and diesel fuels. The study reveals that diesel HCCI combustion has suffered from difficulties in homogenous mixture formation and an excessively high combustion rate. It also provides an overview about how HCCI combustion can be used in commercial vehicles.

Ming et al. (2011): In this analytical study a full-cycle computational fluid dynamics simulation coupled with detailed chemical kinetics mechanism has been used to investigate the effect of start of injection timing and intake valve close timing on

performance and emissions of diesel premixed charge compression ignition engine. The study reveals that to minimize HC, CO, NO_x and soot emissions, start of injection timing must be carefully adjusted within a limited range.

Pandiyarajan et al. (2011): In this work, a shell and finned tube heat exchanger integrated with an IC engine setup to extract heat from the exhaust gas and a thermal energy storage tank used to store the excess energy available is investigated in detail. It is proposed as a method for utilizing the heat energy of waste exhaust gases. The performance of the engine with and without heat exchanger is evaluated. It is found that nearly 10–15% of fuel power is stored as heat in the combined storage system, which is available at reasonably higher temperature for suitable application.

Abdul et al. (2011): In this study combined first and second law of thermodynamic approach is applied for a HCCI engine operating on wet ethanol and computational analysis is performed to investigate the effects of turbocharger compressor ratio, ambient temperature, and compressor adiabatic efficiency on first law efficiency, second law efficiency, and exergy destruction in each component. From the analysis it was found that First law and second law efficiencies are found to be an increasing function of the turbocharger pressure ratio, while they are found to be a decreasing function of the ambient temperature. The effect of turbocharger pressure ratio on exergy destruction is found to be more significant than compressor efficiency and ambient temperature.

Magnus et al. (2011): From the tests, it was found that ethanol's auto ignition timing has the lowest sensitivity to addition of simulated EGR (CSP). This low sensitivity stems primarily from ethanol's exceptionally low sensitivity to a reduction of the intake [O₂] in the 21–17% range. Computations show that ethanol is a stable molecule that does not break down until just prior to the hot-ignition point. Contributing some to ethanol's low sensitivity to CSP addition is a slight enhancement of auto ignition due to the presence of water. For operation with real EGR, trace species have an enhancing effect as well, reducing the retarding effect compared to CSP.

Zhang et al. (2011): The effects of intake temperature and mixture concentration on HCCI combustion characteristics and emissions were analyzed in this paper. The results

indicate that with the increase of intake temperature, the in-cylinder peak pressure significantly increases and the crank angle corresponding to it gets a visible advance. But for gasoline, the changing trend is a little different. The emissions of HC and CO both decrease and NO_x emission for gasoline slightly increases with the increase of intake temperature.

Rakesh and Avinash (2011): In this investigation, port injection technique is used for preparing homogeneous charge. The combustion and emission characteristics of a HCCI engine fuelled with ethanol were investigated on a modified two-cylinder, four-stroke engine. The experiment is conducted with varying intake air temperature (120–1500 °C) and at different air–fuel ratios, for which stable HCCI combustion is achieved. The experimental results indicate that the air–fuel ratio and intake air temperature have significant effect on the maximum in-cylinder pressure and its position, gas exchange efficiency, thermal efficiency, combustion efficiency, maximum rate of pressure rise and the heat release rate.

Shuaiqing et al. (2011): An opposed-piston hydraulic free piston engine operating with homogenous charge compression ignition (HCCI) combustion, has been proposed by State Key Laboratory of Engines as a means of significantly improving the IC engine's cycle thermal efficiency and lowering exhaust emissions. Intake heating, variable compression ratio and internal EGR are utilized to control the combustion phasing and duration in the cycle simulations, revealing the critical factors and possible limits of performance improvement relative to conventional crank engines. It was found that Over-compression of the cylinder charge after auto ignition leads to shorter burn duration, resulting in increasing indicated thermal efficiency at adiabatic case.

Annarita and Vinicio (2012): In this work, HCCI combustion mode, by using ethanol as fuel, is analyzed in order to clarify the role of specific technical solutions, such as power boosting, downsizing, swirl motion, and of the thermo-physical properties of ethanol on emissions and performance of the engine. A multidimensional numerical approach, coupled with a kinetic reaction mechanism for ethanol oxidation and NO_x formation, is proposed and validated against experimental measurements. Specifically, CO emissions

assessment is a major issue of this work, as this pollutant is strictly related to inhomogeneity in the combustion chamber near the walls and a multidimensional approach with an adequate grid resolution is mandatory for a correct simulation.

Mustafa (2012): In this study, the effect of inlet air pressure on the combustion characteristics and exhaust emissions of a direct injection homogeneous charge compression ignition gasoline engine is investigated. The experiments were performed at three different inlet air pressures while operating the engine at the same equivalence ratio and intake air temperature as in normally aspirated HCCI engine condition at different engine speeds. The NO_x and CO emissions of the engine decreased when the boosting is employed, while UHC emissions increased remarkably. It is also revealed that with the increasing boost pressure, the brake thermal efficiency increased while the combustion efficiency decreased.

Ivan et al. (2012): An experimental study was conducted to study the effects of equivalence ratio, inlet absolute pressure and inlet charge temperature on combustion characteristics and emissions of a biogas fueled HCCI engine. For lean biogas air mixtures, slight increases in inlet absolute pressure and inlet charge temperature can be used to increase engine power output, increase indicated efficiency, decrease cycle-to-cycle variability, and decrease HC and CO emissions. However, at high equivalence ratios, this strategy can lead to excessive ringing intensities and slightly higher NO_x emissions without a proper control of inlet charge conditions

Junnian and Jerald (2012): In this analytical study a single zone thermodynamic model with detailed chemical kinetics is used to determine the effect of operating parameters on nitrogen oxides emissions for a natural gas fuelled HCCI Engine. The results show significant changes in nitrogen oxides concentrations with varying engine operating conditions. From this particular study, 50% reduction in nitrogen oxides emissions could result from IMEP decrease from 300 kPa to 200 kPa, or an EGR level increase from 0% to 20%.

Qiang et al. (2012): In this study the HCCI-DI combustion mode was achieved in a heavy-duty diesel engine using the early pilot injection in the intake stroke and the main

injection around compression top dead center. The effects of pilot injection quantity and EGR rate on HCCI-DI combustion and emissions are investigated. This study reveals that NO_x emission is decreased as the pilot injection quantity increased, but CO and HC emissions were increased. This study concludes that the HCCI-DI combustion with low level of EGR is an effective method to reduce NO_x emission further.

Rakesh and Avinash (2012): In this study, tuning of input parameters is carried out by using cumulative heat release calculations of cylinder pressure during motoring. Input parameters used in these investigations are intake air temperature, intake air pressure, phasing between the acquired pressure and crank angle position, compression ratio and scaling factor of heat transfer coefficient. Results shows that measurement errors in phasing between pressure and crank angle position, compression ratio and inlet air pressure affect estimated combustion and performance parameters significantly.

Yaopeng et al. (2013): An improved multi-dimensional model coupled with detailed chemical kinetics mechanism was applied to investigate the combustion and emission characteristics of a methanol/diesel reactivity controlled compression ignition (RCCI) engine. The effects of mass fraction of premixed methanol, start of injection (SOI) of diesel and initial in-cylinder temperature at intake valve closing (IVC) on engine combustion and emission were investigated in detail. The results show that both methanol mass fraction and SOI have a significant impact on cetane number (CN) distribution.

Tao et al. (2014): In this work, research was carried out on a single cylinder engine equipped with fully variable valve lifts and timing devices in order to identify the appropriate engine control strategies to extend the HCCI low load limit. Negative valve overlap (NVO) with port fuel injection and direct gasoline injection were investigated for achieving the appropriate environment for auto-ignition at idle and the optimal tradeoff between the combustion stability and fuel consumption. The result shows that the early intake valve opening (EIVO) strategy is most conducive to produce stable combustion at low load conditions.

Gajendra et al. (2014): In this experimental study the effect of biodiesel content on homogeneous charge compression ignition engine combustion is investigated.

Experiments are performed in a modified two cylinder engine, in which, one cylinder is operated in HCCI mode while other was operated in conventional CI mode. An external device is used for fuel vaporization and mixture formation. The combustion results are found to be more stable for biodiesel HCCI compared to diesel HCCI due to lower rate of heat release for biodiesel. A small increase in CO, HC and smoke emissions was observed with increasing biodiesel content due to slower evaporation rate of biodiesel.

Jacek (2014): During the experiments, air excess ratio values were varied from a stoichiometric mixture to lean mixtures, limited by misfire occurrences. A Fourier transform infrared analytical system and simple gas sampling method from the intake port were applied in order to analyze changes in fuel composition resulting from the reforming process during the NVO period. As a result of reforming, which took place after fuel injection during exhaust compression, up to 10.2% of fuel carbon was converted into CO carbon. NVO reforming reactions and the presence of reforming products did not influence auto-ignition temperature to a significant extent. However, early NVO injection at lean mixtures advanced 5% mass fraction burned when compared to late NVO injection due to the thermal effects of NVO heat release. Nevertheless, the presence of auto-ignition promoting species increased the rate of heat release.

Hui et al. (2014): In this study systematic engine experiments were carried out to investigate the individual and combined effects of residual gas trapping and intake charge heating on HCCI/CAI combustion characteristics, fuel consumption, and emissions, on a single cylinder port fuel injection gasoline 4-stroke engine equipped with variable valve lift and timing control devices. It provides a possible solution for the relatively slow response of fast thermal management system, with adjustable residual gas trapping to cope with the quick response and controlled intake temperature to optimize the fuel economy.

Rakesh and Avinash (2014): This experimental study was carried out to investigate performance, combustion and emission characteristics of HCCI engine fueled with ethanol and methanol and compare it with baseline gasoline fuel. The experiments were conducted on a modified four cylinder four-stroke engine at different engine speeds using

port fuel injection technique for preparing homogeneous charge. It was found that IMEP was mainly affected by the air–fuel ratio in the HCCI operating mode and combustion phasing was mainly affected by the intake air temperature. HCCI operating envelope decreased with increasing engine speed for all test fuels.

Javad et al. (2015): This study investigates the performance and emission characteristics of HCCI engines fueled with oxygenated fuels. The investigation is done through a combination of experimental data analysis and artificial neural network (ANN) modeling. This study uses HCCI experimental data to characterize variations in seven engine performance metrics including indicated mean effective pressure (IMEP), thermal efficiency, in-cylinder pressure, net total heat released, nitrogen oxides (NO_x), carbon monoxide (CO), and total hydrocarbon (THC) concentrations. Two types of ANNs including radial basis function (RBF) and feed forward (FF) are developed to predict the seven engine performance metrics.

Can et al. (2015): The aim of this study is to determine the effects of reduced valve lifts, air/fuel ratio and inlet air temperature for the problem of limited HCCI operating range. In this way variable valve mechanisms were used in order to determine the knocking and misfiring regions. One of the most feasible and practical method is to trap the hot exhaust gases via variable valve mechanisms in order to control HCCI combustion phasing. Test results also showed that HCCI combustion has been achieved at leaner mixtures with higher inlet air temperature at misfiring boundary. It is also possible to say that the HCCI combustion has been achieved at lower engine speeds. It caused to realize HCCI combustion at larger engine speed range.

Kyeonghyeon et al. (2015): The objectives of this study were to extend the operating range of gasoline HCCI combustion and to develop control logic. To extend the high load operating range, several strategies including external EGR (exhaust gas recirculation), EGR stratification, fuel stratification and valve timing swing were adopted. Among these strategies, EGR stratification, asymmetric injection and open valve injection are novel techniques. The high load boundary of the low speed region was improved more than that of the high speed region. The improvement in the low load boundary was due to the

direct injection during negative valve overlap. In terms of stabilizing the HCCI combustion phase, the peak pressure value and pressure rising rate of a cycle were important factors when considering the ringing intensity equation.

Bang et al. (2015): In this study it was observed that auto ignition timing for alcohol–gasoline blends is dependent on alcohol types and its concentration in the blend, engine speed and intake valve opening (IVO)/exhaust valve closing (EVC) timing. In the operating conditions with the residual gases more than 38% by mass in the mixture, alcohol–gasoline blends auto ignite more easily than gasoline. Auto ignition timing for n-butanol–gasoline blend is earlier than that for ethanol–gasoline blend with the same alcohol volume fraction at 1500 rpm in most cases while the auto ignition timings for the blends with alcohol are relatively close at 2000 rpm at the same IVO/EVC timing. Combustion stability is improved with advanced EVC timing at a fixed IVO timing.

Wang et al. (2015): In this study, methanol port injection was used for preparing homogenous charge for diesel methanol dual fuel operation on a 6-cylinder turbocharged intercooler heavy duty (HD) diesel engine. The testing work was operated at a constant load and constant engine speed of 1500 rpm. The experimental results show that there was a strong coupling between the intake air temperature and the methanol fraction to performance and emissions of the engine.

Pranab et al. (2015): This study introduces a novel dual injection strategy to modify a single cylinder direct injection diesel engine to run on homogeneous combustion mode. Effect of main injection timing is investigated covering a range from 26 to 8 crank angle degrees before top dead center with an interval of 3^o. Retarded main injection timing is identified as a control strategy for delaying combustion phasing and a means of controlled combustion phasing of direct injection homogeneous charge compression ignition combustion. Two load conditions are investigated and it is observed that at higher load, start of combustion depends more on fuel air equivalence ratio than main injection timing, whereas at low load, it significantly varies with varying main injection timing. Significant improvements in smoke and oxides of nitrogen emissions are observed when compared with the baseline conventional combustion.

Rakesh and Nekkanti (2016): Present study computationally investigates the HCCI operating range of ethanol at different compression ratios by varying inlet air temperature and engine speed using stochastic reactor model. A newly developed reduced ethanol oxidation mechanism with NO_x having 47 species and 272 reactions is used for simulation. It was found that engine operating condition with richer mixture and lower inlet air temperatures have higher IMEP. NO_x emissions was found ultralow for IMEP less than 4 bar and NO_x emission increases exponentially on increasing engine load for all the compression ratio and engine speeds.

Mathivanan et al. (2016): In this work, diesel injected in five timed pulses has been investigated in a compression ignition (CI) engine operating in HCCI mode. The influence of varying the first, middle and last injection pulse durations alone, in sequence, while maintaining all the other injection pulse durations equal has been studied. In addition, the influence of the injection timing of the last injection pulse was also studied. The results show that, multiple pulse (MP) injection is better than injecting the fuel in a single pulse (SP) as it leads to lower emissions and higher thermal efficiency. This is because of better combustion phasing and higher heat release rates.

Pravin and Rehman (2016): This paper reviews the concepts and methods of HCCI combustion and provides an overview of use of biodiesel in conventional compression ignition direct injection (CIDI) and HCCI engine. In HCCI combustion, the entire combustion process lacks a direct method for the control of ignition timing and combustion rate, which are rather controlled primarily by chemical kinetics, and to a lesser degree, by turbulence and mixing. Biodiesel and its blends with diesel, if coupled properly with HCCI combustion concept, has the potential to reduce the exhaust emissions substantially, while maintaining the performance standards close to the conventional compression ignition (CI) engines.

Chunhua et al. (2016): It was observed that that the intake charge temperature influences both the combustion phasing and heat release rate significantly, which is the most sensitive parameter among tested parameters for methanol HCCI combustion. Equivalence ratio has obvious influence on IMEP and cyclical variation but has little

influence on thermal efficiency. The engine speed scopes are dominated by operation conditions and the optimized speed where highest thermal efficiency obtained increases gradually with equivalence ratio increasing.

Khandala et al. (2017): In this study a newer concept of homogeneous charge compression ignition (HCCI) operation using CRDI is reviewed. It was found that it reduces the particulate matter (PM) and NO_x emission to almost zero level with slightly lower BTE. Such engines however have higher hydrocarbon (HC) and carbon monoxide (CO) emissions in the engine exhaust gas. Hence, there is a need to discuss the performance, emission and combustion of CI, CRDI and HCCI engine operation fuelled with alternative fuels.

Morteza et al. (2017): In this study, the control structure of the HCCI engine is investigated. Since the implementation of HCCI combustion is a control problem, an optimized control structure is required for getting the utmost of this combustion concept superiorities, including high thermal efficiency, fuel flexibility, and low soot-NO_x emissions. It is required that HCCI engine control oriented representation has enough accuracy and speed, simultaneously. The speed-accuracy compromise of the representation is an issue of great importance in control structure development. The drawbacks of HCCI combustion can be significantly improved by an integrated control of suitable parameters. Combustion phasing, load, exhaust gas temperature and engine-out emissions are parameters which have to be controlled provided that their optimum trajectory is known.

Hiremath et al. (2017): Experiments were conducted at different compressed natural gas energy ratio, brake mean effective pressure and charge temperatures to perform the comparative analysis of homogeneous charge compression ignition (HCCI) and dual fuel (DF) engines. Maximum BTE achieved in HCCI operation was 8–9% lower than the neat CI mode of engine operations while in DF mode it was 20–24% lower. Smoke emissions were 70–75% lower in HCCI mode than CI mode of engine operation but at same CNGER and BMEP the smoke emissions were 6–9% lower in DF mode as compared to CI mode.

Sunmeet and Subramanian (2017): In this experimental study tests are done for determining the effect of varying percentage of CO₂ content biogas and its different energy shares on the combustion, performance and emissions characteristics of a dual fueled diesel engine. It is identified from the conducted study that the engine could be operated with up to the maximum biogas energy share at high as well as part loads. Brake thermal efficiency of the engine decreases with increase in CO₂ content in biogas.

2.2 ION SENSOR TECHNOLOGY

The fact that ions are produced in flames has been known for many years. HCCI is a lean and low temperature combustion event, which leads to small quantities of ions being produced during the combustion event. Ion sensors using standard spark plugs are inexpensive sensors which are ideal for production engines. In this section development of ion sensor for combustion monitoring is discussed in detail.

Andreas et al. (2003): This work is focused on studying the in-cylinder pressure fluctuations caused by rapid HCCI combustion. A number of pressure transducers are mounted in the combustion chamber to analyze the pressure waves traversing through it. Experiments showed that direction of pressure wave was random which gives the absence of hot spot ignition. The study reveals that there is no evidence of damage of engine parts during rapid HCCI combustion.

Anders et al. (2004): In this study the ion current at different locations inside the combustion is measured and analyzed. This is because the ion current is a local measurement and pressure is global inside the combustion chamber. For making it global ion current is measured at seven locations inside the combustion chamber. Individual DC source of 85 volts is applied across those spark plugs. The study indicates that the combustion timing depends on the wall temperature at different spark plug locations.

Andreas et al. (2005): This study investigates the effect different fuels on ion current strength. The test is done on a Scania engine in single cylinder operation and ion current was measured at 7 locations simultaneously. The fuels investigated are isooctane, n-heptane, PRF80, gasoline, diesel, ethanol and methanol. The study reveals that fuels with

high octane number gives ion current signal more easily and with fuels such as n-heptane and diesel the ion current is only achieved at rich mixtures.

Mehresh et al. (2005): In this investigation the ion current signal in homogenous charge compression ignition engines is studied. The effects of the equivalence ratio, the intake mixture temperature, and the applied bias voltage on the ion signal are studied through a series of experiments. It is shown that a measurable ion current exists even in the very lean combustion in an HCCI engine.

Gregory et al. (2009): This experimental study measures ion signals produced from the combustion of gasoline, ethanol, and n-heptane in a 4-cylinder HCCI engine with different equivalence ratios and intake pressures. It is found that the ion signal is reduced with an increase in intake pressure, reducing equivalence ratio and decreasing the bias voltage source. Results from a Well-Mixed-Reactor (WMR) model suggest that gasoline and ethanol produces more ions than n-heptane during combustion under the same operating conditions. This study proves that ion sensors can be used reasonably to detect the combustion event for various fuels used in HCCI engines over a wide range of operating conditions

Saxena et al. (2011): This study discusses experimental research that uses the potential of enhancing ion signals at low equivalence ratios by adding small amounts of potassium acetate to ethanol fuel. For each concentration, the study examines the additive's effects on the ion signal and any side effects from this additive. The experimental results reveal significant increases in ion signals with addition of just 180 mg/L of potassium acetate at low equivalence ratios. The study also reveals a side effect, where increasing potassium acetate concentrations cause a reduction in the heat release rates and therefore a lower engine power output.

Zhongquan et al. (2012): In this research work the relationship between ion current and local temperature is investigated with compressed natural gas (CNG) as a fuel. The ion current is measured using a pair of ignition electrodes and a pair of detector electrodes inside of a constant volume combustion bomb. The study indicated that, when ignition electrodes were used for detection, the current showed ignition, front flame and post

flame stages. However, the ignition and part of the front-flame current are lost, when detector electrodes were used.

2.3 RESEARCH GAP

A thorough review of the available literature on evolution of HCCI Technology and the use of ion sensor is performed. However based on the literature it is found that studies related external mixture in diesel HCCI technology is insufficient. The limitation of vaporization of diesel may be the reason for this. Hence the present study introduces a novel technique for external mixture formation by mixing diesel vapour obtained from a heat exchanger and fresh air. It also deals with investigating the effect of injection pressure and injection timing on engine performance, combustion and emissions in a DI modified HCCI engine. The use of ion sensor with diesel HCCI is introduced for monitoring combustion events. The air preheating method can be employed to extend the operating range of the engine. The main purpose of this investigation is to optimize different parameters to achieve HCCI mode of combustion with a better performance and lean combustion.

2.4 OBJECTIVES OF THE RESEARCH

This study aims at converting a CI engine into HCCI engine with better efficiency and low emissions. The proposed mode of HCCI operation will be achieved by combined direct diesel injection and diesel vapour induction. The main objectives of the work are:

- To convert the existing diesel engine in to HCCI mode of operation.
- To control the combustion in low temperature bettering the emission characteristics and to increase the life of the engine.
- To recover the exhaust gas heat which amounts to 35% of the heat generated to vaporize the diesel through a suitably designed, fabricated heat exchanger.
- To develop a low cost spark plug based ion sensor for detecting and controlling the combustion events in HCCI mode.
- To analyse the performance of the engine in direct injection mode and HCCI mode separately.
- To combine the direct injection and vapour induction mode of fuel supply expecting the range of engine operation to increase.

- To apply air preheating to increase the range of operation.
- Optimize the parameters like inlet air temperature, injection timing, injection pressure etc.
- To analyse the performance of the engine in HCCI mode and compare with DI engine.

CHAPTER 3

ION SENSOR TECHNOLOGY

This section of the report deals with generating a method by which the in cylinder pressure measurement in an Internal Combustion engine by ion sensor technology. The replacement of piezoelectric pressure by an ordinary spark plug based ion sensor is explained in detail. Initially the single cylinder DI diesel engine is operated with pressure sensor and ion sensor at the rated condition of 27.5 deg. bTDC and 180 bar injection pressure.

3.1 MODIFICATIONS FOR ION SENSOR

Traditionally, in HCCI research engines, sensing of combustion timing is accomplished using piezo-electric pressure transducers, however these sensors are to date too expensive for use in production engines. Ion sensors are significantly less expensive than pressure transducers (Andreas et al. 2003). For example, an existing spark plug can often be used as an ion sensor. An ion sensor signal has been used for combustion diagnostics, combustion stability control and peak pressure position control.

Here a standard spark plug about 12 mm diameter is chosen as ion sensor. A hole is drilled at the centre of the cylinder head to place this ion sensor. The centre portion of the cylinder head contains passages for the cooling water. Therefore extreme care is taken to locate the sensor so that it is placed exactly in between intake and exhaust valve without blocking the passage of cooling water. The photographic view if the spark plug is given in Fig. 3.1. A bias voltage of about 100 volt is attached to the spark plug (positive side) and the engine head (negative side). By attaching the negative side to the engine head the cylinder walls along with the side electrode become negatively charged (cathode) and receives the ions which are produced during the combustion event. The centre electrode is positively charged (anode) and receives the electrons which are responsible for conducting the current across the spark plug gap. The voltage drop across a known resistance is measured. National Instruments Labview “Visual Instruments” programs are

used to monitor the values which are obtained by using a high capacity Data Acquisition Card.



Fig. 3.1 Spark Plug

The circuit as shown in Fig. 3.2 comprises of a step down transformer to convert 230 V AC to 100 V AC. A bridge rectifier is used to convert this 100 V AC to corresponding DC. Then Capacitors regulate this fluctuated DC voltage to a constant DC voltage of $100\sqrt{2}$ V. A potential divider is used to adjust this constant DC voltage to the required level. The current to spark plug is made to flow through a known Resistance, so that the voltage drop across the resistance will give a proportional current value.

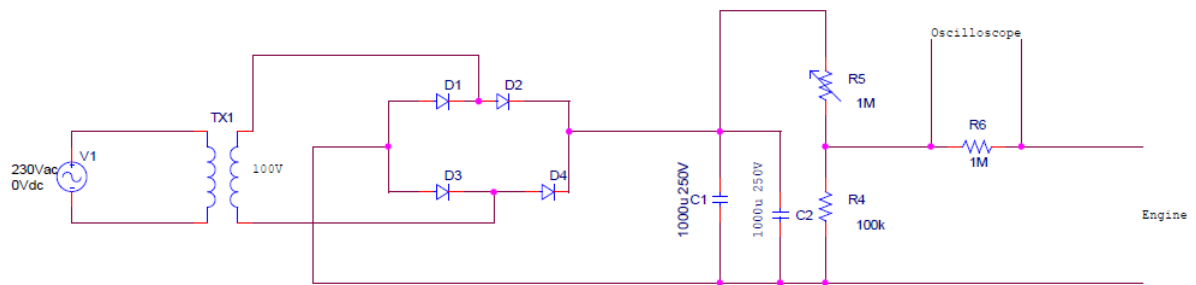


Fig. 3.2 Electrical circuit of the ion sensor in an HCCI Engine

The photographic view of spark plug fitted on the cylinder head is shown in Fig. 3.3. It is placed centrally over the cylinder head and the bottom side of the cylinder head is perfectly machined to avoid any kind of mismatches.

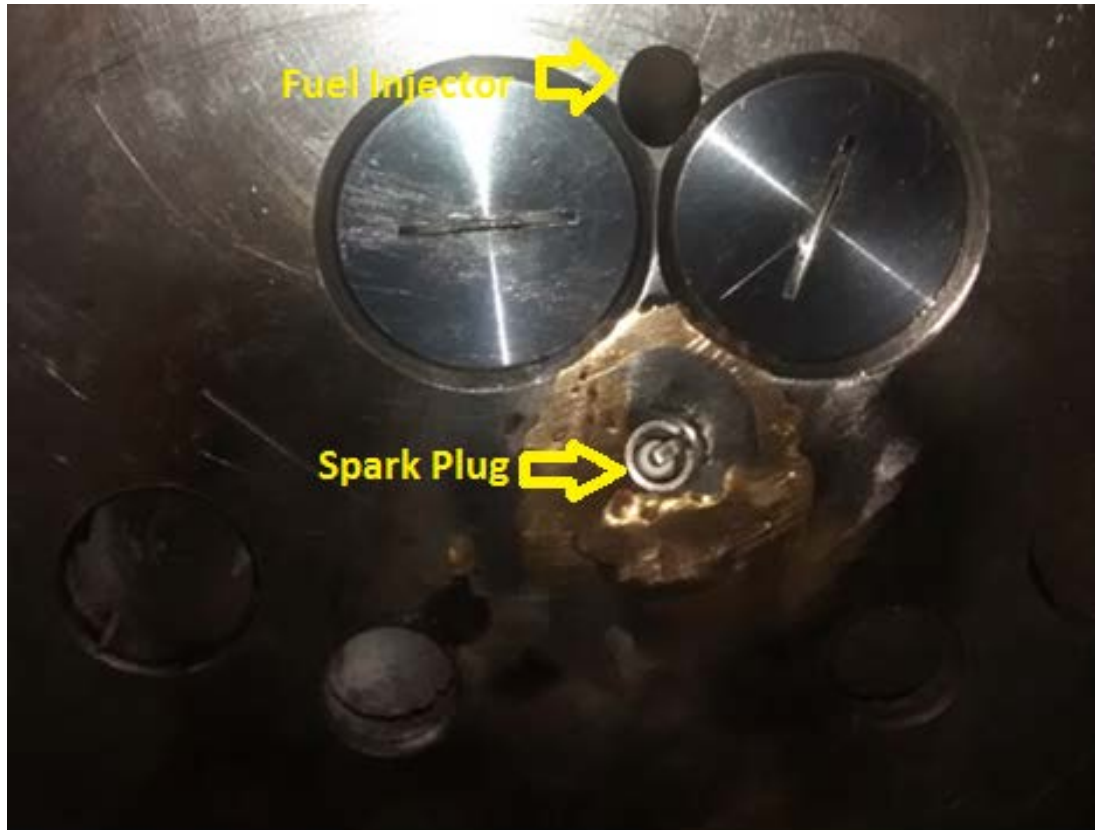


Fig. 3.3 View of Spark Plug ion sensor fitted on the cylinder Head

Performance test has been done for the engine after fitting the new cylinder head with spark plug ion sensor and different characteristics are tabulated in Table 3.1. It reveals that engine is having almost same efficiency even with modification to HCCI mode.

Table 3.1 Performance Characteristics of Diesel Engine after modification

Load	Exhaust Gas temp	Fuel Consumption	BP	BMEP	BSFC	BTE (Normal Engine)	BTE (Modified Engine)
(%)	° C	kg/hr	kW	bar	kg/kW.hr	(%)	(%)
0	134.31	0.46	0	0	--	0	0
25	198.47	0.56	1.05	1.27	0.533	15.88	14.35
50	350.67	0.91	2.01	2.43	0.452	18.71	20.05
75	405.86	1.09	3.29	3.98	0.331	27.94	26.18
100	417.09	1.51	4.98	6.02	0.35	25.35	23.12

3.2 P- θ DIGRAM FOR CONVENTIONAL DIESEL ENGINE WITH ALL LOADS

The cylinder pressure is calculated for conventional mode of operation. In conventional mode of operation the cylinder pressure is measured by using Pressure sensor (piezoelectric sensor). As given in Fig. 3.4 the maximum value of pressure noticed here is 74.9 bar at crank angle of 379 deg. As the % load increases the peak pressure increases and the maximum value of pressure inside the cylinder is measured at full load condition.

It is found that all the pressure curves follow the same Gaussian pattern and this characteristic is used for developing a correlation between incylinder pressure and ion voltage which is discussed in the next section.

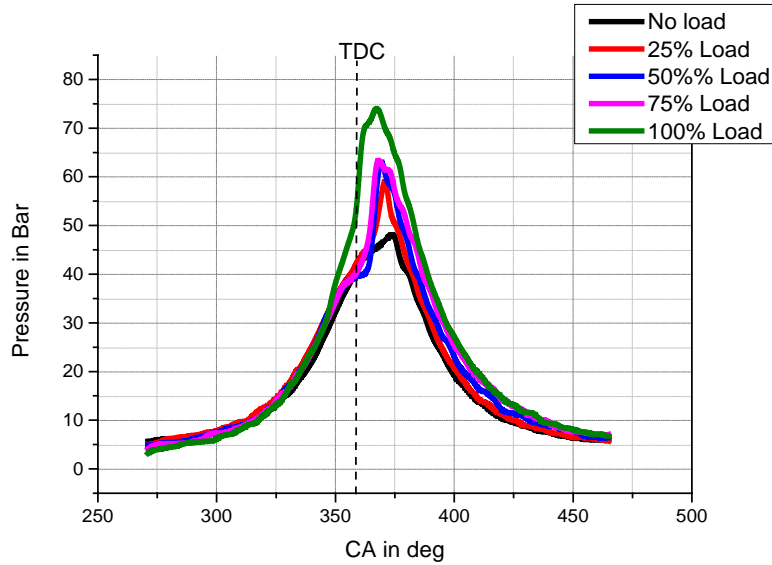


Fig. 3.4 Pressure (bar) vs crank angle (deg) for conventional diesel engine with all load at 180 bar Injection pressure and Injection timing 27.5 deg bTDC.

3.3 ION voltage vs Pressure

As per the Ion sensing technology the Ion voltage is measured by sparkplug which is designed as Pressure sensor with modified circuit. Ion voltage generated is recorded by Lab view software in computer. The ion voltage and cylinder pressure are related with the crank angle in a Gaussian pattern (Zhongquan et.al. 2012). Using non linear regression analysis the recorded experimental data is correlated. The measured Ion voltage is correlated with pressure by the following correlation,

$$p = a_1 + \{(a_2 - a_1) \left[\left(\frac{k}{1+10^{(l1-x)l2}} \right) + \left(\frac{1-k}{1+10^{(l2-x)h2}} \right) \right]\} \text{-----} \quad (1)$$

Where,

p = Cylinder pressure in bar

$a_1 = 2.3289842864$ (Constant value)

$$a_2 = 6.8013750629 \times 10^7 \text{ (Constant value)}$$

$$k = 2.701079627 \times 10^{-7} \text{ (Constant value)}$$

$$l_1 = -0.3549565786 \text{ (Constant value)}$$

$$l_2 = 2.1604372764 \text{ (Constant value)}$$

$$h_2 = 3.2055235874 \text{ (Constant value)}$$

x = Ion voltage in mv

The above correlation was generated by using ORIGIN lab software. Here the maximum value of ion voltage is taken as peak pressure which is measured by pressure sensor. Then the corresponding ion voltage value is equated with the actual pressure value which is already measured during the combustion. Then depending on the condition the constant values has been introduced to get the correlation. The method for generating the above correlation is given in Appendix II.

By using the above correlation the cylinder pressure has been measured with respect to Ion voltage followed by the crank angle. Based on the pressure value calculated by the above co relation the graphs are plotted cylinder pressure vs crank angle for different load conditions and which have been compared with the original cylinder pressure value.

Fig. 3.5 shows the Ion voltage measured by using spark plug in conventional mode of operation at all load conditions. The injection pressure was set as 180 bar and injection timing was 27.5 deg. The ion voltage measured here is then converted as pressure by using the co relation generated. The time along with Ion voltage is converted as crank angle in degree.

The rated Engine speed is 1500 rpm and the tests are done on a four stroke engine. It will complete 750 cycles in one minute and hence almost 0.08 seconds are required for completing one cycle.

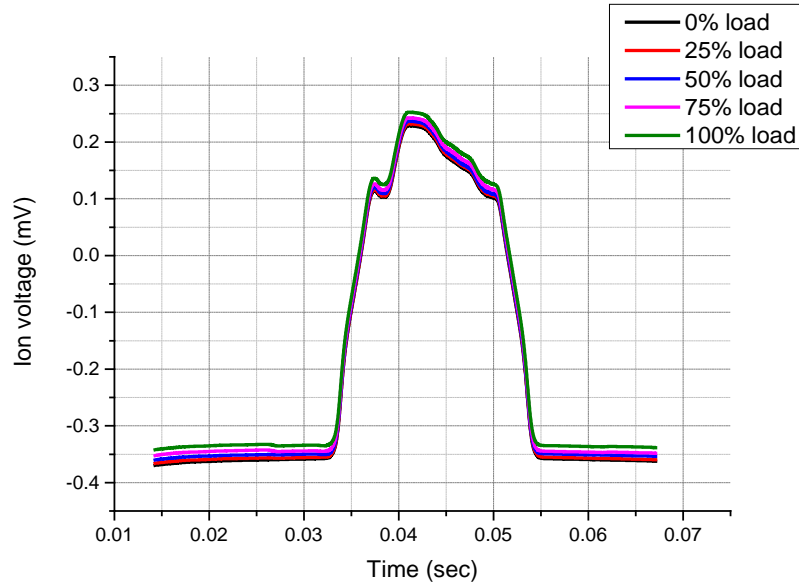


Fig. 3.5 Ion voltage (mV) vs Time (sec) for conventional diesel engine at 180 bar Injection pressure with Injection timing 27.5 deg bTDC.

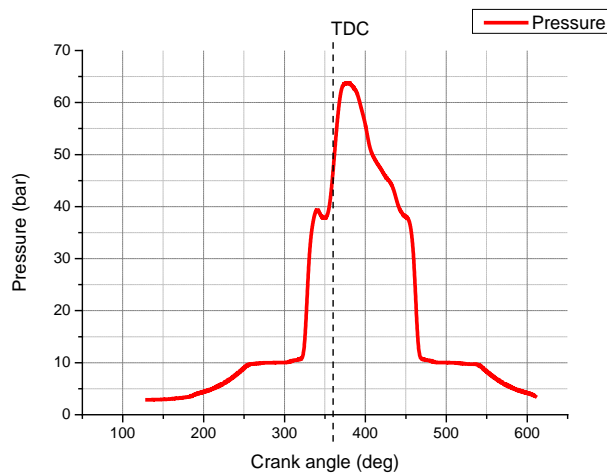


Fig. 3.6 Pressure (Bar) vs crank angle (deg) for conventional diesel engine at 50% Load based on Ion voltage value and 180 bar Injection pressure with Injection timing 27.5 deg bTDC.

Fig. 3.6 shows the variations in cylinder pressure found based on Ion voltage using the correlation and the maximum pressure value is recorded as 63.95 bar in conventional mode of operation at 370 deg of crank angle.

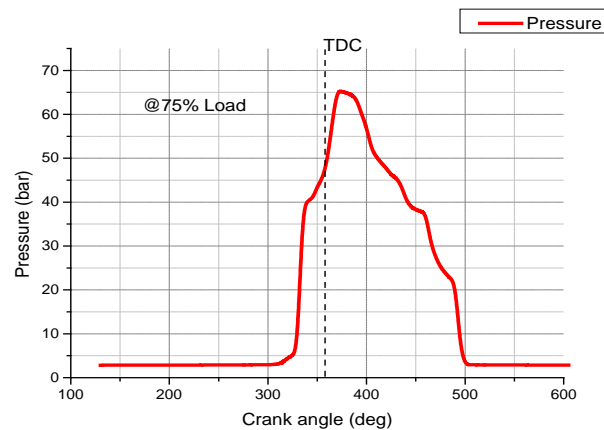


Fig. 3.7 Pressure (bar) vs crank angle (deg) for conventional diesel engine at 75% Load based on Ion voltage value and 180 bar Injection pressure with Injection timing 27.5 deg bTDC.

Fig 3.7 shows the variations in cylinder pressure found based on Ion voltage using the correlation and the maximum pressure value is recorded as 65.52 in conventional mode of operation at 370 deg of crank angle.

Fig 3.8 shows the variations in cylinder pressure found based on Ion voltage using the correlation and the maximum pressure value is recorded as 71.00 in conventional mode of operation at 380 deg of crank angle.

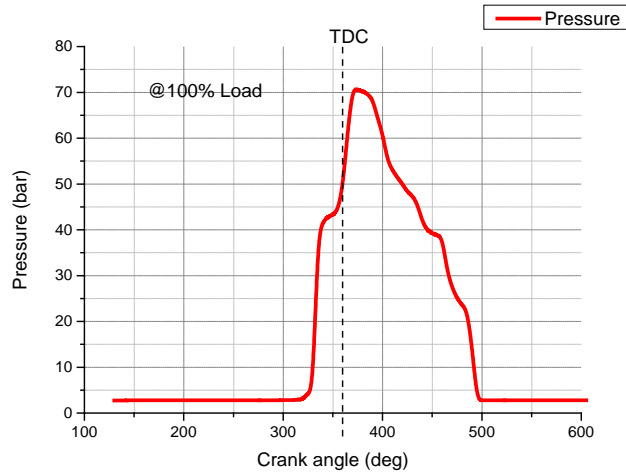


Fig. 3.8 Pressure (bar) vs crank angle (deg) for conventional diesel engine at 100% Load based on Ion voltage value and 180 bar Injection pressure with Injection timing 27.5 deg bTDC.

The Figures 3.9 to 3.11 gives the comparison between in cylinder pressure values given by pressure sensor and obtained by the co-relation generated at different crank angles.

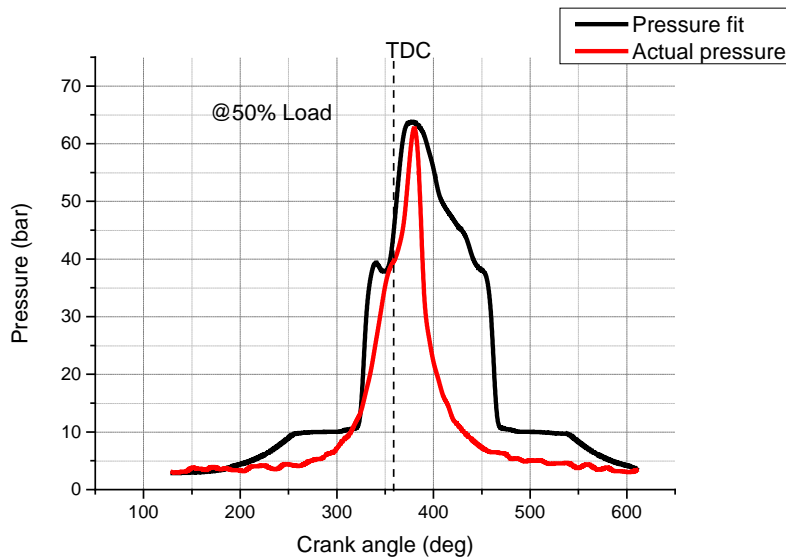


Fig. 3.9 Comparison between actual pressure and pressure based on Ion voltage at 50% Load

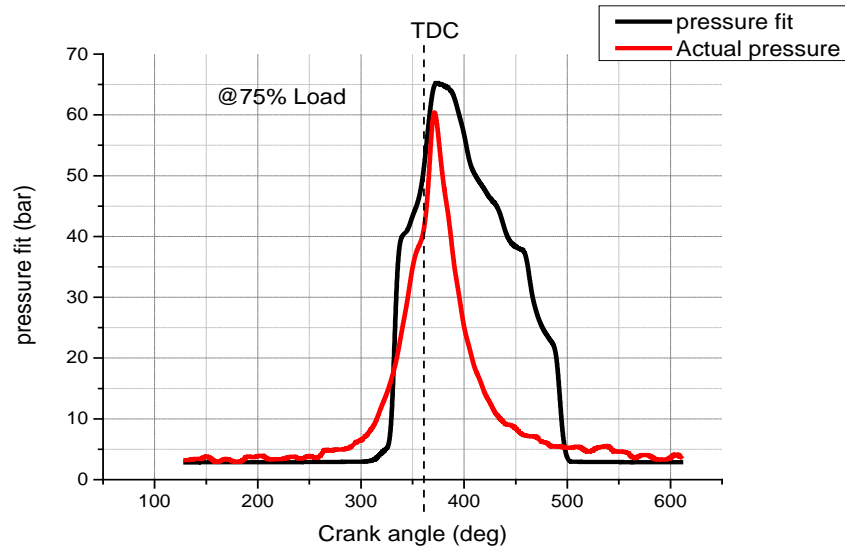


Fig. 3.10 Comparison between actual pressure and pressure based on Ion voltage at 75% Load

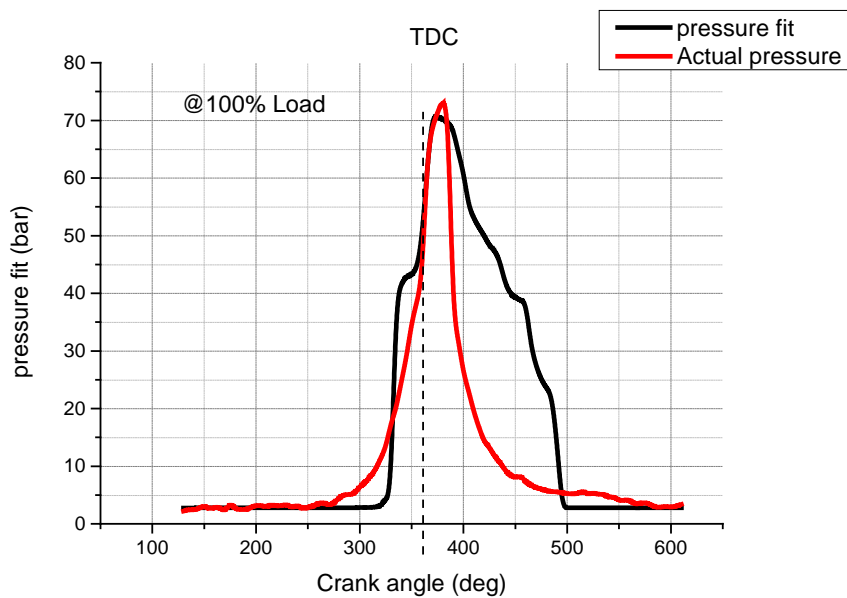


Fig. 3.11 Comparison between actual pressure and pressure based on Ion voltage at 100% Load

The correlation is used for calculating the Pressure value by using the Ion voltage measured during the time of conventional combustion mode. The pressure value calculated is then compared with the actual pressure in the same mode of operation. The comparison graphs show the peak pressure value for actual and the calculated value is almost same with the error of around 8%.

In 50% load condition the actual peak pressure was 65.29 bar and in calculated peak pressure value by Ion voltage was 63.94 bar. In 75% load condition the actual peak pressure was 64.11bar and in calculated peak pressure value by Ion voltage was 66.28 bar. In the same way for 100% load condition the actual peak pressure was 73.72 bar and calculated peak pressure value was 71.00 bar.

From the above study it can be concluded that variation between pressure measured by piezosensor and pressure value obtained through the correlation is less than 10% before the engine attains the peak pressure condition. After the peak the values gives much difference and it may be due to the fact that ion voltage is a local measurement where as pressure change is much more global inside the combustion chamber. It is proved that ion sensing technology is a cheaper combustion diagnosis tool so that overall installation and maintenance cost can be reduced. The further studies use only the ion sensor for the pressure measurement.

[This Page is kept intentionally blank]

CHAPTER 4

EXPERIMENTAL SETUP AND METHODOLOGY

4.1 EXPERIMENTAL SETUP

The existing set up is a computerized single cylinder four stroke naturally aspirated direct injection water cooled diesel engine test rig. The engine is directly coupled to an eddy current dynamometer. The engine and the dynamometer are interfaced to a control panel which is connected to a computer. The software engine soft 2.4 records the engine performance and combustion characteristics. The engine specifications are given in table 4.1.

Table 4.1 - Specifications of the Diesel engine test rig

Engine	4 stroke single cylinder CI engine
Make	Kirloskar
Power	5.2 KW @ 1500 RPM
Bore × Stroke	87.5 × 110 mm
Compression ratio	17.5:1
Connecting rod length	234mm
Dynamometer type	Eddy current with load cell
Fuel and air flow measurement	Differential pressure unit
Speed measurement	Rotary encoder
Interfacing	ADC card PCI 1050

4.2 MODIFICATIONS FOR HCCI MODE

The experimental set up shown in Fig. 4.1 and Fig. 4.2 depicts the vapour induction through a customized heat exchanger which controls the rate of flow of exhaust gas and diesel through it at demand. The liquid diesel to be vapourised is stored in a fuel tank kept at a suitable height and the diesel flows into the heat exchanger entirely on gravity basis.

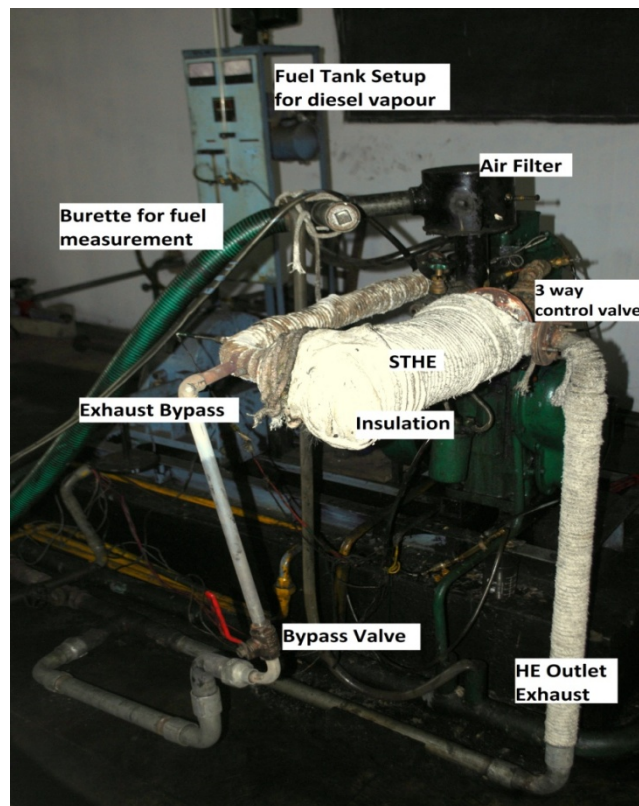


Fig. 4.1 Experimental Setup for Vapour Induction

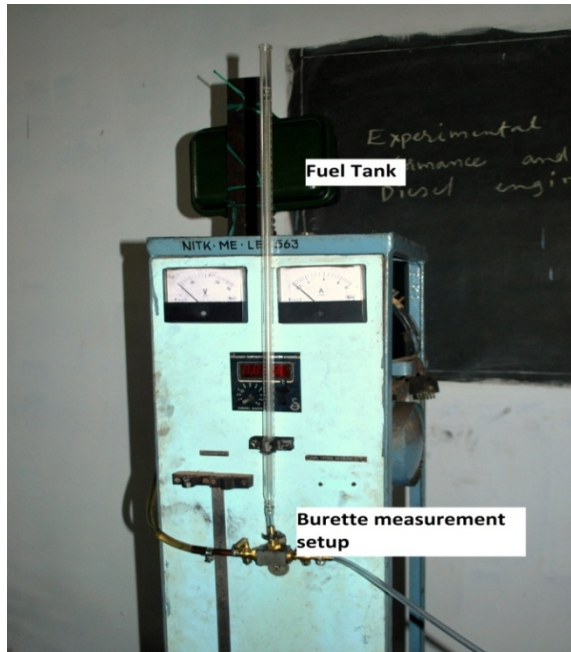


Fig. 4.2 Fuel tank and flow measurement for diesel vapour production

The sectional views of heat exchanger and fabricated assembly are shown in figures 4.3 and 4.4 respectively. The heat exchanger is mounted in a horizontal orientation in a way to minimize the flow path of the vapourised diesel to the combustion chamber. The exhaust gas pipe is connected to the shell side inlet of the heat exchanger and the shell side outlet is connected to a long pipe to give off the exhaust gas away from the setup. This is shown in Fig. 4.5. The diesel vapour outlet from the heat exchanger is connected to the combustion chamber via two three-way valves as shown in Fig. 4.6. One valve regulates the entry of the vapour into the combustion chamber while the other ensures the complete vapour formation. In order to keep the superheat within control a bypass is also constructed which provides a path for the exhaust gas to skip the heat exchanger. The specification of the heat exchanger is given in table 4.2.

The design procedure and calculations of the shell and tube heat exchanger is given as Appendix I.

Table 4.2 - Specification of Heat Exchanger

Length of the Heat Exchanger(shell)	0.45 m
Shell Diameter	0.06 m
Thickness of the shell wall	0.002 m
Length of the tube	2.25 m
Diameter of the Tube	0.006 m
Tube Thickness	0.5 mm
Tube material	Copper
Shell material	GI
Number of passes	7
Thermal Conductivity of the tube material	386 W/mK
Critical Radius of Insulation	0.0525 m

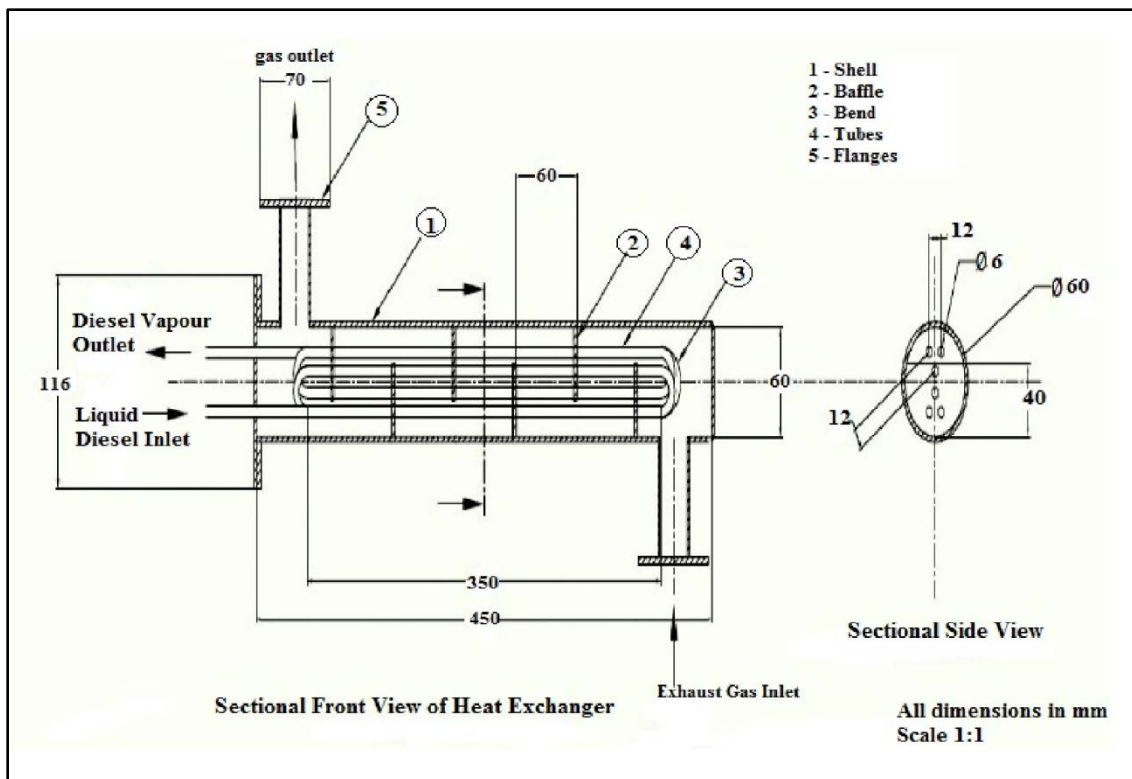


Fig. 4.3 Shell and Tube Heat Exchanger – front and sectional side view



Fig. 4.4 Shell and Tube Heat Exchanger - Inner and Outer Assembly

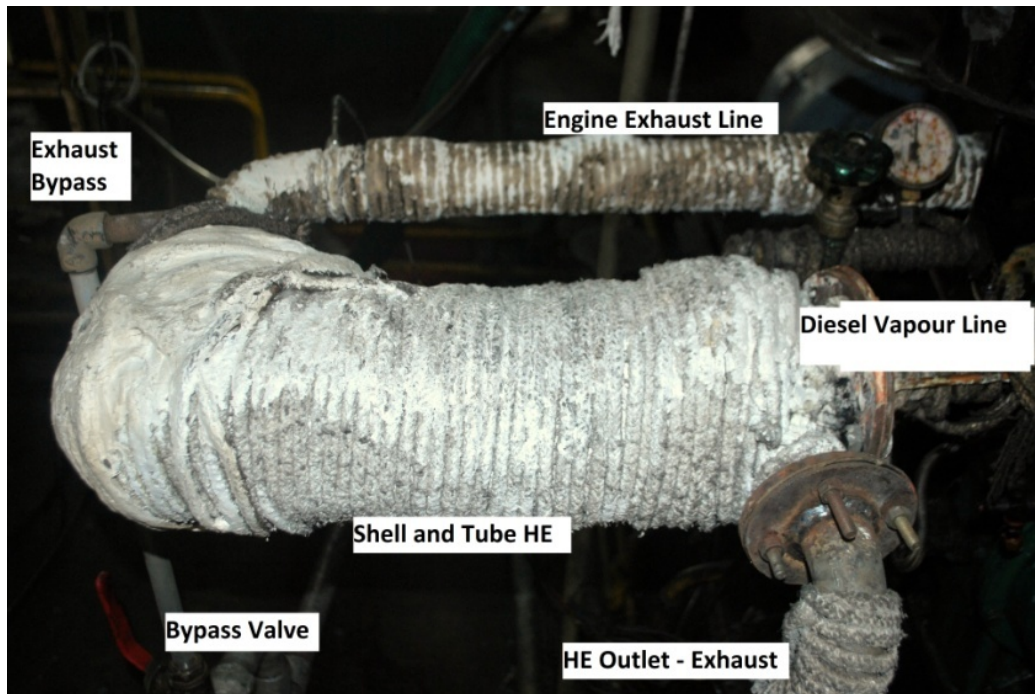


Fig. 4.5 Heat Exchanger Connections

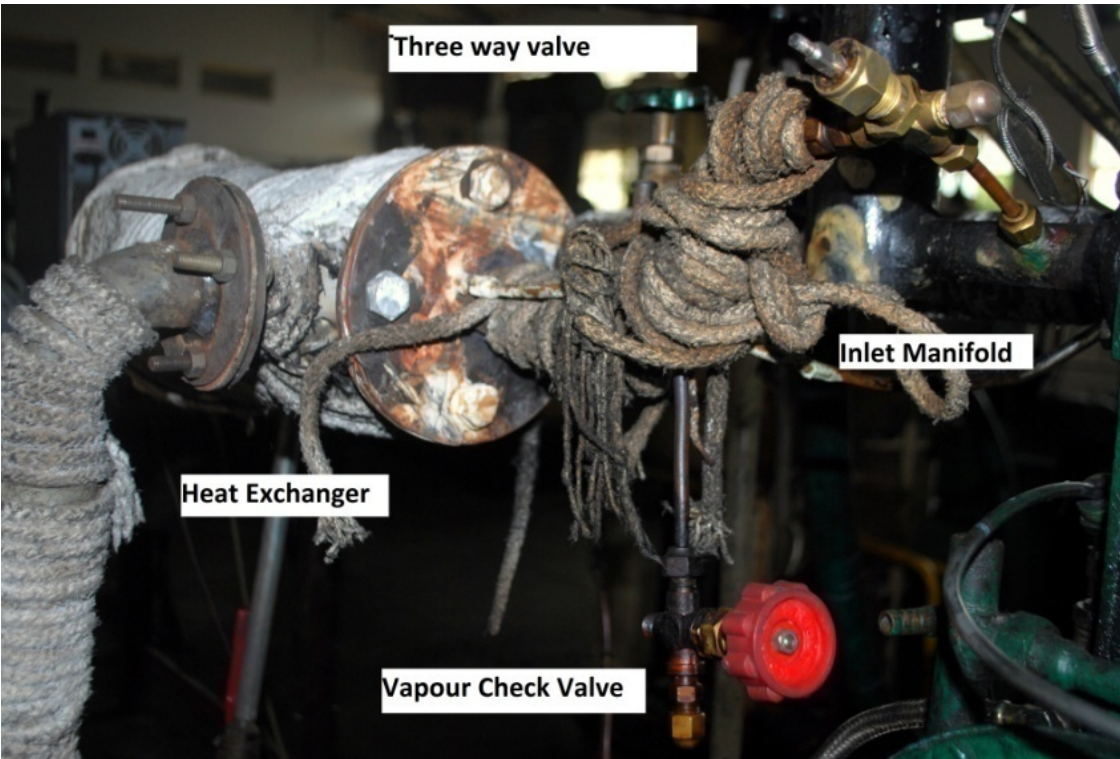


Fig. 4.6 Three way valve for vapour quality checking and connection to inlet manifold

A coil type heater is fitted near the intake manifold to increase the temperature of intake charge. It has a temperature sensor and closed loop feedback system for maintaining a constant temperature for incoming air. This heated air is allowed to mix with diesel vapor produced by the heat exchanger near intake manifold. This part is perfectly insulated to avoid any kind of heat leakage. The schematic of the complete experimental setup is shown in fig. 4.7. The supply of fuel to injector is from main fuel tank and supply of diesel to the shell and tube heat exchanger is from the other fuel tank. The exhaust bypass is for controlling the flow of exhaust gas to the heat exchanger so that the diesel vapour produced is at a constant degree of superheat. Air Preheater is installed very near to intake manifold and the flow of diesel vapour from the heat exchanger is controlled by valves.

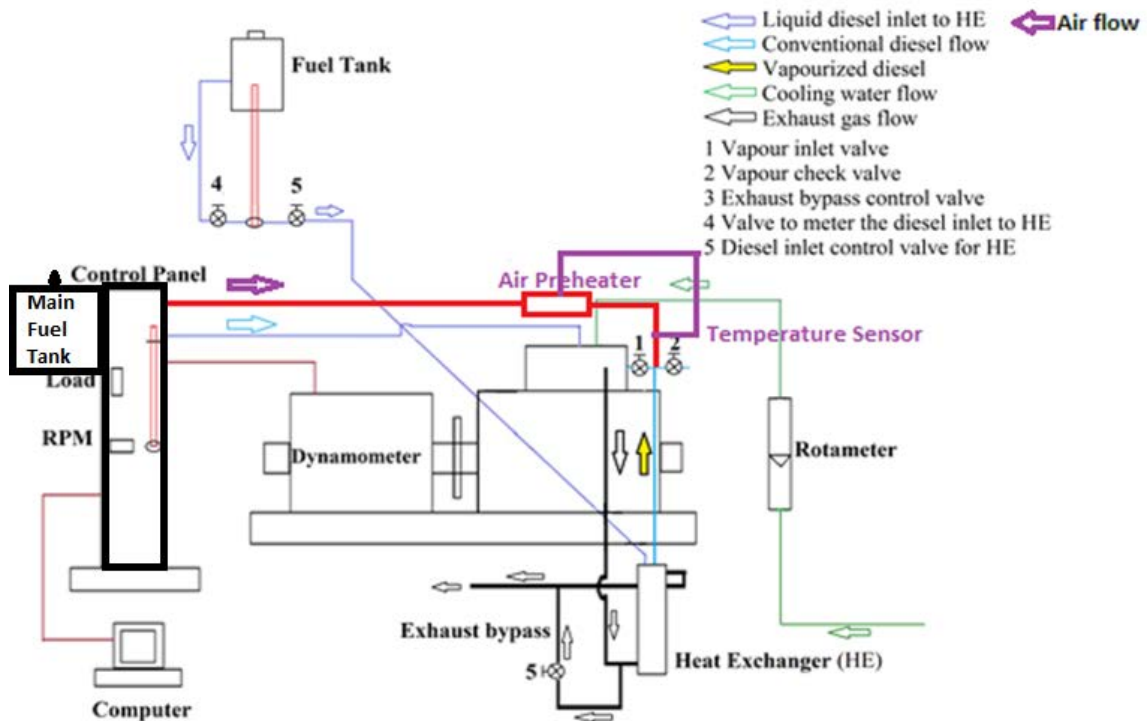


Fig. 4.7 Schematic Diagram of the Experimental Setup.

4.3 METHODOLOGY

The experiments are done according to the experimentation matrix given in Table 4.3. The readings are taken with combined diesel injection and vapour induction. The flow rate of liquid diesel passed through the heat exchanger is measured by the burette connected to the fuel line. The flow rate is varied by the fuel cock valve and when the flow rate of inducted vapour is increased the flow rate of injected diesel will decrease by the operation of governing system of the diesel engine. Thus the diesel flow rate and diesel vapour flow rate can be separately measured. The experiments are repeated with three injection timings (27.5, 29.5 & 31.5 deg. bTDC) and three injection pressures (180, 200 and 220 bar). The bias voltage given can be varied by a differential potentiometer connected across the supply emf.

Table 4.3 Scheme of Experiments of the Research Work

Variables	Type of variables	Details of Variables	Remarks
Independent	Fuel Used	Diesel,	
	Load (%)	25,50,75 and 100	
	Injection Pressure(bar)	180,200 & 220	
	Injection Timings (deg. bTDC)	27.5,29.5 & 31.5	
	% Diesel Vapour Induction	0 to 100%	
	EGR rate	0 to 30%	
	Air inlet temperature	30 to 100 °C	
	Bias Voltage	50 to 150 V	
Dependent	Brake Thermal Efficiency (%)	25%, 50%, 75 % and 100% Load	
	Ion Voltage	25%, 50%, 75 % and 100% Load	
	Emissions - CO,HC,CO ₂ ,NO _x and Smoke Opacity	25%, 50%, 75 % and 100% Load	
	Cylinder Pressure(bar)	25%, 50%, 75 % and 100% Load	
	Heat Release Rate(J/deg. CA)	25%, 50%, 75 % and 100% Load	

Here, Diesel Vapour Content (%)

$$\% \text{ Vapour} = (m_v/m_f) \times 100 \%$$

m_v = Mass of vapour diesel inducted in kg/hr.

m_f =total mass of fuel consumed in kg/hr.

AVL Exhaust Gas Analyzer was used for the measurement of exhaust gases. CO, HC, CO₂, O₂ and NO_x emissions were measured for different operating conditions. AVL smoke meter was used for measuring smoke opacity. The current produced by the electrons across the spark plug gap was measured by measuring the voltage drop across a known resistance. National Instruments Labview “Visual Instruments” programs are used to monitor the values which are obtained by using a high capacity Data Acquisition Card.

4.4 OBSERVATIONS

A sample experimental observation for 200 bar injection pressure at 31.5 deg. bTDC injection angle is shown in the following table 4.4 to 4.9. A sample calculation for one set of readings is also shown in section 4.4.1.

Table 4.4 -50% load readings at 31.5 deg. bTDC and 200 bar injection pressure

Trials	Direct Injection (cc/min)	Vapour Induction (cc/min)	Diesel Vapour Temperature (°C)	Exhaust Gas Temperature (°C)	RPM
1	15.78	0	0	340	1500
3	10.5	3.4	175	320	1500
4	7.31	6.2	186	316	1500
6	3.9	12.4	190	312	1420
8	1	13.9	186	308	1280

Table 4.5 - 75% load readings at 31.5 deg. bTDC and 200 bar injection pressure

Trials	Direct Injection (cc/min)	Vapour Induction (cc/min)	Diesel Vapour Temperature (°C)	Exhaust Gas Temperature (°C)	RPM
1	19.6	0	0	416	1500
2	16.21	2.7	185	404	1500
3	14.6	4.2	190	396	1500
4	10.16	6.1	212	392	1500
5	8.69	10.4	218	372	1450

Table 4.6 - 100%load readings at 31.5 deg. bTDC and 200 bar injection pressure

Trials	Direct Injection (cc/min)	Vapour Induction (cc/min)	Diesel Vapour Temperature (°C)	Exhaust Gas Temperature (°C)	RPM
1	31.57	0	0	584	1500
2	26.08	4.2	235	572	1500
3	24	6	245	568	1500
5	18.75	9	274	564	1500
6	17.64	12.9	277	560	1500

Table 4.7 - Emissions at 50% load -31.5 deg. bTDC and 200 bar injection pressure

Trials	CO (%)	HC (ppm)	CO ₂ (%)	O ₂ (%)	NO _x (ppm)	Smoke opacity(%)
1	0.03	11	4.1	14.7	775	35
2	0.09	14	5.1	13.54	578	52.5
3	0.2	16	3.8	15.02	425	48
4	0.31	34	49	13.27	1225	91

Table 4.8- Emissions at 75% load - 31.5 deg. bTDC and 200 bar injection pressure

Trials	CO (%)	HC (ppm)	CO ₂ (%)	O ₂ (%)	NO _x (ppm)	Smoke Opacity(%)
1	0.04	7	5	13.67	1183	55
2	0.1	15	5.3	13.03	1111	43
3	0.12	18	5.4	12.91	981	28
4	0.19	27	4.9	13.56	999	37

Table 4.9 - Emissions at 100 % load - 31.5 deg. bTDC and 200 bar injection pressure

Trials	CO (%)	HC (ppm)	CO ₂ (%)	O ₂ (%)	NO _x (ppm)	Smoke opacity(%)
1	0.28	12	7.1	10.34	1206	89
2	0.32	18	5.7	12.36	794	67
3	0.11	30	3.9	14.73	636	65
4	0.44	42	3.7	14.24	581	91

4.4.1 Sample Calculations

In the observation tables shown above the highlighted readings corresponds to the optimum vapour induction condition. A sample calculation for optimum vapour induction condition at 50 % load and 31.5 deg. bTDC, 200 bar injection pressure is done below.

Direct injected diesel flow rate = 7.31 cc/min

Vapour injected diesel flow rate = 6.2 cc/min

Total fuel consumption = 13.51 cc/min = $0.81 \times 60 \times 13.51/1000$ kg/hr
= 0.66 kg/hr

$$\begin{aligned} \text{Percentage Vapour Utilization} &= 6.2/13.51 \times 100 \\ &= 45.89\% \end{aligned}$$

(i) Brake Power (kW)

$$BP = \frac{2\pi N W g R}{60000} \text{ kW}$$

Where, g = Acceleration due to gravity, 9.81 m/sec^2

R = Arm length of dynamometer in meters = 0.175 m

$$\begin{aligned} BP &= 2\pi \times 1500 \times 8.8 \times 9.81 \times 0.185 / 60000 \\ &= 2.51 \text{ kW} \end{aligned}$$

(ii) Brake specific fuel consumption (kg/kWhr):

$$BSFC = \frac{\text{Fuel Consumption}}{\text{Brake Power}} \text{ kg/kWhr}$$

$$BSFC = \frac{m_f}{BP}$$

Where, m_f = Mass flow rate of fuel in kg/hr

BP = Brake power in kW

$$\begin{aligned} BSFC &= 0.66 / 2.51 \\ &= 0.26 \text{ kg/kWhr} \end{aligned}$$

(iii) Brake Thermal Efficiency (BTE):

$$BTE = \frac{\text{Brake Power} \times 3600 \times 100}{C.V \times \text{Fuel Consumption}} \%$$

$C.V$ = 43610 KJ/kg

$$BTE(\%) = \frac{BP \times 3600 \times 100}{CV \times m_f}$$

$$BTE = \frac{2,51 \times 3600 \times 100}{43610 \times 0.66}$$

$$= 31.52\%$$

[This Page is kept intentionally blank]

CHAPTER 5

RESULTS AND DISCUSSION

5.1 EFFECT OF INJECTION PRESSURE AND INJECTION TIMING ON THE PERFORMANCE AND EMISSION CHARACTERISTICS

The experiments are conducted on a single cylinder direct injection diesel engine connected to an eddy current dynamometer. The shell and tube heat exchanger made according to the requirements is attached and a bypass is made so as to control the flow rate of exhaust gas to the heat exchanger. A dedicated fuel tank stores fuel for diesel vapour production and a burette measurement system controls the flow rate of diesel to the heat exchanger. At each load condition the readings were taken up to that point where engine starts knocking or when the power was decreasing considerably as indicated by a drop in rpm. Exhaust gas temperature readings were found to be varying and the results and discussions were done for the same.

This section of the report deals with the analysis of the performance and emission characteristics of the engine working in a dual fuel mode - vapour diesel induction and direct diesel injection. The steady state performance and emission tests were conducted at rated engine speed of 1500 rpm for three different injection timings i.e. 27.5 deg. bTDC, 29.5 deg. bTDC and 31.5 deg. bTDC and at 180 bar injection pressure. Later the set of experiments were repeated for two more injection pressures - 200 bar and 220 bar. The experimental results obtained for conventional direct injection diesel mode were taken as baseline data for comparison.

5.1.1 Performance Parameters

The combustion performance of the engine was assessed by calculating and comparing the brake thermal efficiency (BTE) and brake specific fuel consumption (BSFC). Exhaust gas temperature variation was also taken as one performance parameter. The variation of exhaust gas temperature with the increasing amount of diesel vapour induction was

plotted. The replacement efficiency of vapour diesel as compared to direct injected diesel is discussed under this section.

5.1.1.1 Effect of vapour induction on Brake Thermal Efficiency

Figures 5.1 to 5.9 indicate the variation in BTE for fuel injection pressures of 180 bar, 200 bar and 220 bar and three injection timings, i.e. 27.5 deg. bTDC, 29.5 deg. bTDC and 31.5 deg. bTDC. Comparisons are made for three constant load conditions –50%, 75% and 100% load. For lower loads the quality of the vapour produced by heat exchanger was very less. When vapour was inducted for 25% load the engine power was dropping considerably and eventually engine stalled. There was also loud noise as the low temperature vapour was being condensed while mixing with inlet air.

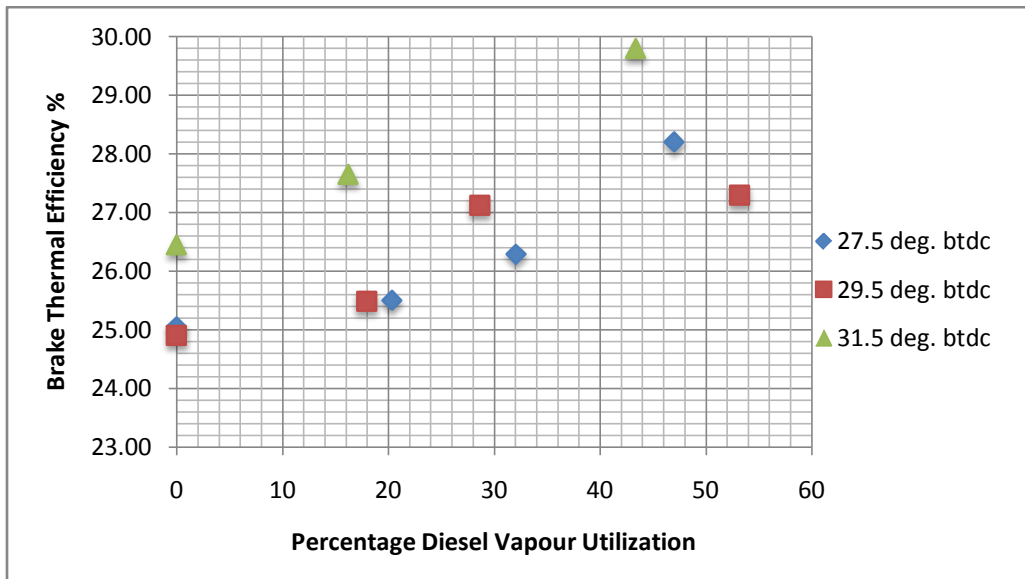


Fig. 5.1 Effect of diesel vapour induction on BTE for various injection timings at 50% load and 180 bar injection pressure

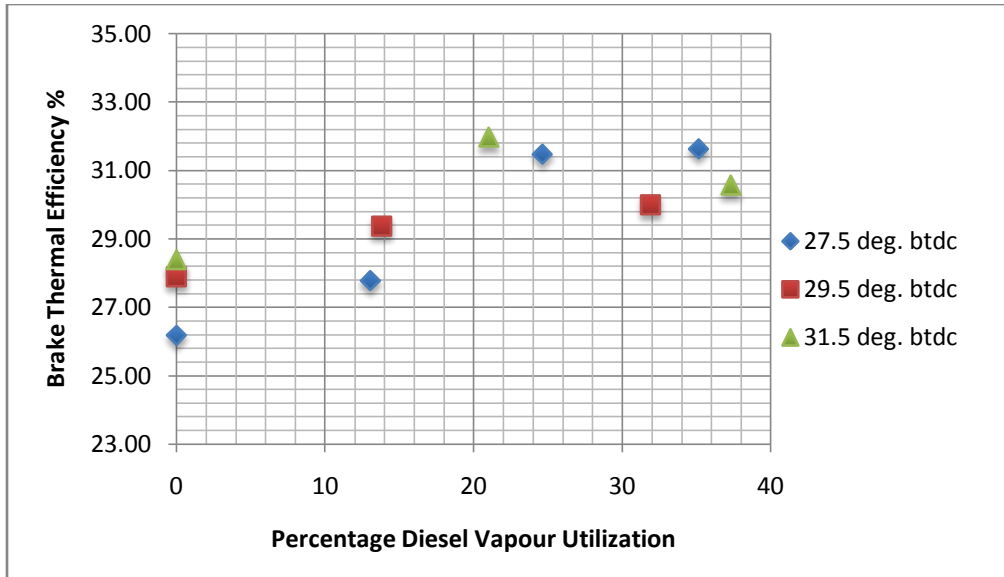


Fig. 5.2 Effect of diesel vapour induction on BTE for various injection timings at 75% load and 180 bar injection pressure

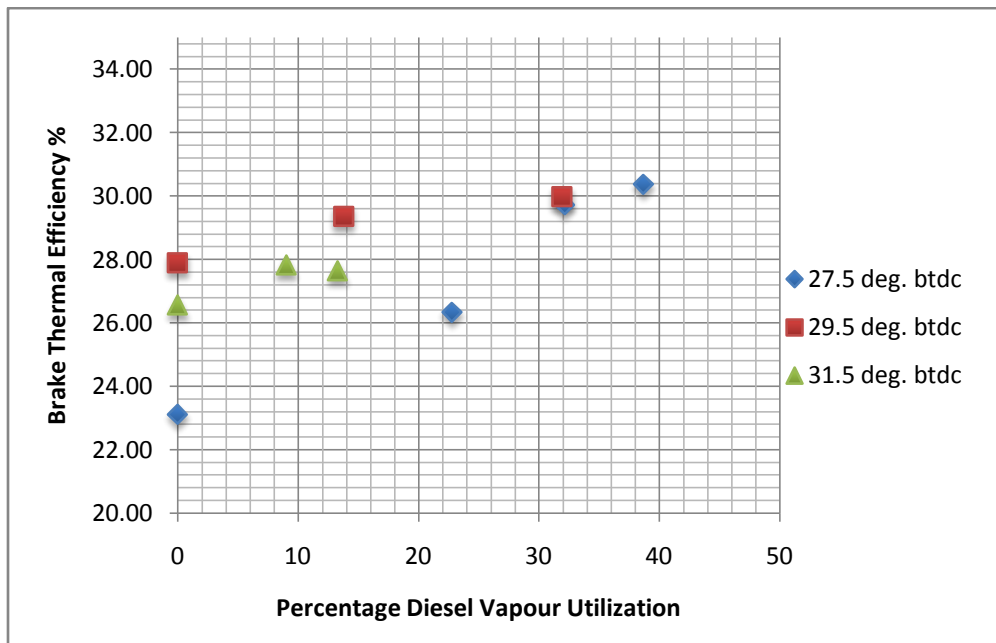


Fig. 5.3 Effect of diesel vapour induction on BTE for various injection timings at 100% load and 180 bar injection pressure

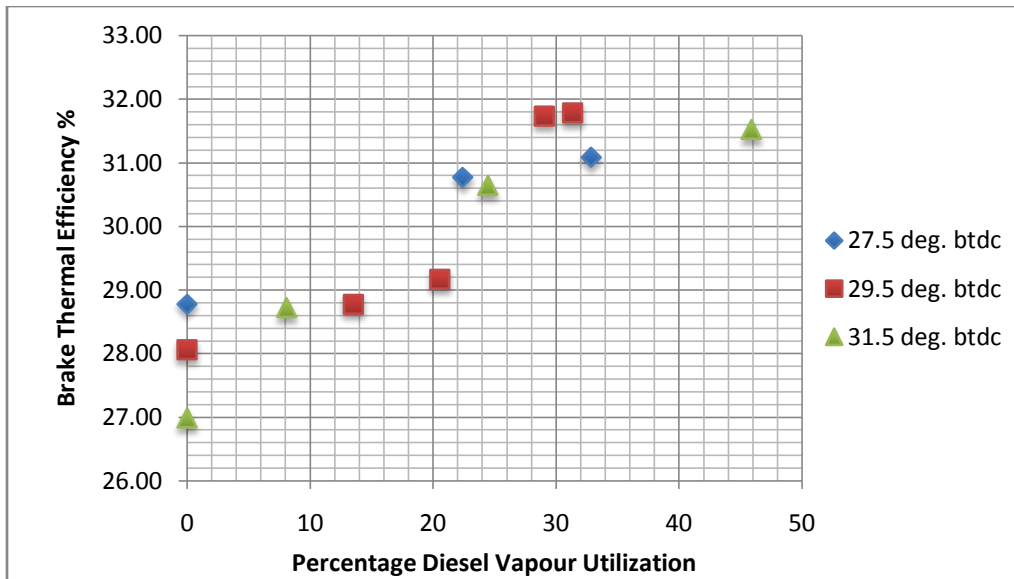


Fig. 5.4 Effect of diesel vapour induction on BTE for various injection timings at 50% load and 200 bar injection pressure

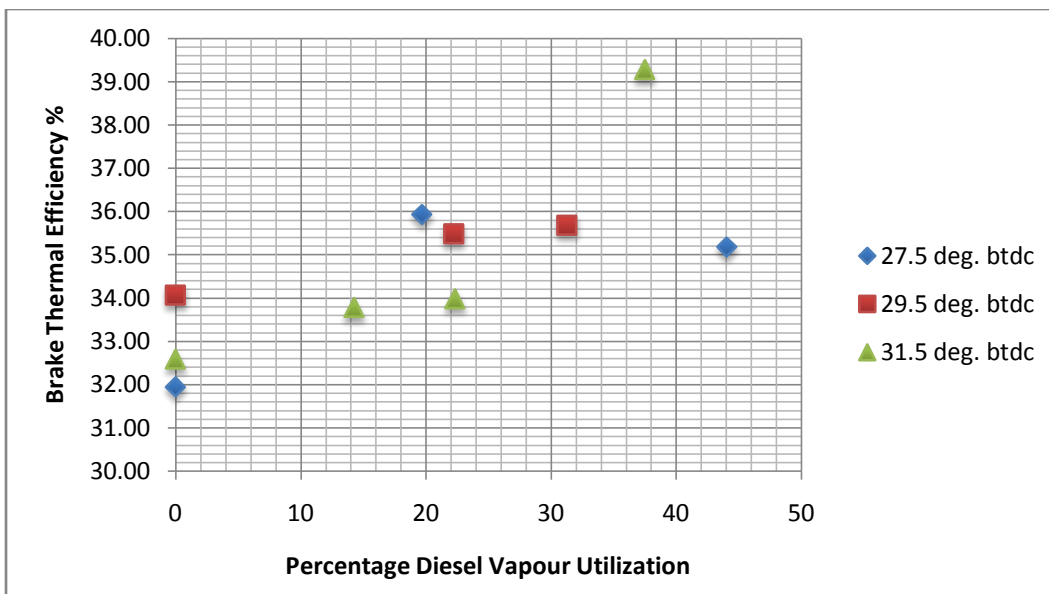


Fig. 5.5 Effect of diesel vapour induction on BTE for various injection timings at 75% load and 200 bar injection pressure

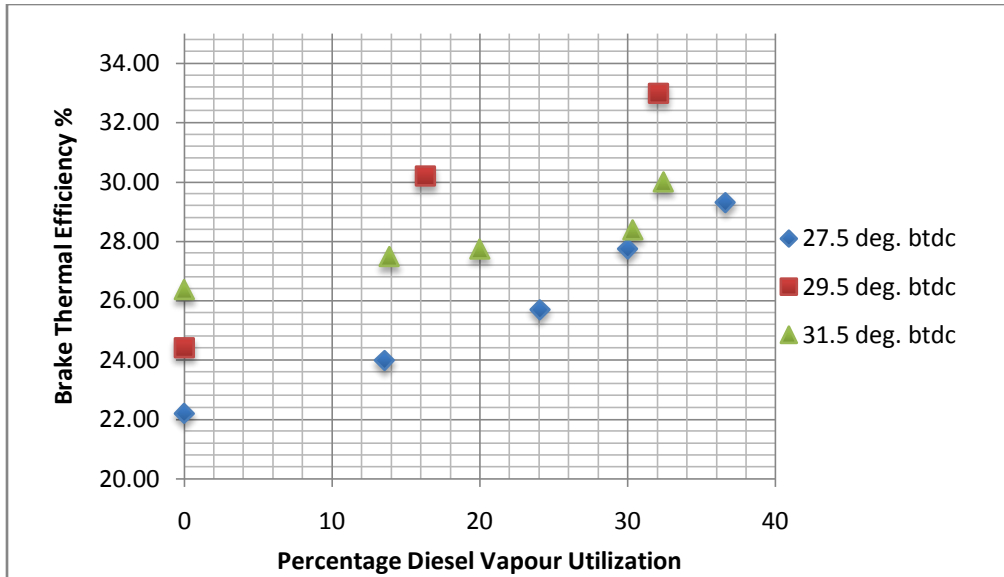


Fig. 5.6 Effect of diesel vapour induction on BTE for various injection timings at 100% load and 200 bar injection pressure

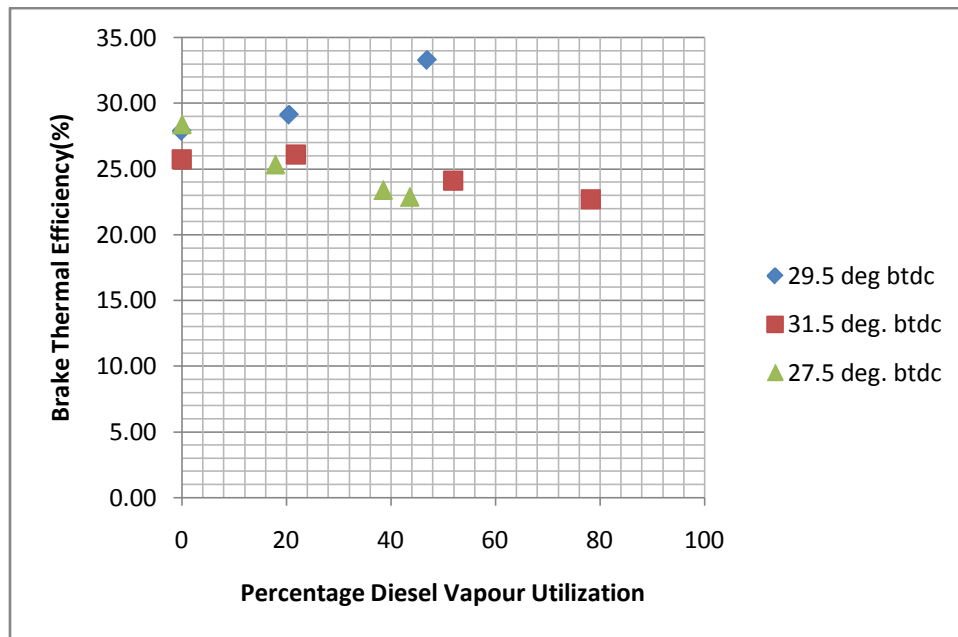


Fig. 5.7 Effect of diesel vapour induction on BTE for various injection timings at 50% load and 220 bar injection pressure

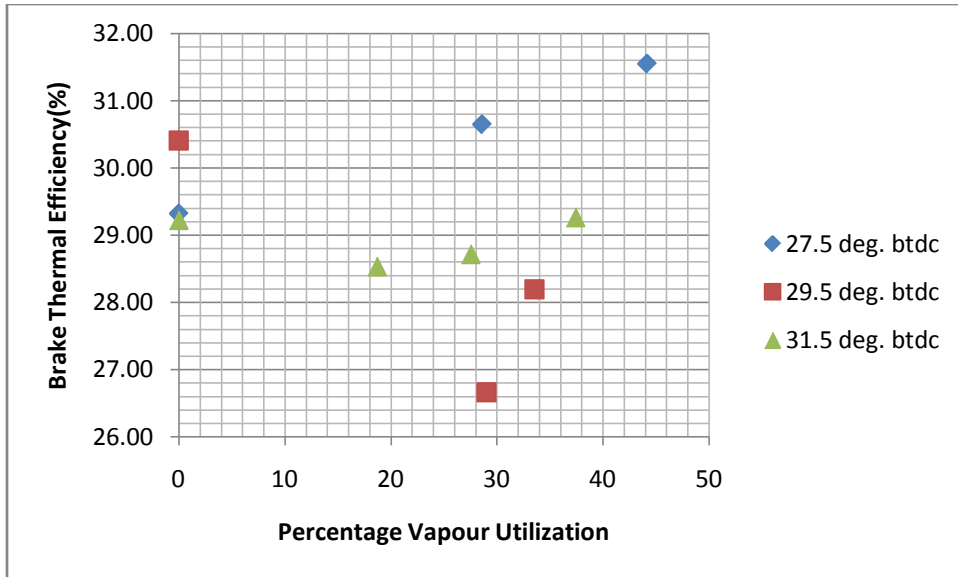


Fig. 5.8 Effect of diesel vapour induction on BTE for various injection timings at 75% load and 220 bar injection pressure

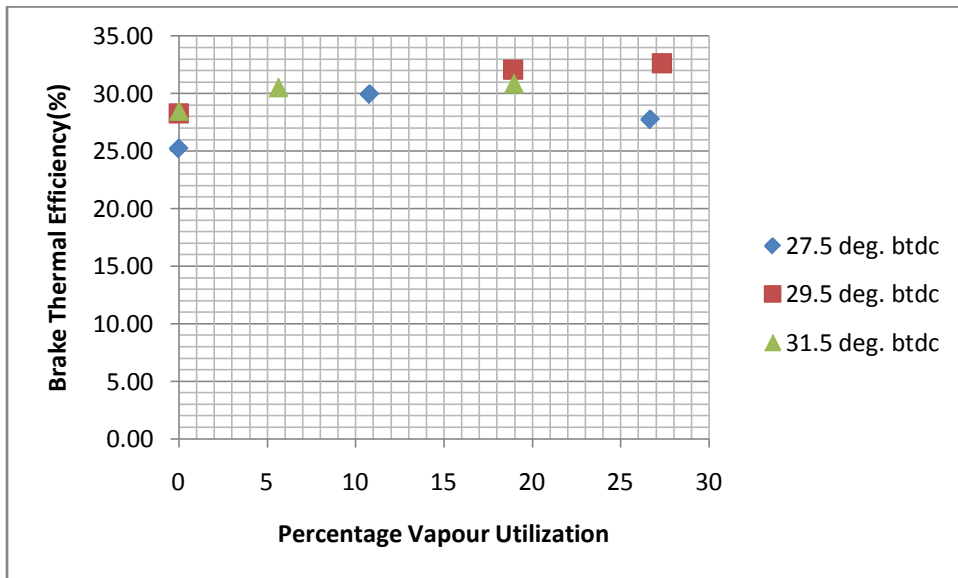


Fig. 5.9 Effect of diesel vapour induction on BTE for various injection timings at 100% load and 220 bar injection pressure

As shown in figures 5.1 to 5.9 the induction of vapour fuel improves the thermal efficiency of the engine. The value of brake thermal efficiency without vapor induction

indicates the normal DI mode of operation. As fuel is inducted as vapour the amount of fuel injected is decreased by the action of the governing system of the engine. All the tests are conducted at a constant speed of 1500 rpm. This may be the reason for improvement in Brake thermal efficiency.

But beyond a certain condition if more vapour is inducted it leads to decrease in BTE. The drop in efficiency is because, as the vapour mass fraction increases the start of combustion is no longer controlled by the injection of fuel and it is controlled by the auto ignition of the fuel. And this caused the heat release to retard. The decreased performance was associated with knocking and increase in emissions.

Table 5.1 Maximum brake thermal efficiency obtained by vapour induction at different operating conditions.

Pressure (bar)	Injection Timing (deg. bTDC)	Load (%)	Maximum Brake Thermal Efficiency (%)	% Vapour Utilisation (%)
180	27.5	50	28.21	47.02
		75	31.63	35.13
		100	30.38	38.69
	29.5	50	27.3	53.2
		75	29.99	31.92
		100	30.05	34.29
	31.5	50	28.9	43.38
		75	30.57	37.32
		100	27.66	13.28
200	27.5	50	31.09	32.85
		75	35.18	44.05
		100	29.31	36.62

	29.5	50	31.78	31.34
		75	35.69	31.28
		100	32.98	32.09
	31.5	50	31.52	45.89
		75	39.29	37.52
		100	30	32.43
220	27.5	50	23.41	38.48
		75	31.55	44.12
		100	27.77	26.77
	29.5	50	33.37	46.88
		75	28.19	33.51
		100	32.6	27.33
	31.5	50	24	51.93
		75	29.27	37.4
		100	30.88	18.93

From Table 5.1 it is very much clear that 180 bar and 200 bar injection pressures the performance was found to be improving, but as the engine started in taking vapour at 220 bar injection pressures there was loud knocking noise and the total amount of fuel intake was increasing considerably resulting in decrease of thermal efficiency. It can be assumed that for 180 bar and 200 bar a better combustion and homogeneity of charge inside the cylinder were responsible for improved thermal efficiency. For this the auto ignition events of both fuels - direct injected atomized diesel and premixed diesel vapour-air mixture should occur simultaneously. This will happen only if the final mixture is enough homogeneous. To obtain this it is better to advance the fuel injection timing so that the delay period increases and there will be more time for proper mixing. This led to the conduction of tests at 29.5 deg. bTDC and 31.5 deg. bTDC. And from the graphs it can be identified that the combustion is improving as the injection angle advances.

One other parameter that could increase the possibility of homogeneous vapour mixture is fuel injection pressure. As the fuel injection pressure increases the atomization increases and the quality of atomized fuel increases. This enhances the mixing as the droplet size of fuel is reducing as well as velocity of the fuel injected is increased. Therefore at an earlier injection angle and at a higher injection pressure an improved homogeneous mixture formation can be expected. By comparing the graphs it can be seen that at 200 bar injection pressure and at 31.5 deg. bTDC, the BTE curve was at its maximum and also the percentage increase in BTE (20.54% for 75% load) as compared to the conventional combustion was maximum. So with induction of vapour the engine shows a considerable shift in its rating from 27.5 deg. bTDC, 180 bar injection pressure to 31.5 deg. bTDC and 200 bar injection pressure.

Therefore the maximum increase in efficiency with vapour induction was at an injection pressure of 200 bar and injection timing of 31.5⁰ bTDC and the % increase in BTE at different load condition is given in Table 5.2.

Table 5.2 Maximum increase in Brake Thermal Efficiency

Percentage Load (%)	Percentage Vapour Utilization (%)	Percentage Increase in BTE (%)
50	45.89	16.80
75	37.52	20.54
100	32.43	13.76

The percentage vapour utilization shown in Table 5.2 corresponds to the maximum increase in BTE. The experiments thus showed a shift in the rating of the engine. This was because the engine was mechanically and thermally designed to run in CI mode and in the experiment HCCI mode of combustion was approached.

The figures 5.10, 5.11 and 5.12 show the variation of BTE at different injection timings - 27.5 deg. bTDC, 29.5 deg. bTDC and 31.5 bTDC for different injection pressures respectively. The values for BTE in HCCI mode corresponding to the maximum values obtained during the respective conditions, which is discussed in the previous pages.

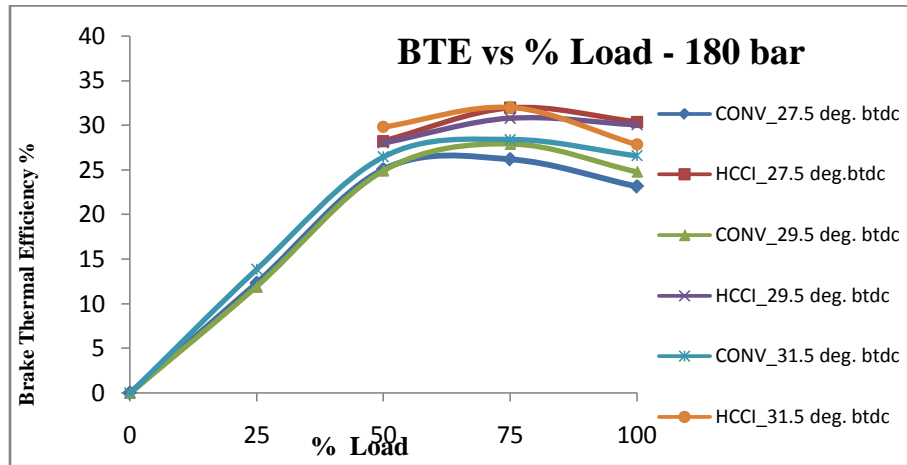


Fig. 5.10 Effect of vapour induction on BTE at different injection timings and 180 bar injection pressure

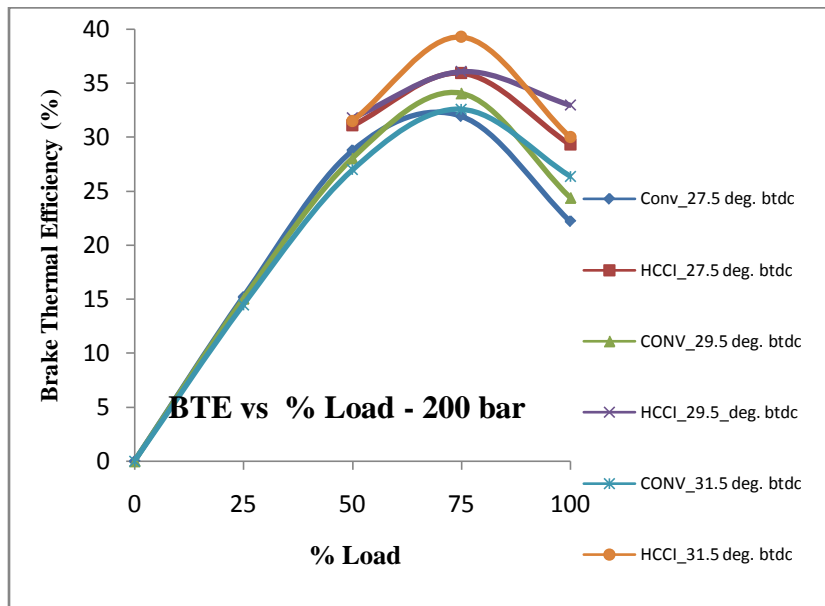


Fig. 5.11 Effect of vapour induction on BTE at different injection timings and 200 bar injection pressure

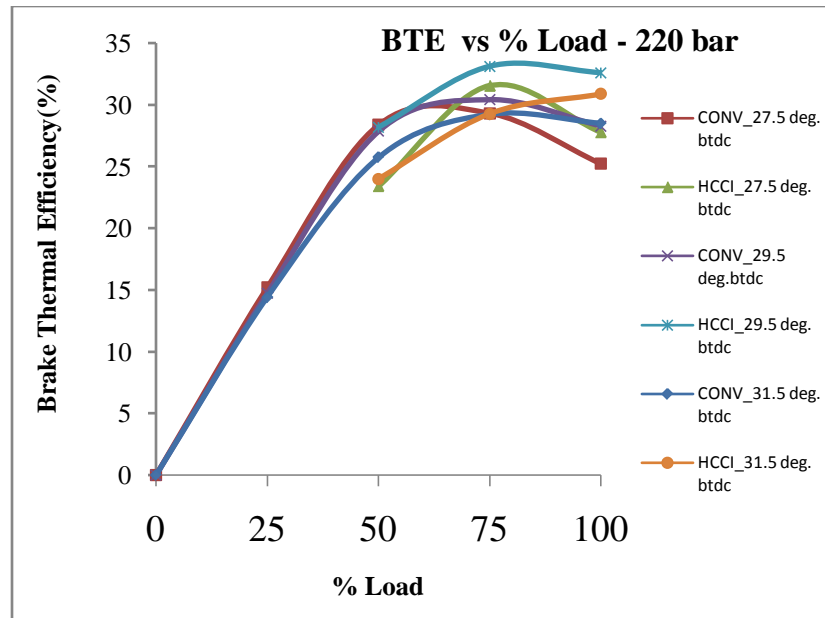


Fig. 5.12 Effect of vapour induction on BTE at different injection timings and 220 bar injection pressure

Figures 5.10 to 5.12 indicate the variation in BTE for different fuel injection pressures. For lower loads the quality of the vapour produced by heat exchanger was very less. When vapour was inducted for 25% load the engine power was dropping considerably and eventually engine stalled. There was also loud noise as the low temperature vapour was being condensed while mixing with inlet air.

5.1.1.2 Brake Specific Fuel Consumption

The figures 5.13, 5.14 and 5.15 show the variation of BSFC at different injection timings - 27.5 deg. bTDC, 29.5 deg. bTDC and 31.5 bTDC for different injection pressures respectively. The values for BSFC in HCCI mode are corresponding to the minimum values obtained during the respective conditions. It is found that the BSFC is reduced by inducting vapour at 180 bar and 200 bar injection pressures and for all injection timings.

Minimum value is corresponding to injection pressure of 180 bar and injection timing of 31.5 deg. bTDC.

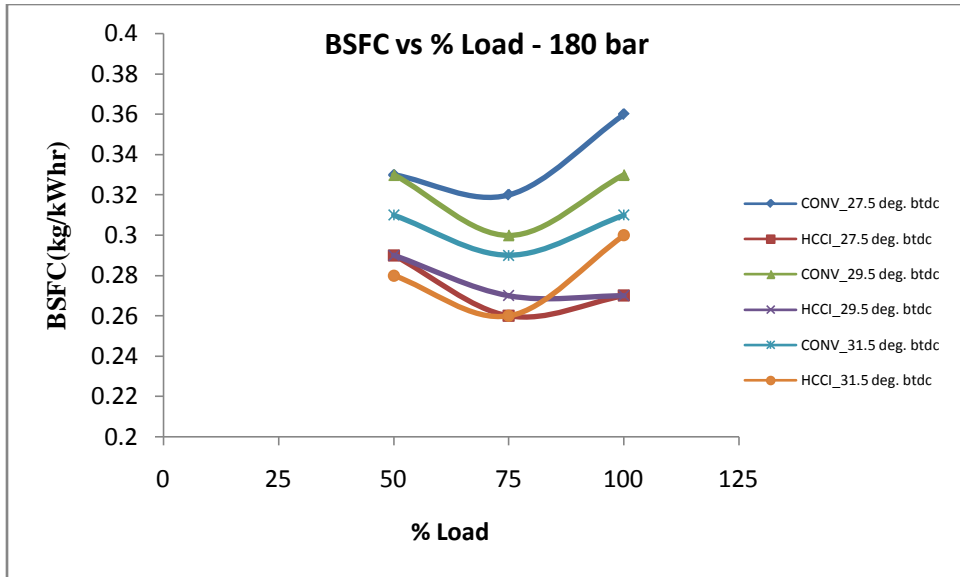


Fig. 5.13 Effect of vapour induction on BSFC at different injection timings and 180 bar injection pressure

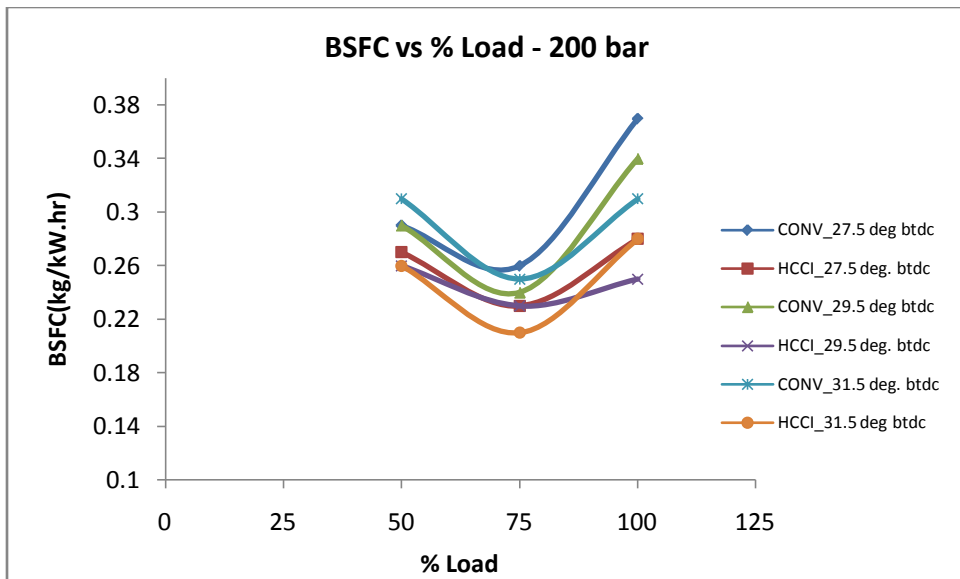


Fig. 5.14 Effect of vapour induction on BSFC at different injection timings and 200 bar injection pressure.

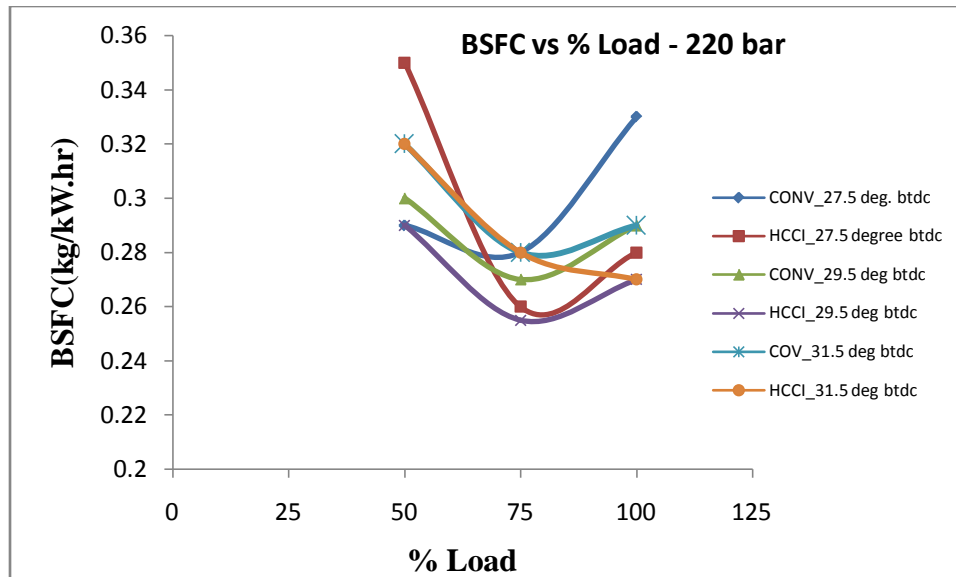


Fig. 5.15 Effect of vapour induction on BSFC at different injection timings and 220 bar injection pressure

But when the engine is operated at 220 bar, the fuel consumption is increased and the variation is irregular as given in Fig. 5.15. At this condition engine was running with loud noise and knocking tendency is detected.

The experimental results showed an improvement in BSFC with HCCI mode of operation. But there was always some value of BSFC beyond which an increase in vapour induction causes increase in BSFC. Vapour induction beyond that limit caused loss of power and rpm, the total fuel consumption also started creeping up.

The improvement in BSFC is because of lean combustion of the charge. The well mixed mixture due to vapour induction causes a lean combustion. The better distribution of pressure on to the piston means that major part of the energy generated is directed towards the piston this makes it possible to run the engine at lower fuel consumption than normal.

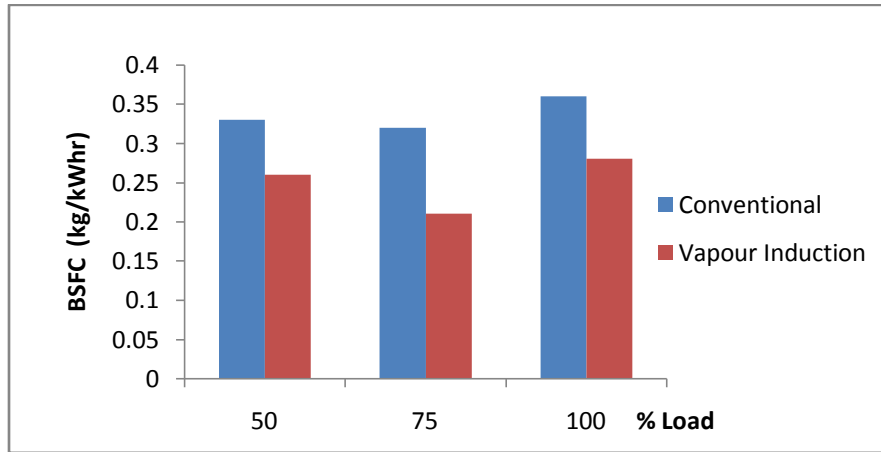


Fig. 5.16 BSFC with direct diesel injection at old rated condition (27.5 deg. bTDC and 180 bar) and vapour induction at new rated condition(31.5 deg. bTDC and 200 bar)

The comparison between the minimum BSFC attained to the BSFC of the existing CI engines at various loads is plotted in the Fig. 5.16. It was seen that the maximum decrease in BSFC was seen for the engine running at 31.5 deg. bTDC and 200 bar injection pressure.

5.1.1.3 Exhaust Gas Temperature

Exhaust gas temperature is one of the most important parameters in the HCCI mode of operation of the engine as it is a direct measure of the in-cylinder temperature at that point of time. The in cylinder temperature is responsible for most of the merits and demerits of the HCCI engine. For example the increase in thermal efficiency of the engine can also be attributed to the comparatively lesser amount of heat that is lost to the engine cooling water. It can also as will be seen later be held responsible for the decrease of NO_x .

The decrease in the temperature as the engine approaches HCCI mode of operation is because of the homogeneity of the charge in the engine cylinder. As the charge is homogenous and well distributed there would not be any fuel rich area.

The figures 5.17 and 5.18 show the variation of exhaust gas temperature at rated engine condition - 180 bar, 27.5 deg. bTDC and at optimized vapour induction mode 31.5 deg. bTDC and 200 bar injection pressure respectively.

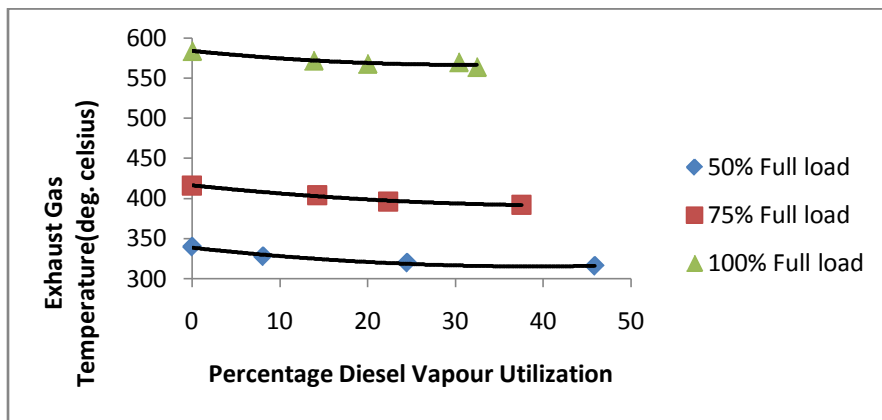


Fig. 5.17 Effect of vapour induction on exhaust gas temperature at different load conditions at 31.5 deg. bTDC and 200 bar injection pressure

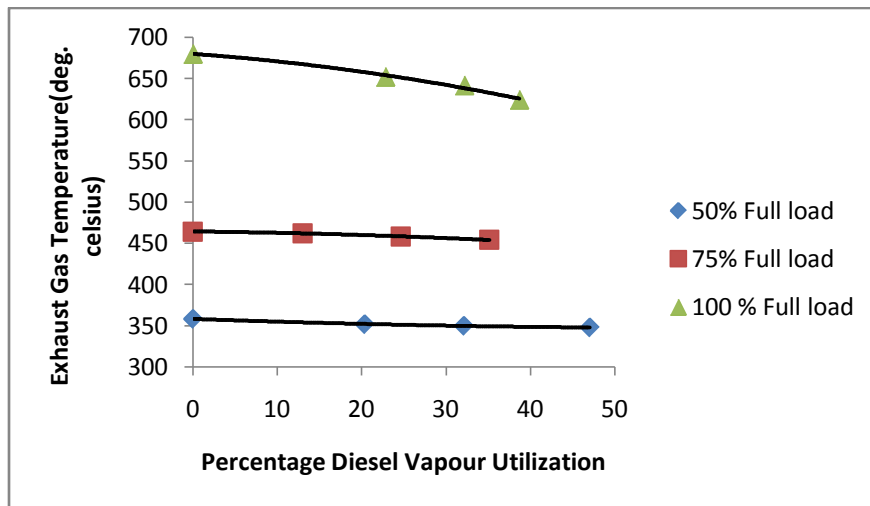


Fig. 5.18 Effect of vapour induction on exhaust gas temperature at different loads at 27.5 deg. bTDC and 180 bar injection pressure

From the graphs it can be analyzed that the exhaust gas temperature went on decreasing as the engine inducted more and more vapour. This may reduce the NO_x emissions, which will be discussed later in this chapter.

The comparison between the minimum temperatures of exhaust gas attained in optimized vapour induction mode to the temperature of exhaust gas in the existing CI engines at 50%, 75% and 100% load conditions are plotted in the Fig. 5.19. The maximum decrease in temperature is at 31.5 deg. bTDC and 200 bar injection pressure.

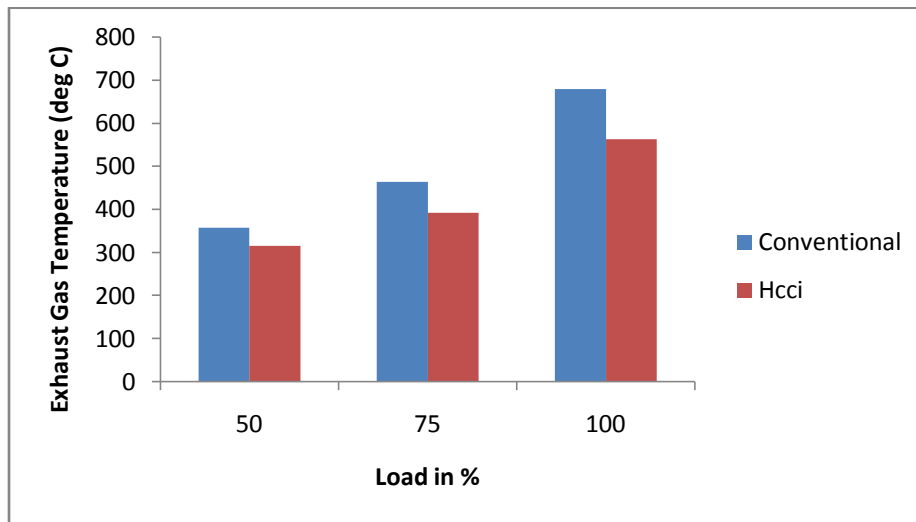


Fig. 5.19 Exhaust Gas Temperatures with new (HCCI mode at 31.5 deg. bTDC and 200 bar) and old (Conventional diesel injection at 27.5 deg. bTDC and 180 bar) rating conditions.

5.1.2 Emission Parameters

Automobile emissions are dealt with stringent rules nowadays. The newer emission norms demand very less amount of emissions. There are several researches being carried on to develop technologies that would reduce harmful emissions or at least minimize the need of costlier after-treatment devices. Here the trend of all the emission parameters at injection pressures of 180 bar, 200 bar and 220 bar and injection timings of 27.5 deg.

bTDC, 29.5 deg. bTDC and 31.5 deg. bTDC for diesel vapour induction are being discussed.

5.1.2.1 Unburned Hydrocarbons

Unburned hydrocarbons are result of incomplete combustion (which can be caused due to lack of air). As the CI engines work in lean mixture they emit comparatively low amount of UBHC (less than 100 ppm) when compared to SI engines. As HCCI engines run of leaner charge it is expected that the HC emissions will reduce. But this is not the case. A slight increase in HC emissions were observed though the increase was only marginal.

As the HCCI mode of operation results in lean combustion, there may be a decrease in in-cylinder temperature, which was evident from the decrease in exhaust gas temperature. This is one of the reasons for the increase in HC emissions. Another reason can be as the homogenous charge is compressed there is a chance that the fuel gets into the crevices and minute cracks in the engine cylinder (Gregory and Chen 2011). These fuel molecules will be kept away from air required for their proper combustion. The variation in HC emissions as the engine approaches HCCI mode of operation is shown in figures 5.20, 5.21 and 5.22. It is found that increasing the injection pressure and advancing the injection timing reduces HC emissions. This is due to the fact that a high pressure and more time for mixture formation always owe better combustion.

From the figures 5.20 to 5.22 it can be seen that there is an increase in UBHC upon vapour induction. However it is not increasing much while working at higher loads. At 50% load, upon vapour induction the percentage increase in UBHC emission is much higher compared to that of conventional diesel engine. At lower loads the quality of the vapour produced by the heat exchanger was less because of lower exhaust gas temperature. Consequently a part of the vapour inducted through a port in intake manifold while mixing with cold air condenses and gets collected in the crevices or minute cracks in the engine. This may comes out as UBHC emissions.

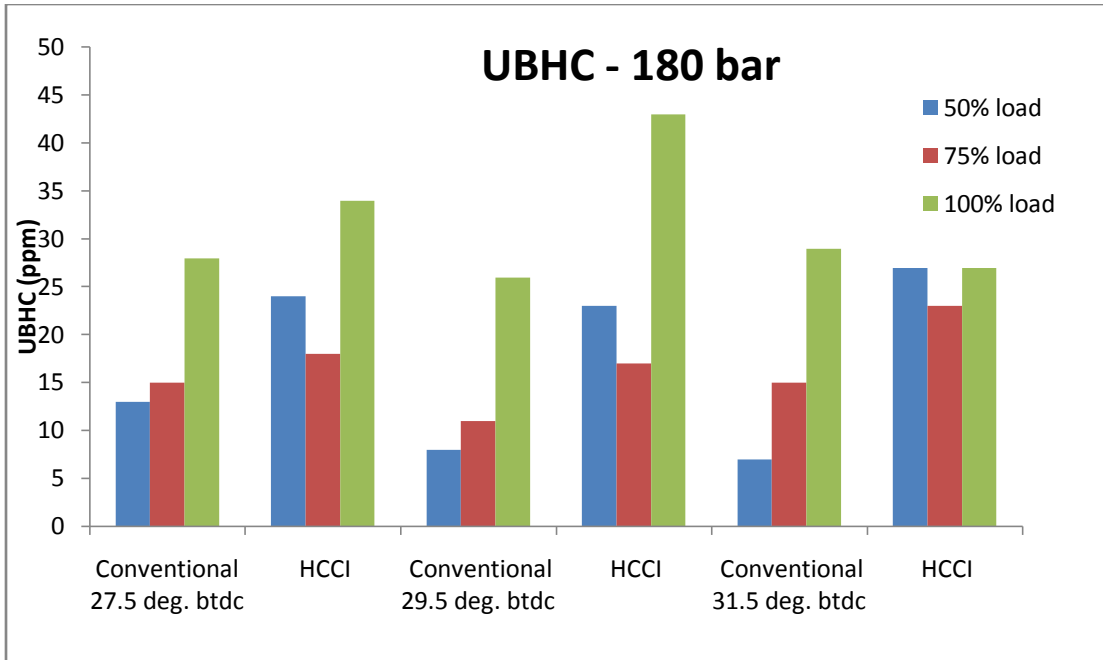


Fig. 5.20 UBHC emissions for conventional and vapour induction mode at different injection timings at 180 bar

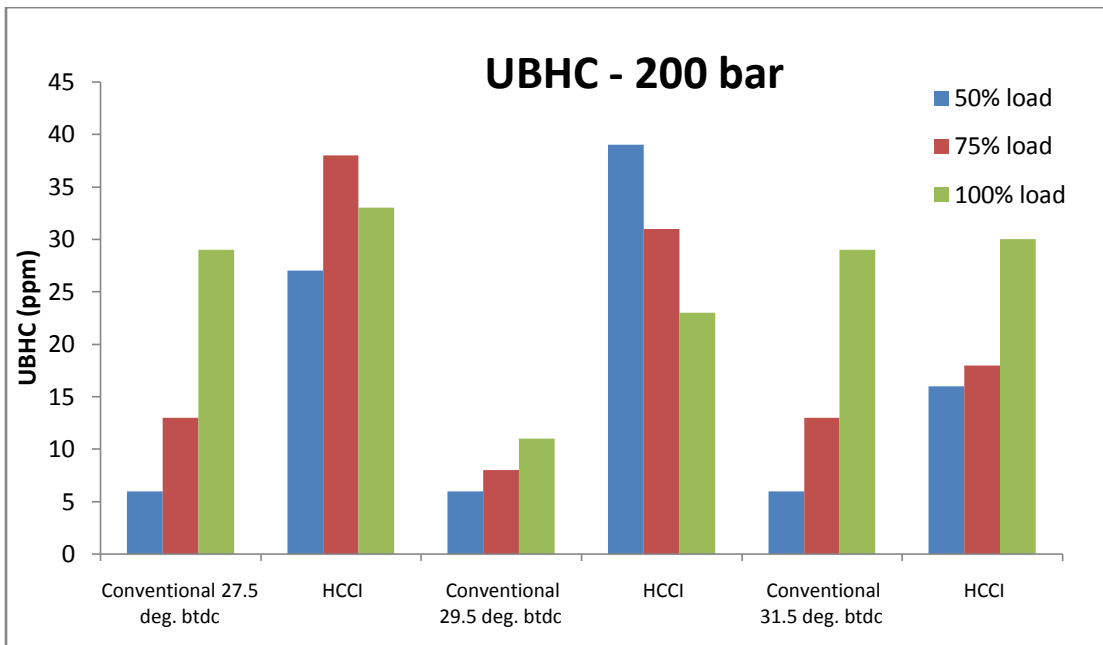


Fig. 5.21 UBHC emissions for conventional and vapour induction mode at different injection timings at 200 bar

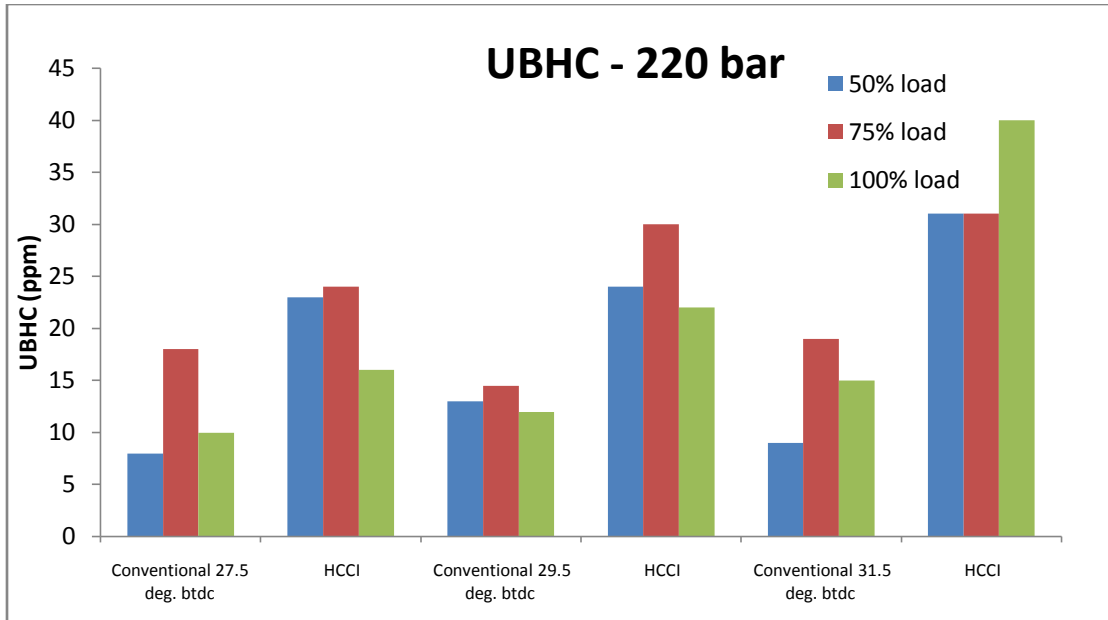


Fig. 5.22 UBHC emissions for conventional and vapour induction mode at different injection timings at 220 bar

Beyond the limit of optimum vapour utilization, intermittent or severe knocking results and the engine emissions vary unpredictably. On an average HC emissions increased by around 53% with vapour induction, however at higher loads HC increased only by 31%. From the study of performance parameters it was found that the better vapour induction working conditions are at 31.5 deg. bTDC, 200 bar injection. An increase in UBHC emissions can be attributed to the combustion of unburned premixed fuel that had entered the crevices or minute cracks within the cylinder.

Fig. 5.23 gives a comparison between the UBHC emissions at optimized vapour induction mode and conventional diesel injection mode. As explained earlier the conventional mode is with 180 bar injection pressure and injection timing of 27.5 deg. bTDC and the vapour induction gives a better performance at 200 bar injection pressure and 31.5 deg. bTDC injection pressure.

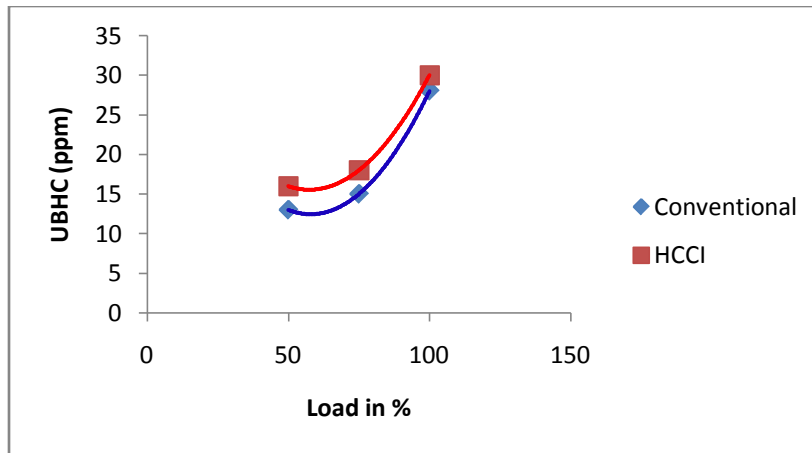


Fig. 5.23 UBHC emissions at optimized vapour induction mode (200 bar injection pressure and 31.5 deg. bTDC) and conventional diesel injection mode (180 bar injection pressure and 27.5 deg. bTDC) at different loads

5.1.2.2 Carbon Dioxide

Carbon dioxide is generally a non-polluting component of the CI engine emissions. Its presence in the exhaust is taken as a measure of the completeness of combustion as ideally, combustion of hydrocarbons should produce only carbon dioxide and water (Sunmeet and Subramanian 2017). It was seen that the carbon dioxide content in the exhaust decreased marginally indicating signs of incomplete combustion.

As the engine approached HCCI mode of operation there was a decrease exhaust gas temperature as shown in figures 5.17 and 5.18. This is one of the reasons for the decrease in carbon dioxide emissions. Another reason can be as the homogenous charge is compressed there is a chance that the fuel gets into the crevices and minute cracks in the engine cylinder. These fuel molecules will be kept away from air required for their proper combustion.

The variation in carbon dioxide emissions as the engine approaches HCCI mode of combustion are shown in figures 5.24, 5.25 and 5.26.

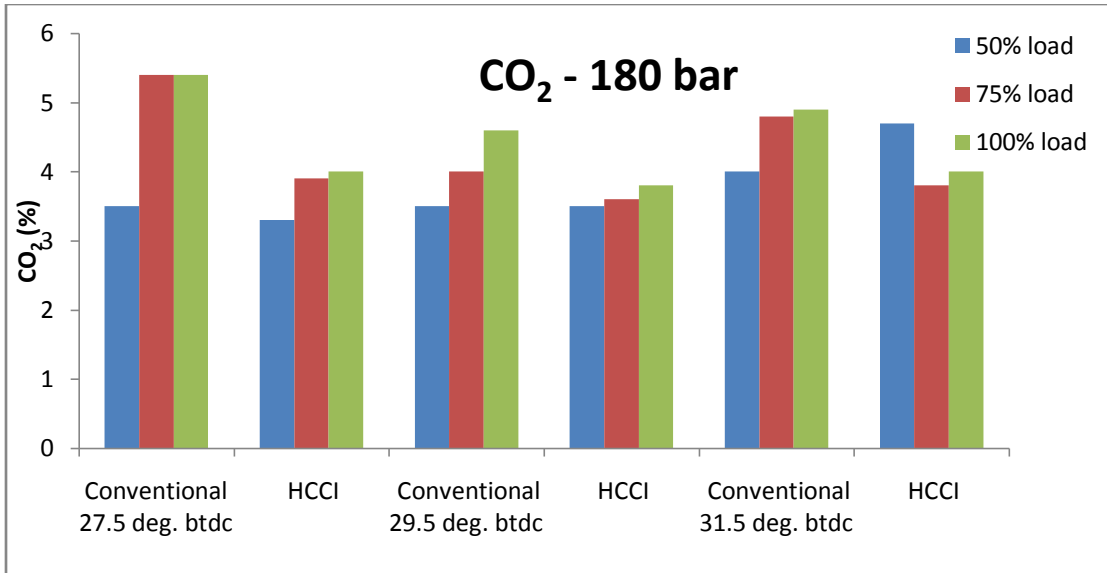


Fig. 5.24 CO₂ emissions for conventional and vapour induction mode at different injection timings at 180 bar

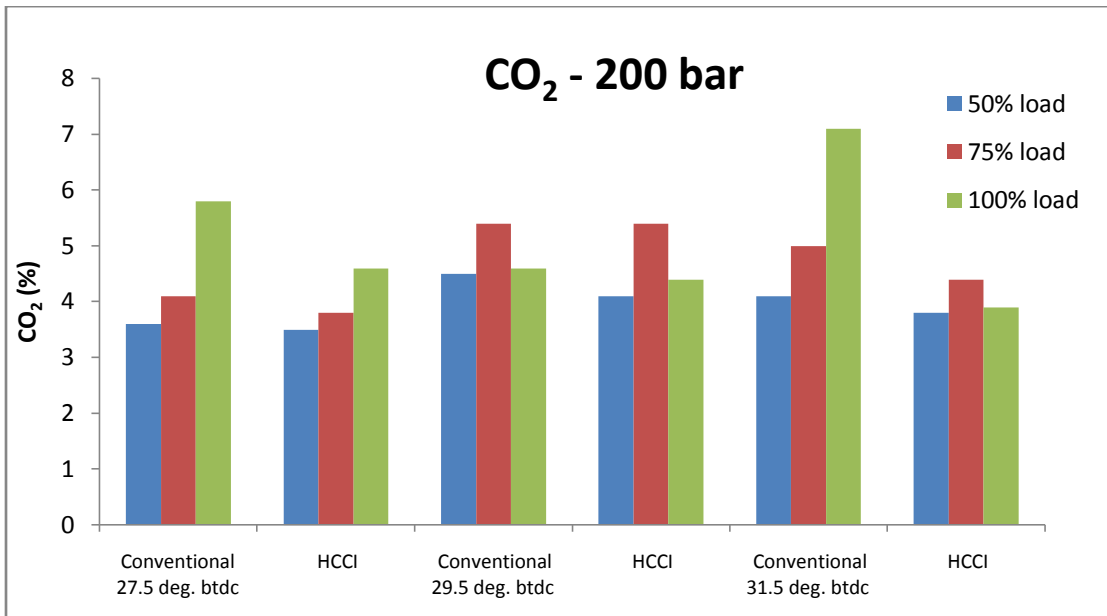


Fig. 5.25 CO₂ emissions for conventional and vapour induction mode at different injection timings at 200 bar

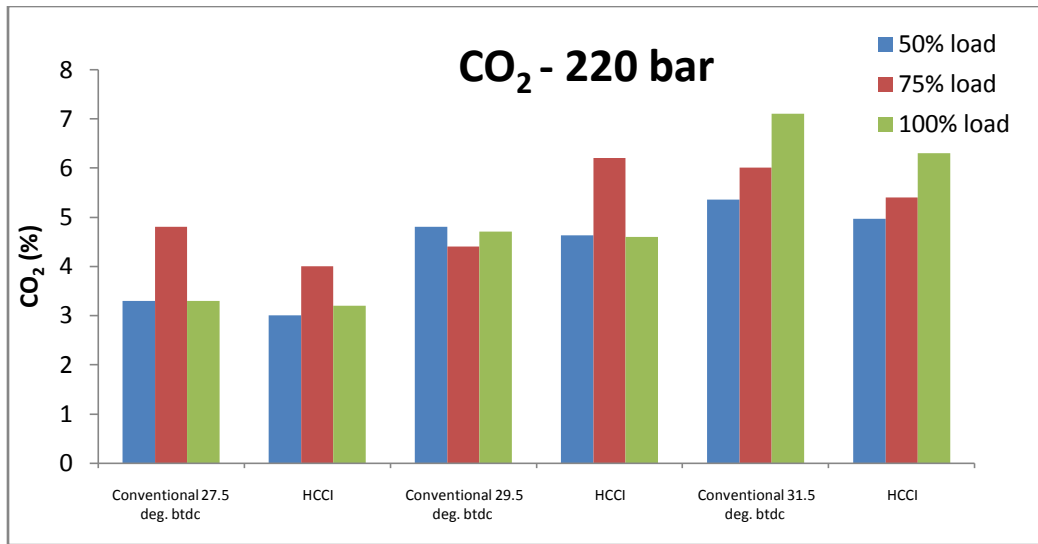


Fig. 5.26 CO₂ emissions for conventional and vapour induction mode at different injection timings at 220 bar

Fig. 5.27 gives a comparison between the UBHC emissions at optimized vapour induction mode and conventional diesel injection mode. As explained earlier the conventional mode is with 180 bar injection pressure and injection timing of 27.5 deg. bTDC and the vapour induction gives a better performance at 200 bar injection pressure and 31.5bTDC injection pressure.

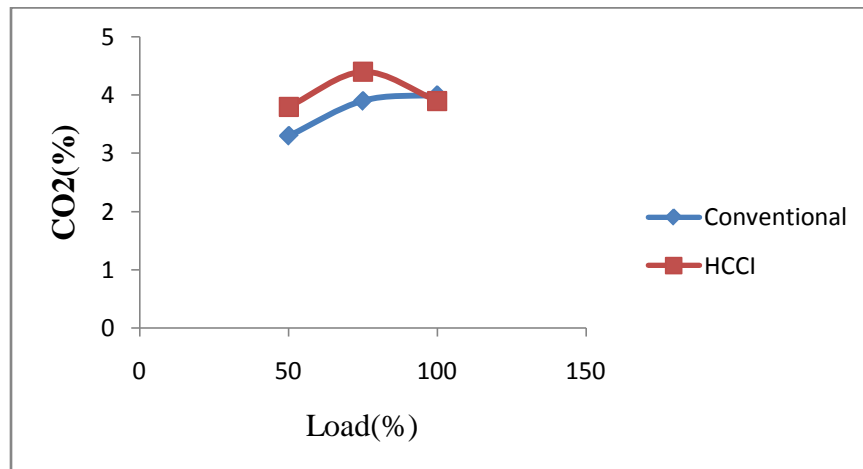


Fig. 5.27 CO₂ emissions at optimized vapour induction mode (200 bar injection pressure and 31.5° bTDC) and conventional diesel injection mode (180 bar injection pressure and 27.5° bTDC) at different loads

5.1.2.3 Carbon monoxide

Carbon monoxide is the toxic byproduct of all hydrocarbon combustion. This is the result of incomplete combustion as enough oxygen would not be present for the carbon monoxide to be converted into carbon dioxide which is harmless.

It was seen that the carbon monoxide emissions increased as the engine approached HCCI mode of combustion. As the engine approached HCCI mode of operation there was a decrease in in-cylinder temperature. This is one of the reasons for the decrease in carbon dioxide emissions and subsequent increase in carbon monoxide emission. Another reason can be as the homogenous charge is compressed there is a chance that the fuel gets into the crevices and minute cracks in the engine cylinder. These fuel molecules will be kept away from air required for their proper combustion. The variation in carbon monoxide emissions as the engine approached HCCI mode of combustion at 200 bar injection pressure are shown in figures 5.28, 5.29 and 5.30. Since 200 bar is the optimized injection pressure for vapour induction, the graphs are plotted at this pressure varying injection timing showing how CO emissions vary as engine approached HCCI mode of combustion. The trend showed % CO increases first but with more vapour induction it was becoming steady. This is because homogeneity of the mixture prevents fuel rich areas thereby reducing CO emissions.

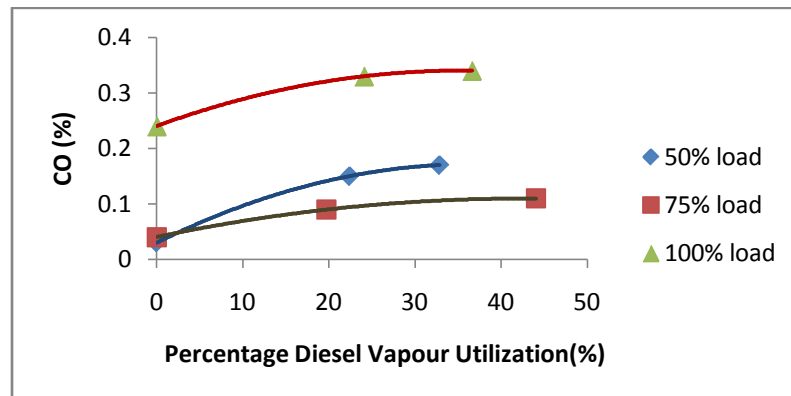


Fig. 5.28 Effect of vapour induction on CO Emissions at 27.5 deg. bTDC and 200 bar injection pressure

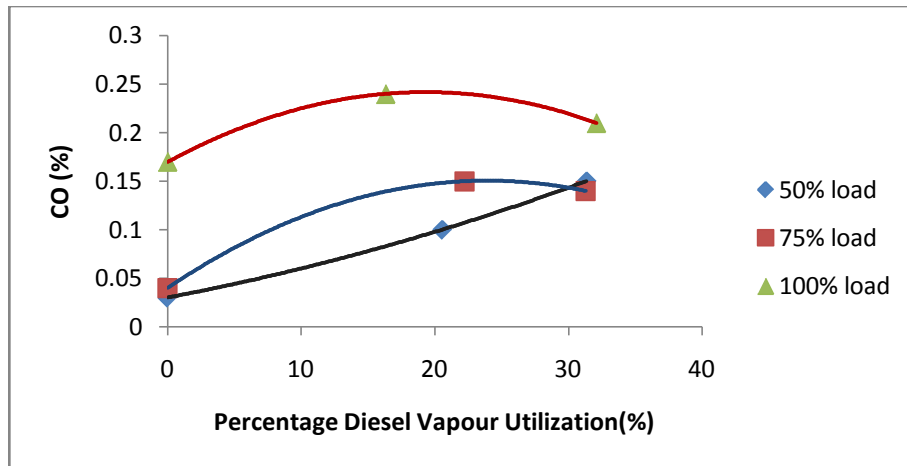


Fig. 5.29 Effect of vapour induction on CO Emissions at 29.5 deg. bTDC and 200 bar injection pressure

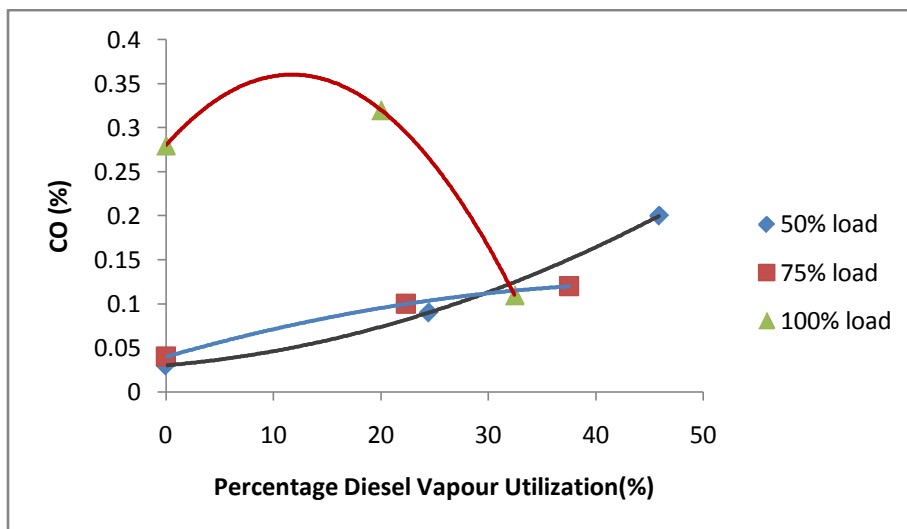


Fig. 5.30 Effect of vapour induction on CO Emissions at 31.5 deg. bTDC and 200 bar injection pressure

Following bar charts (figures 5.31, 5.32 and 5.33) show the comparison of CO emissions from conventional diesel engine and vapour induction mode of the engine. It can be seen that at all the three injection pressures the percentage of CO emissions increased in the vapour induction mode. The rated conditions of the engine ie 180 bar injection pressure and 31.5 deg. bTDC injection timing produced lowest CO emissions.

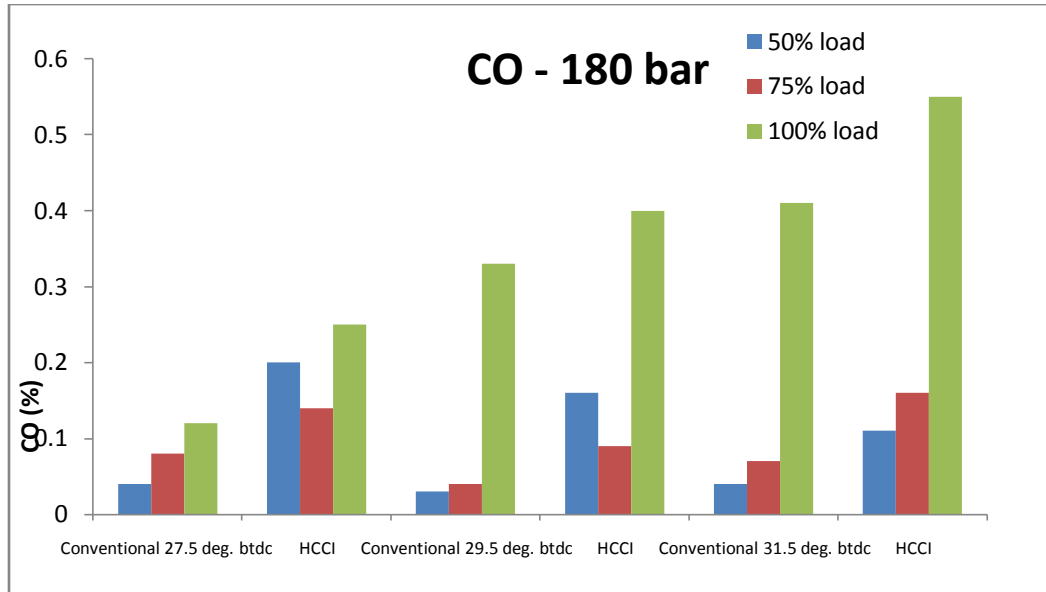


Fig. 5.31 CO emissions for conventional and vapour induction mode at different injection timings at 180 bar

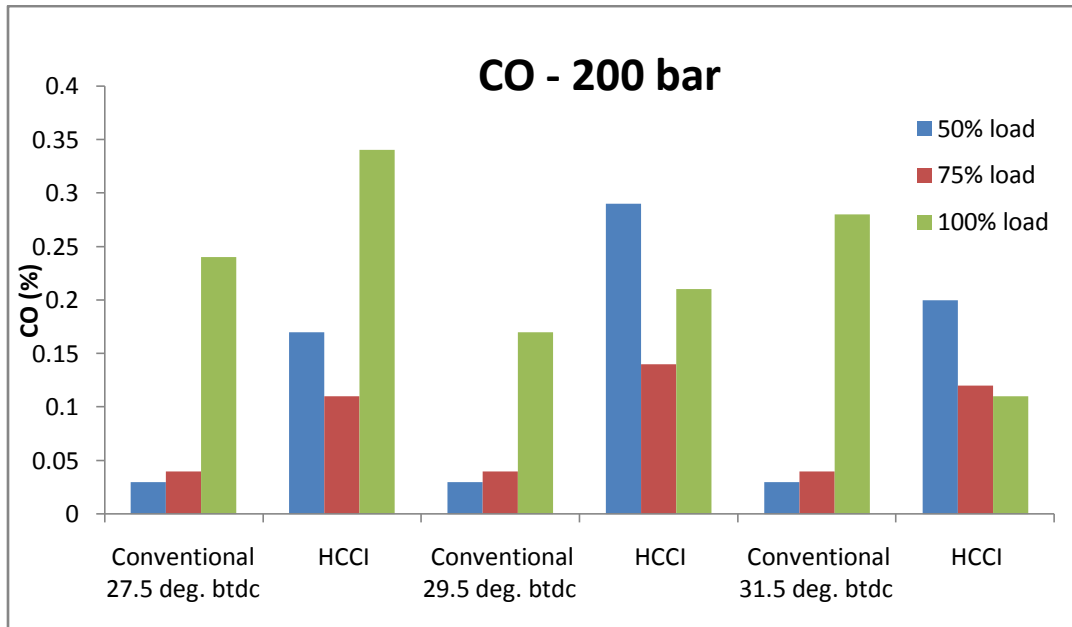


Fig. 5.32 CO emissions for conventional and vapour induction mode at different injection timings at 200 bar

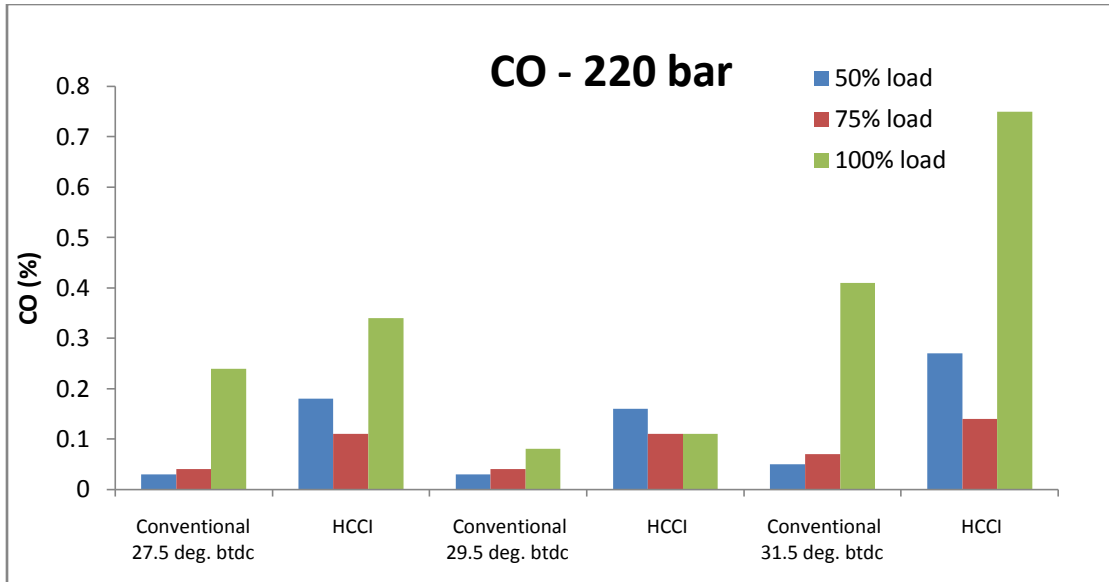


Fig. 5.33 CO emissions for conventional and vapour induction mode at different injection timings at 220 bar

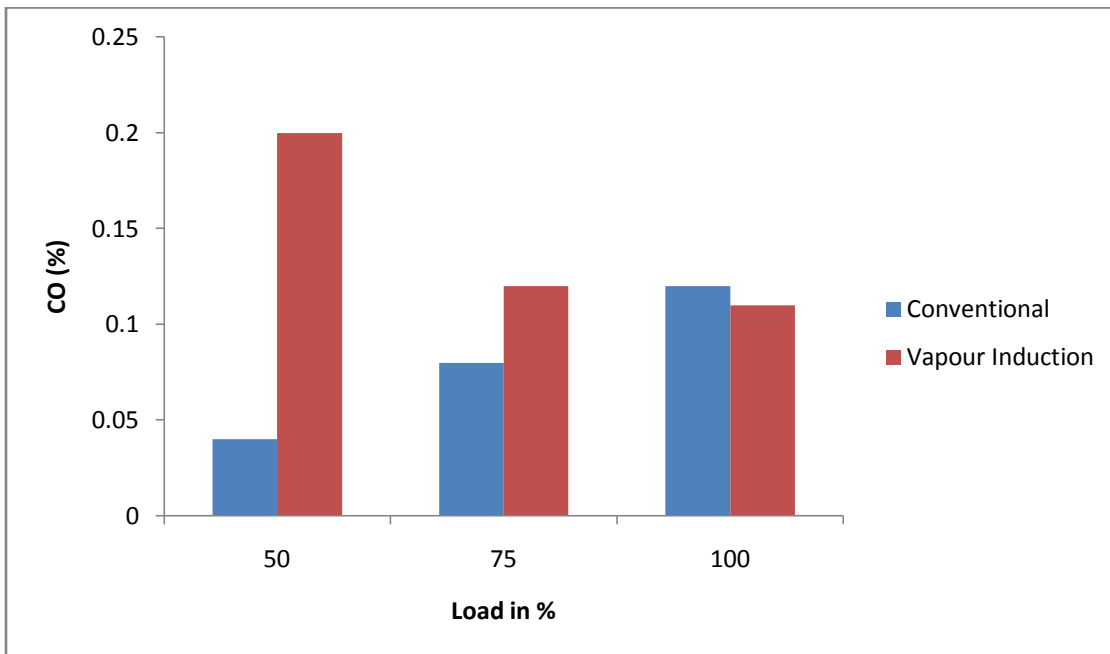


Fig. 5.34 CO emissions of Conventional diesel combustion (27.5 deg. bTDC and 180 bar) and optimized vapour induction at 31.5 deg. bTDC and 200 bar injection pressure at different loads

There was no specific trend for CO curve. It depended much on the particular condition for combustion. In Vapour induction mode, for medium load 50%, the amount of CO was higher compared to that in the conventional case. However the vapour induction at 75% usually showed a decrease in CO as compared with 50% load. In conventional mode, CO was gradually increasing with increase in load. Vapour induction at 100% load showed an increase in CO in most of the cases but not higher than that in 50% load condition. Fig. 5.34 gives the variation CO emissions at conventional diesel combustion at 27.5 deg. bTDC and 180 bar injection pressure are compared with most efficient vapour induction - 31.5 deg. bTDC and 200 bar injection pressure. In this case the trend of CO for vapour induction was to decrease with load. This can attributed to the increase in homogeneity of charge as well as increased quality of diesel vapour. One more finding related to this is that at 100% load at new rated conditions the decrease in CO was not associated with increase in CO₂. The exhaust oxygen increased instead. The average increase in CO emissions considering all the three injection pressures and injection timings is around 31.25%.

5.1.2.4. Nitrogen Oxides

Nitrogen oxides are among the major pollutants in engine exhaust. They have far reaching effects and remain in the atmosphere for a long time. One of the major reasons for developing HCCI mode of combustion is reduction of nitrogen oxide emissions. There are different mechanisms that explain the formation of NO_x in engines. One of the major parameter that controls formation of NO_x is in-cylinder temperature. NO_x formation starts as the in cylinder temperature reaches near 1800 K and it increases much with increase in temperature. HCCI mode of combustion helps in reducing the peak temperature inside the cylinder and thereby reduces thermal NO_x considerably.

One another factor that controls NO_x formation is residence time. As HCCI employs an explosion by production of many autoignition spots, the residence time will be less and hence lesser NO_x production.

Figures 5.35 to 5.43 give the variation of NO_x emissions for all injection pressures and injection timings. This is analysed in detail because variation of NO_x with vapour induction is one of the most important outcome of this experimental study. It is seen that the NO_x emissions started to decrease as more and more vapour was inducted. However after some point of induction a further increase in vapour induction caused a decrease in engine performance. At 50% load, vapour induction can be improved upto utilizing more than 90% vapour. But beyond a limit, increase in vapour induction caused a decrease in rpm of the engine. The engine started working at lower speeds developing lesser power. But the NO_x emissions started rising. Eventually the engine stalled when it was nearing 100% vapour induction.

At 75% load, the maximum amount of vapour utilization decreased. However at the lower utilization conditions the engine performance was increasing considerably (at around 40% vapour utilization). NO_x emissions also showed a steeper decrease with increase in vapour induction. When vapour induction crossed the limit where thermal efficiency started decreasing, engine started knocking. With further increase in vapour induction, the knocking became more audible and was intermittent, speed also started fluctuating. The NO_x emissions became unpredictable - sometimes increasing and sometimes decreasing. This can be related to the exhaust gas temperature. When the vapour induction increased combustion mixture became more homogeneous and the exhaust temperature started decreasing (Junnian and Jerald 2012). But the temperature became sometimes low that the quality of vapour produced was affected. This vapour might have condensed and filled the minute cracks and crevices forming unburnt mixture. This continued and at some point it started igniting all of a sudden causing knocking. Knocking increased temperature which improved vapour quality and again combustion became normal. This can be the explanation of intermittent knock. Further with advance of ignition angle, this effect was found to be increasing, but rpm dropped and engine eventually stopped.

The experiments were then conducted by increasing fuel injection pressure. The increase in fuel injection pressure increased the exhaust gas temperature. And it was found that the degree of superheat was sometimes so high at 75 and 100% load that the inducted vapour auto ignites and heat release started before fuel injection. This can be understood from the sudden loss of power and quite unstable rpm. For controlling this bypass valve was opened that reduced the exhaust gas flow rate to the heat exchanger thereby decreasing the diesel vapour temperature. The temperature was adjusted for optimum working conditions. It showed that at higher injection pressure - 200 bar as injection angle advances combustion becomes more and more stable and the knocking also reduced. The amount of vapour utilization increased to maximum of 54.48% at 31.5 deg. bTDC, 200 bar for 75% load.

At full load conditions vapour utilization decreased much more. The quality of vapour inducted also increased and the bypass valve was opened to control temperature of diesel vapour. NO_x emissions started decreasing with vapour induction, but beyond a particular percentage of vapour induction, there was heavy knocking and increase in NO_x emissions. At 220 bar injection pressure the vapour induction by even small amount decreased the engine performance and it started knocking. The optimum working conditions and low NO_x were obtained at 200 bar injection pressure. At this pressure as the injection angle advanced the delay period was increased slightly and this helped to control the start of combustion. The NO_x was found to be lowest at 31.5 deg. bTDC.

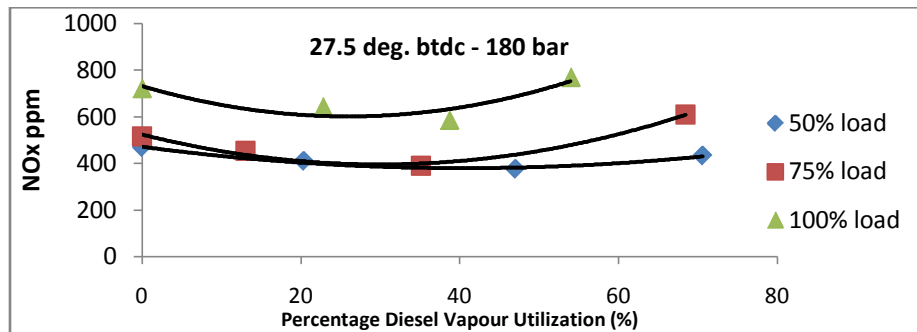


Fig. 5.35 NO_x variation with vapour induction at 27.5 deg. bTDC and 180 bar injection pressure.

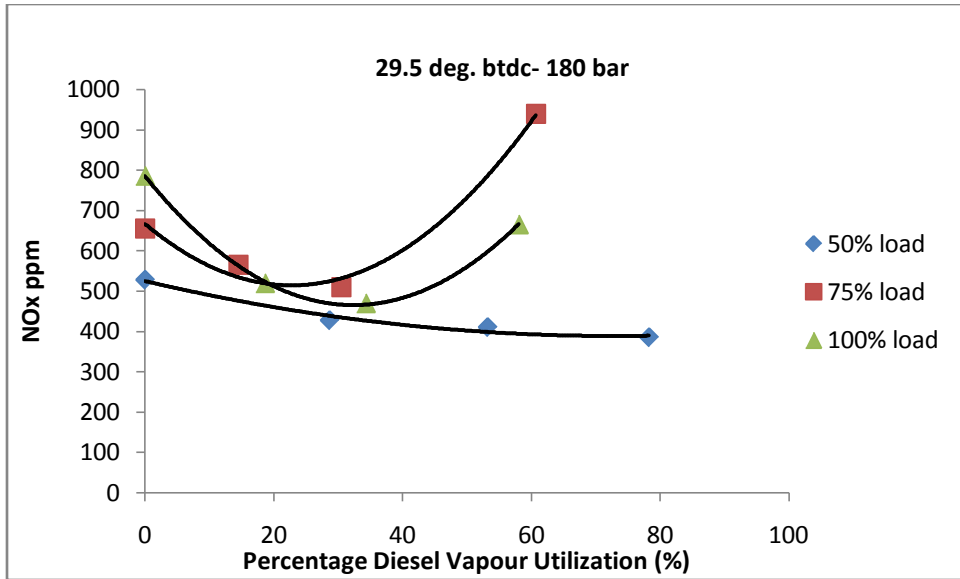


Fig. 5.36 NO_x variation with vapour induction at 29.5 deg. bTDC and 180 bar injection pressure.

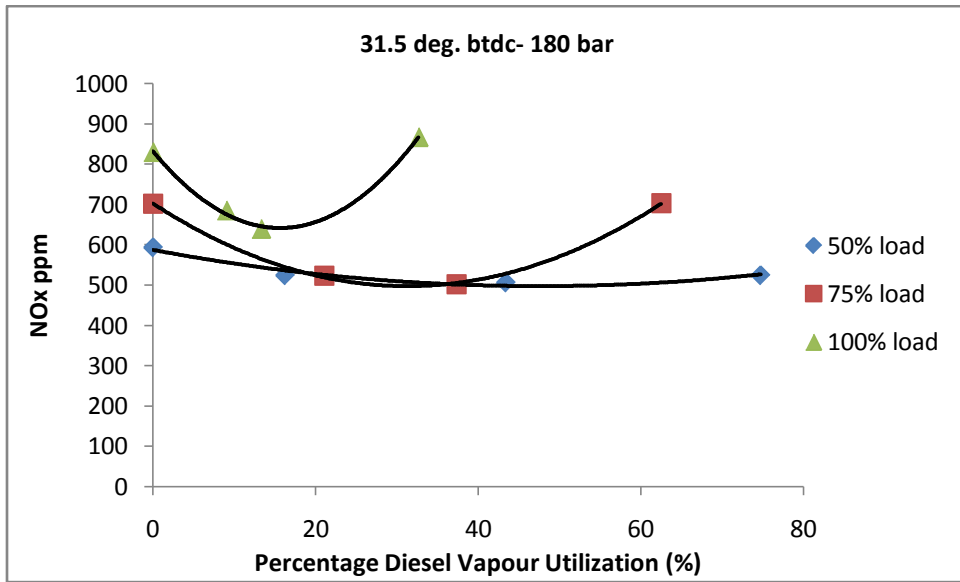


Fig. 5.37 NO_x variation with vapour induction at 31.5 deg. bTDC and 180 bar injection pressure.

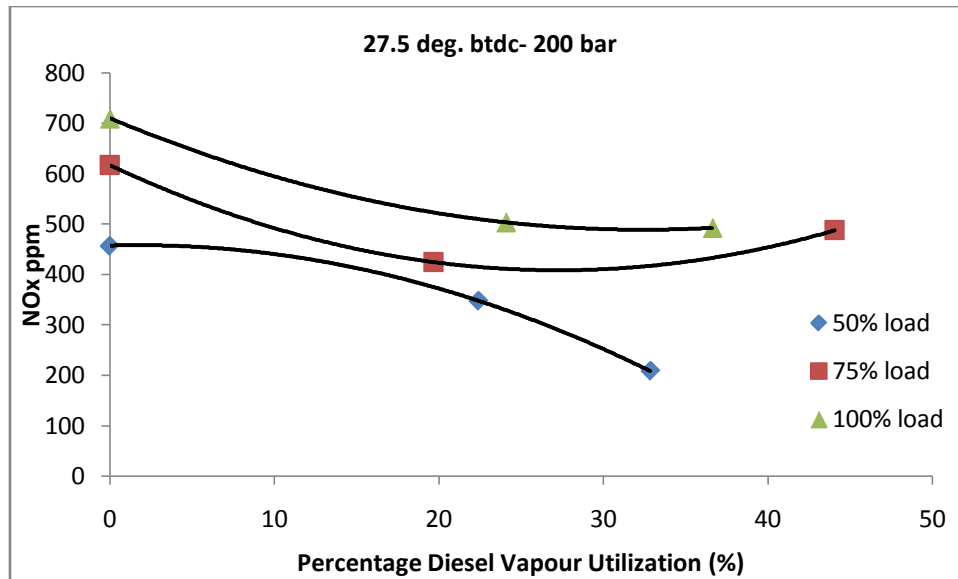


Fig. 5.38 NO_x variation with vapour induction at 27.5 deg. btDC and 200 bar injection pressure.

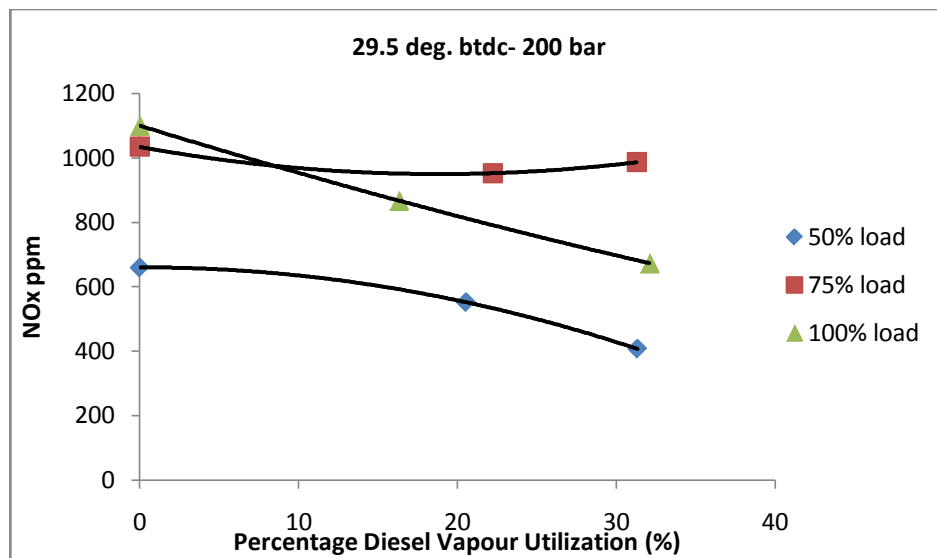


Fig. 5.39 NO_x variation with vapour induction at 29.5 deg. btDC and 200 bar injection pressure.

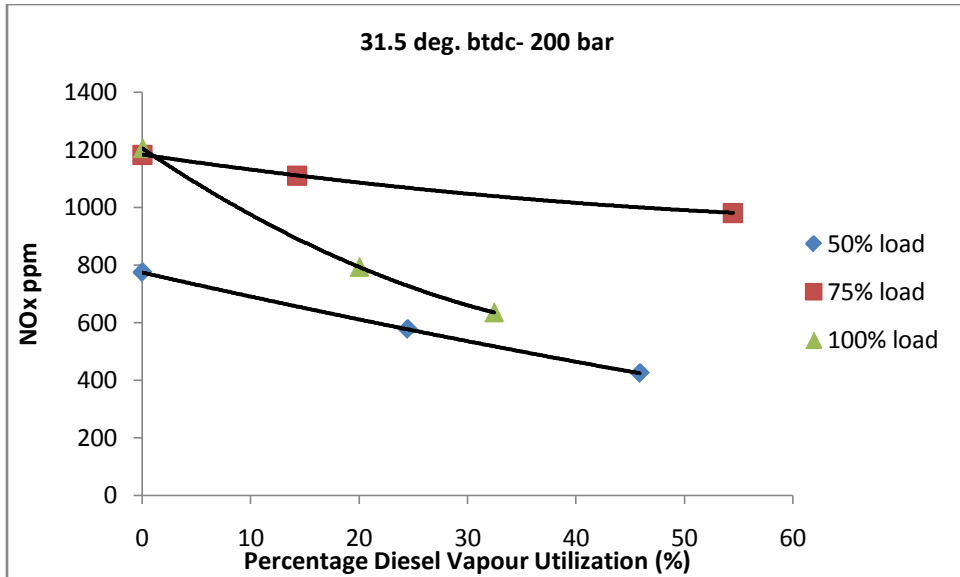


Fig. 5.40 NOx variation with vapour induction at 31.5 deg. bTDC and 200 bar injection pressure.

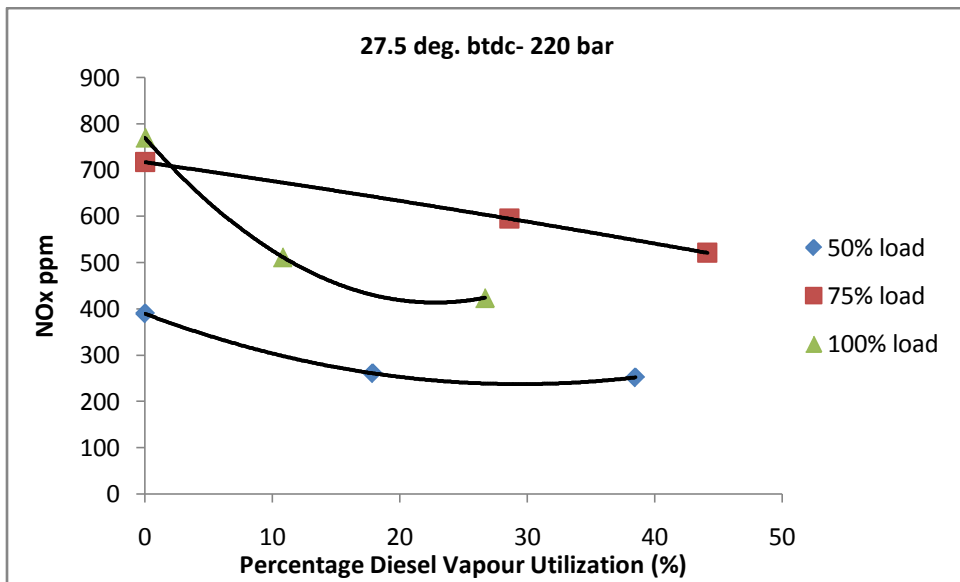


Fig. 5.41 NOx variation with vapour induction at 27.5 deg. bTDC and 220 bar injection pressure

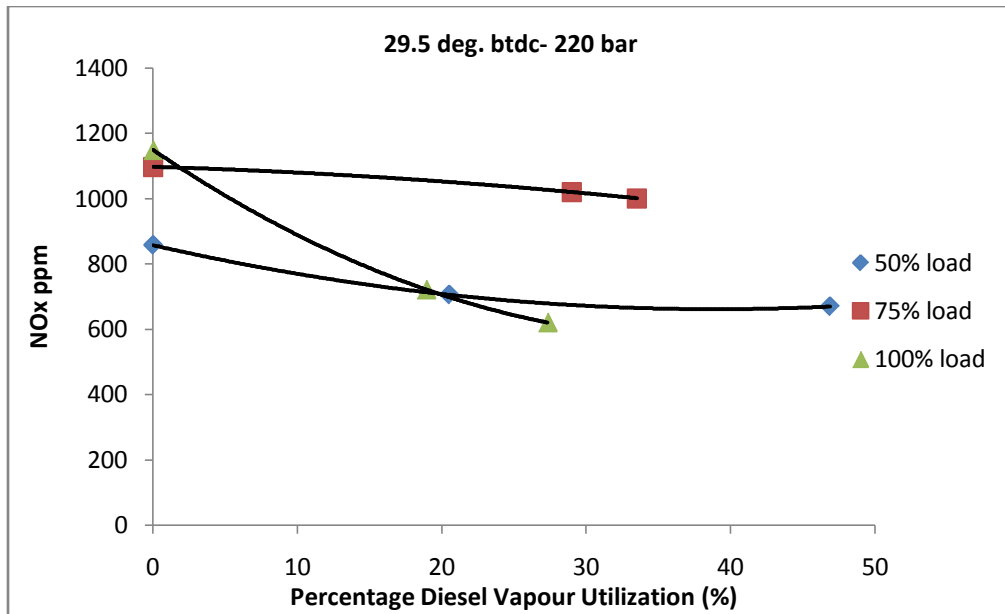


Fig. 5.42 NOx variation with vapour induction at 29.5 deg. bTDC and 220 bar injection pressure

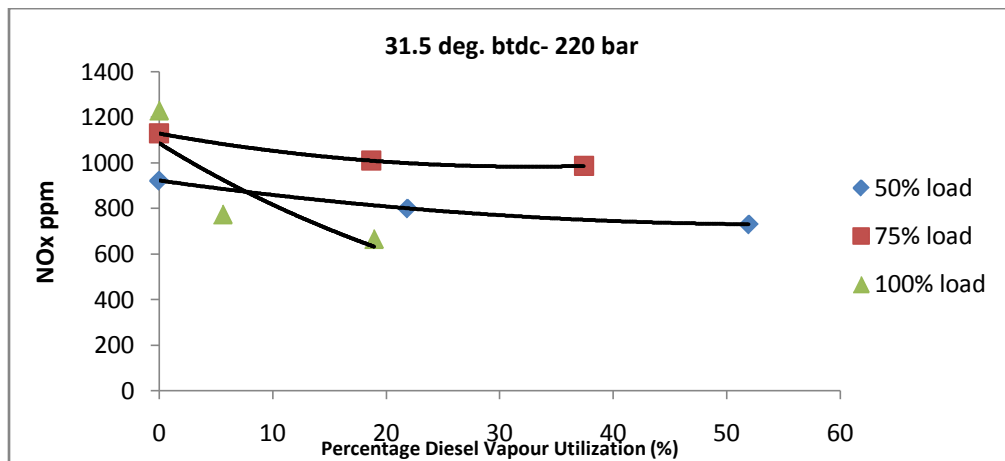


Fig. 5.43 NOx variation with vapour induction at 31.5 deg. bTDC and 220 bar injection pressure

The NOx emissions with CI mode of combustion and the HCCI mode of combustion are compared in the figures 5.44, 5.45 and 5.46.

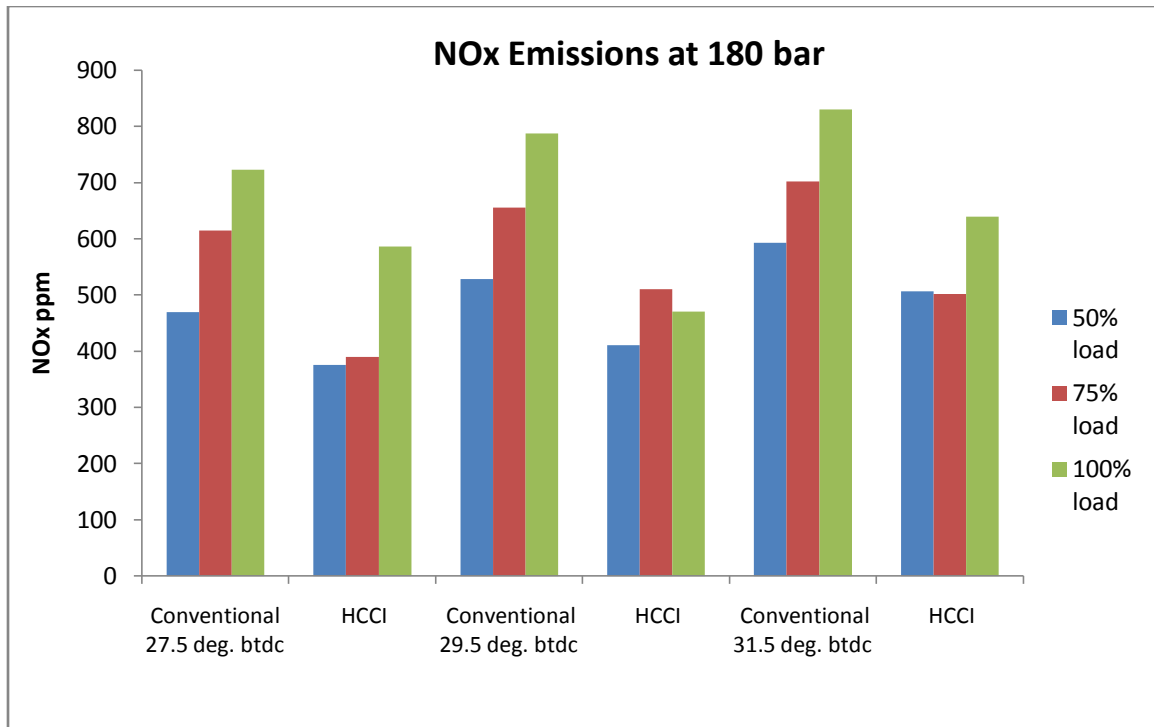


Fig. 5.44 NOx emissions for conventional and vapour induction mode at different injection timings at 180 bar

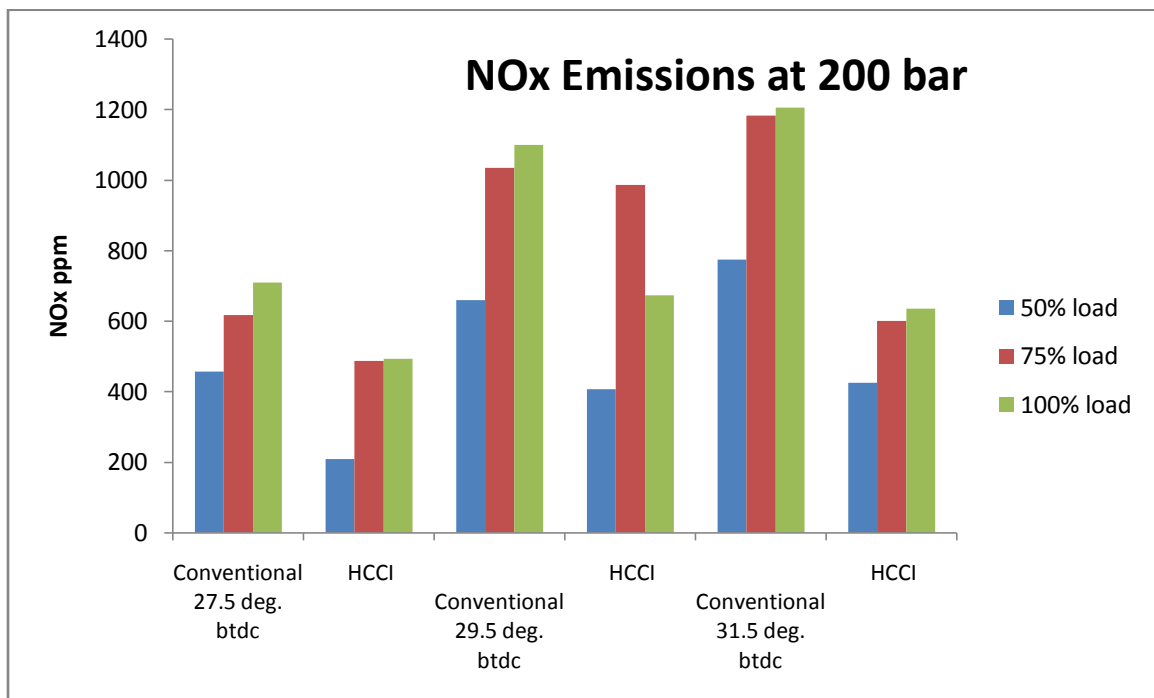


Fig. 5.45 NOx emissions for conventional and vapour induction mode at different injection timings at 200 bar

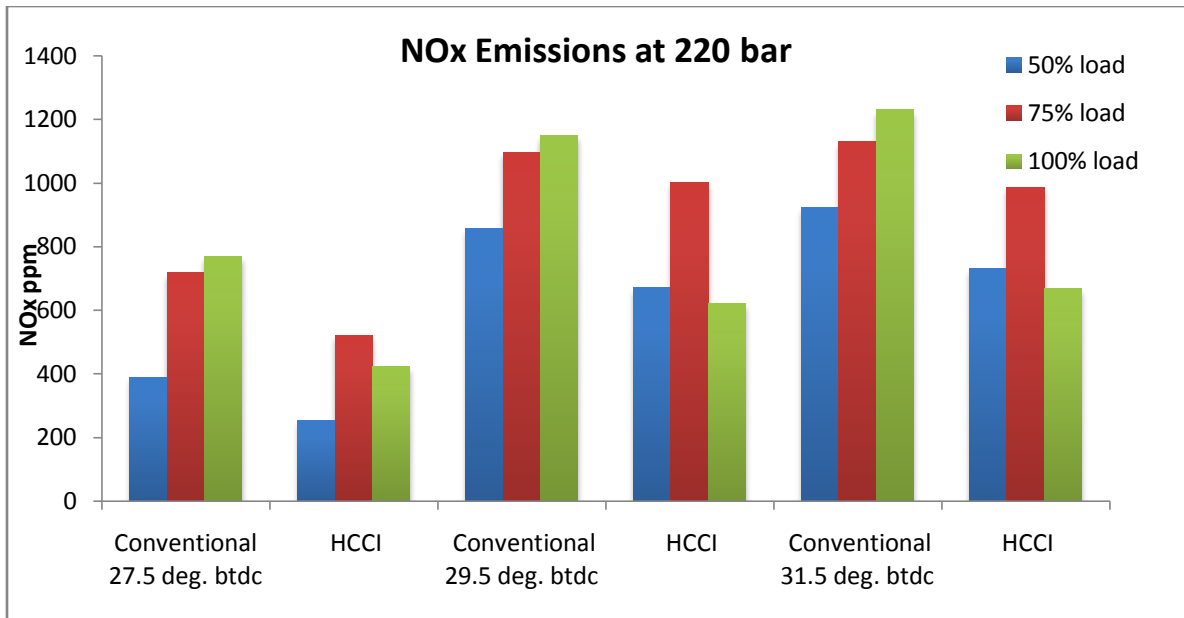


Fig. 5.46 NO_x emissions for conventional and vapour induction mode at different injection timings at 220 bar.

Fig. 5.47 gives a comparison between the NO_x emissions at optimized vapour induction mode and conventional diesel injection mode. As explained earlier the conventional mode is with 180 bar injection pressure and injection timing of 27.5⁰ bTDC and the vapour induction gives a better performance at 200 bar injection pressure and 31.5⁰ bTDC injection pressure.

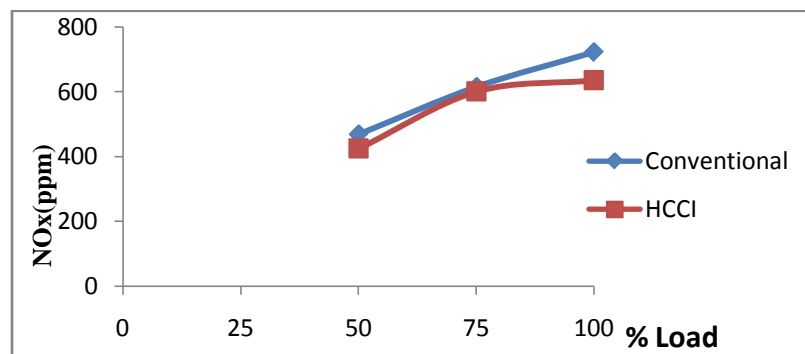


Fig. 5.47 NO_x emissions at optimized vapour induction mode (200 bar injection pressure and 31.5 deg. bTDC) and conventional diesel injection mode (180 bar injection pressure and 27.5 deg. bTDC) at different loads

5.1.2.5. Smoke Opacity

The variation of smoke opacity for Conventional diesel combustion and vapour induction mode at varied injection timings and injection pressures are shown in figure 5.48 to 5.50. Smoke emissions reduced at higher loads with the introduction of vapour. However at 50% full load conditions the introduction of vapour produced more smoke on an average. An overall reduction of smoke by 48% was observed with use of vapour induction. This may be due to decreasing temperature and at higher loads mixture becomes more homogeneous.

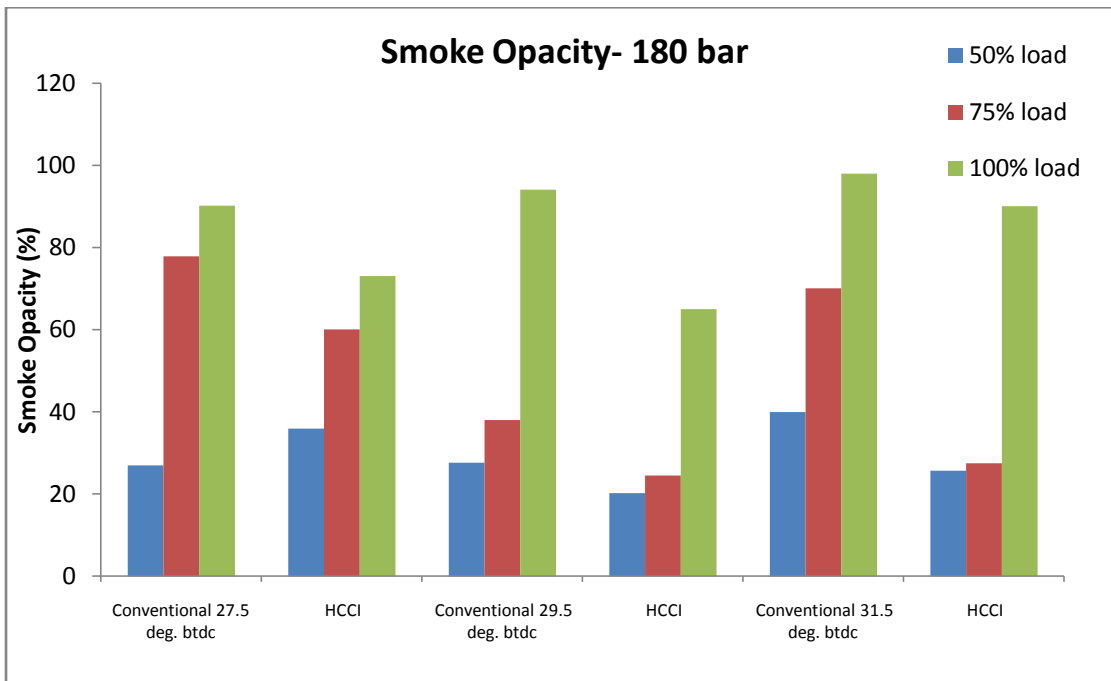


Fig. 5.48 Smoke Opacity for conventional and vapour induction mode at different injection timings at 180 bar

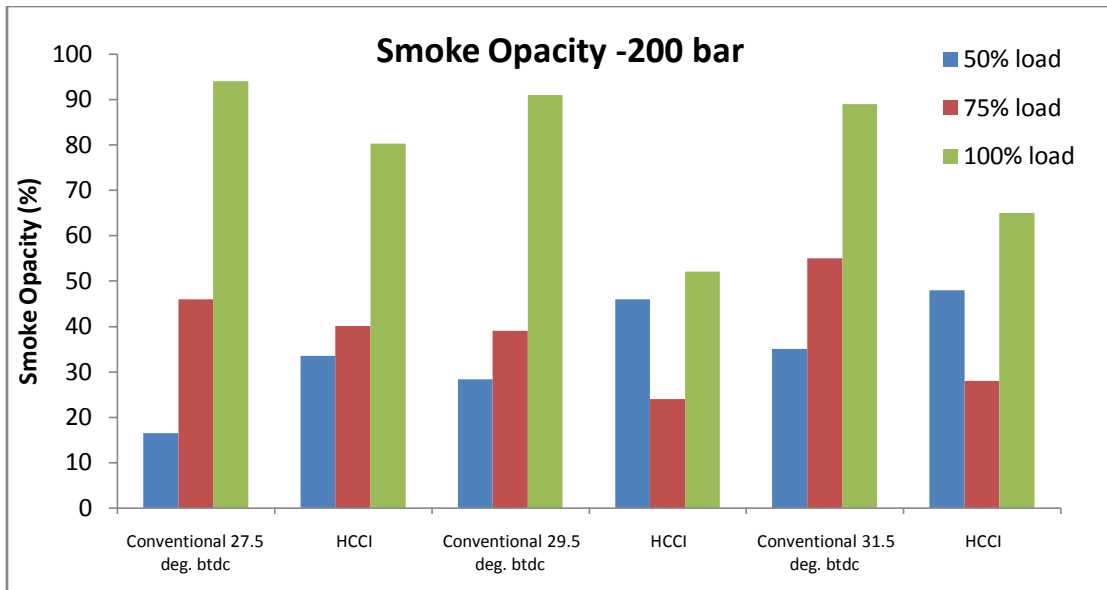


Fig. 5.49 Smoke Opacity for conventional and vapour induction mode at different injection timings at 200 bar

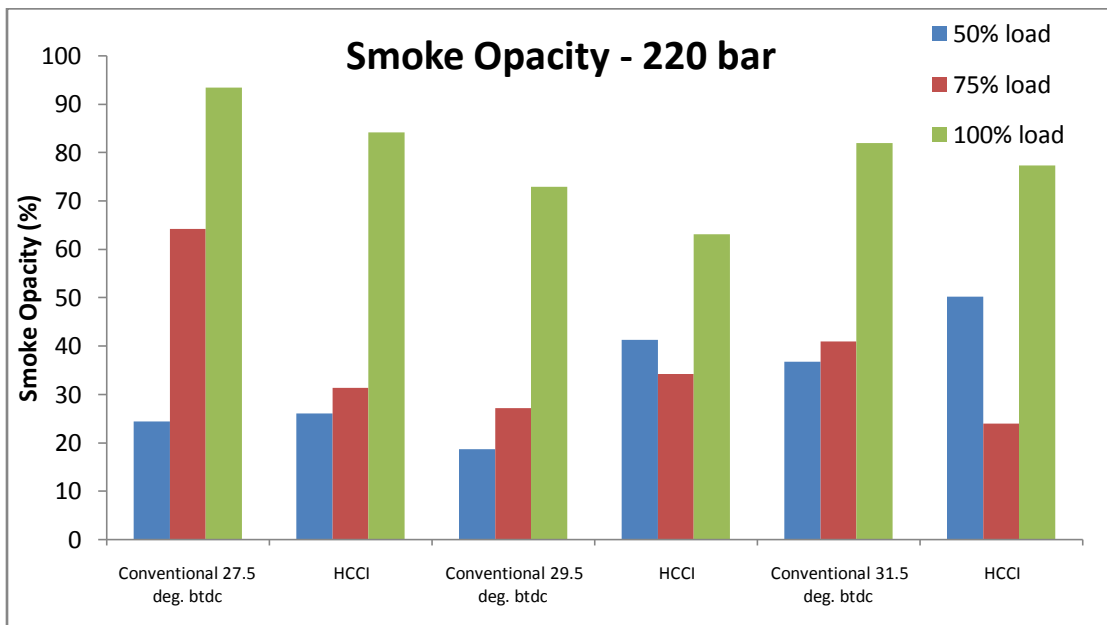


Fig. 5.50 Smoke Opacity for conventional and vapour induction mode at different injection timings at 220 bar

Fig. 5.51 gives a comparison between the NO_x emissions at optimized vapour induction mode and conventional diesel injection mode. As explained earlier the conventional mode is with 180 bar injection pressure and injection timing of 27.5° bTDC and the vapour induction gives a better performance at 200 bar injection pressure and 31.5° bTDC injection pressure.

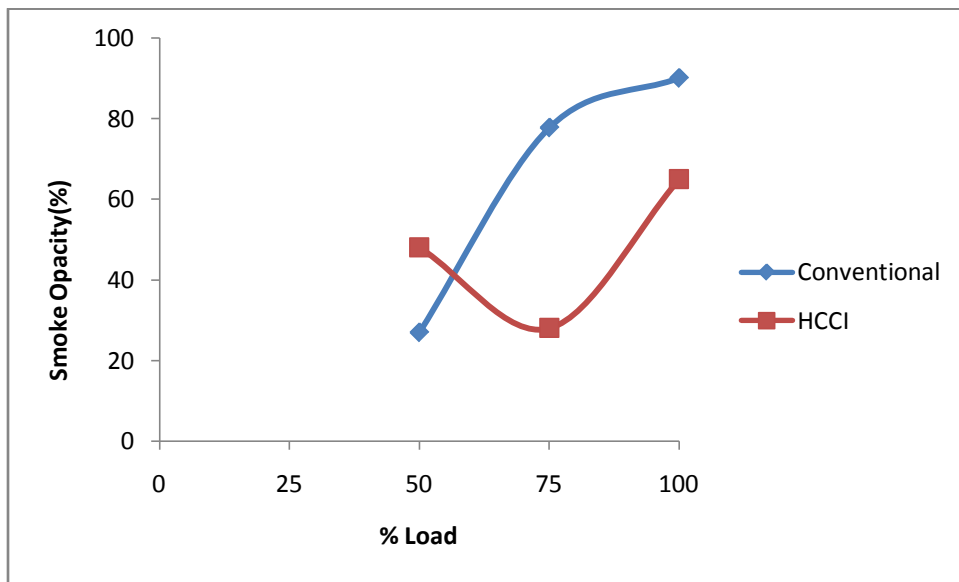


Fig. 5.51 Smoke Opacity at optimized vapour induction mode (200 bar injection pressure and 31.5 deg. bTDC) and conventional diesel injection mode (180 bar injection pressure and 27.5 deg. bTDC) at different loads.

5.1.3 Net Heat Release rate

The variation of net heat release rate with induction of vapour at different load conditions for 200 bar injection pressure and 31.5 deg injection timing are given in Fig. 5.52 to 5.54. It is observed that the heat release rate is advanced by vapour induction in all the conditions. At 50% load the maximum NHRR is decreased by induction of vapour where as at 100% load condition maximum NHRR is increased by vapour induction. This is due to the fact that at higher loads the heat exchanger produces a better vapour with improved degree of super heat and thus the air vapour mixture which is mixed externally becomes more and more homogenous.

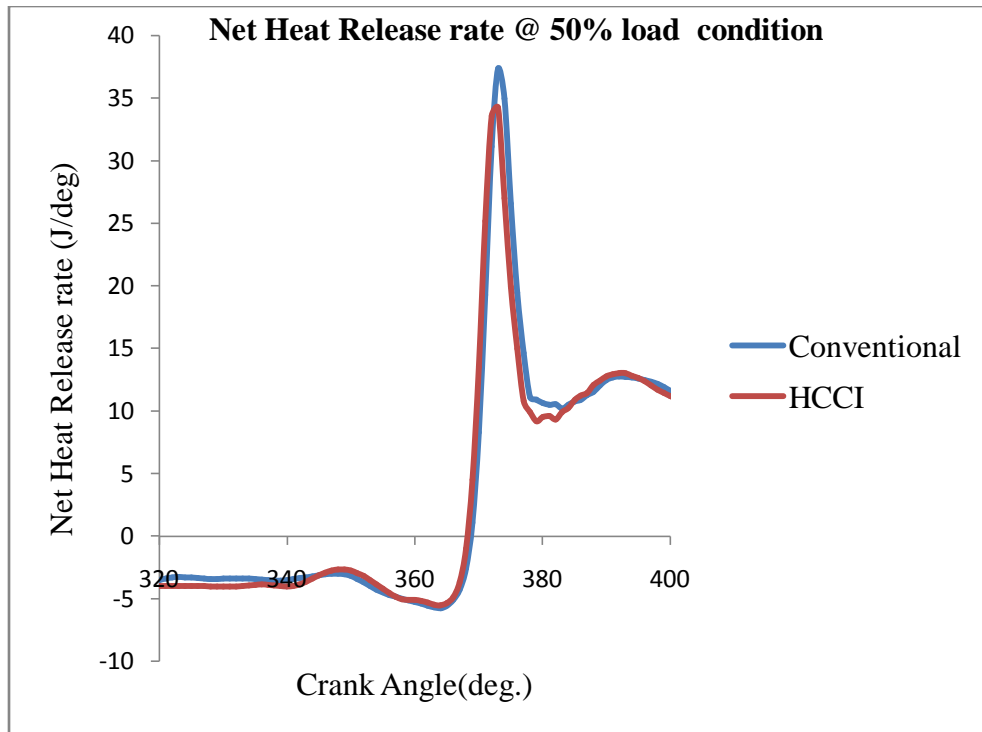


Fig. 5.52 Effect of vapour induction on Net Heat Release rate at 50% load condition

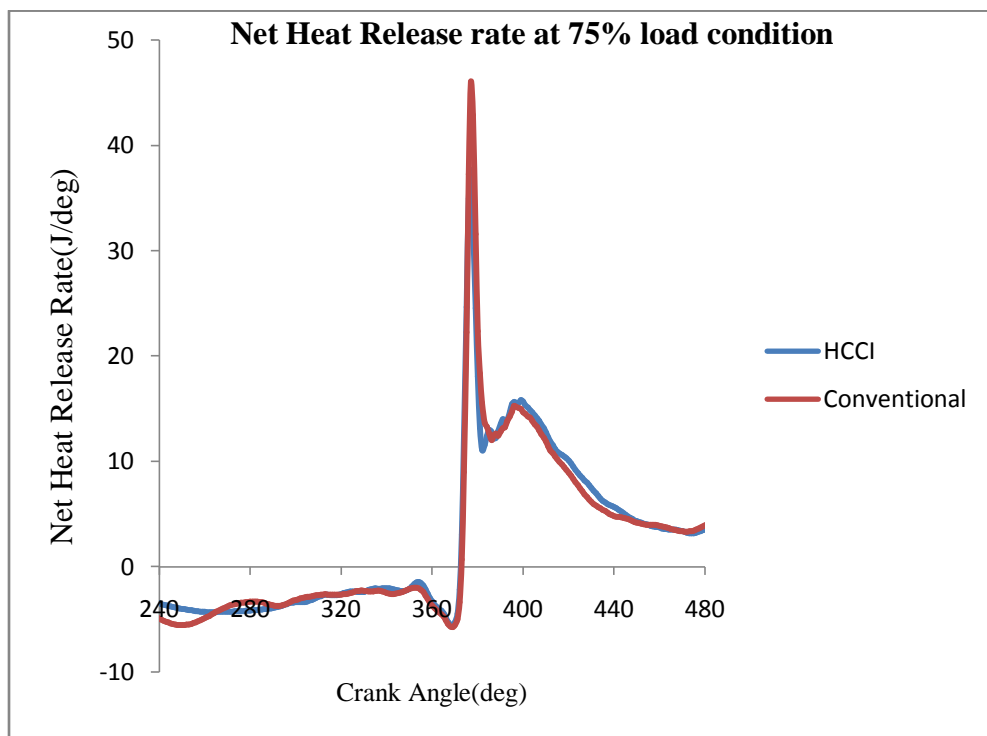


Fig. 5.53 Effect of vapour induction on Net Heat Release rate at 75% load condition

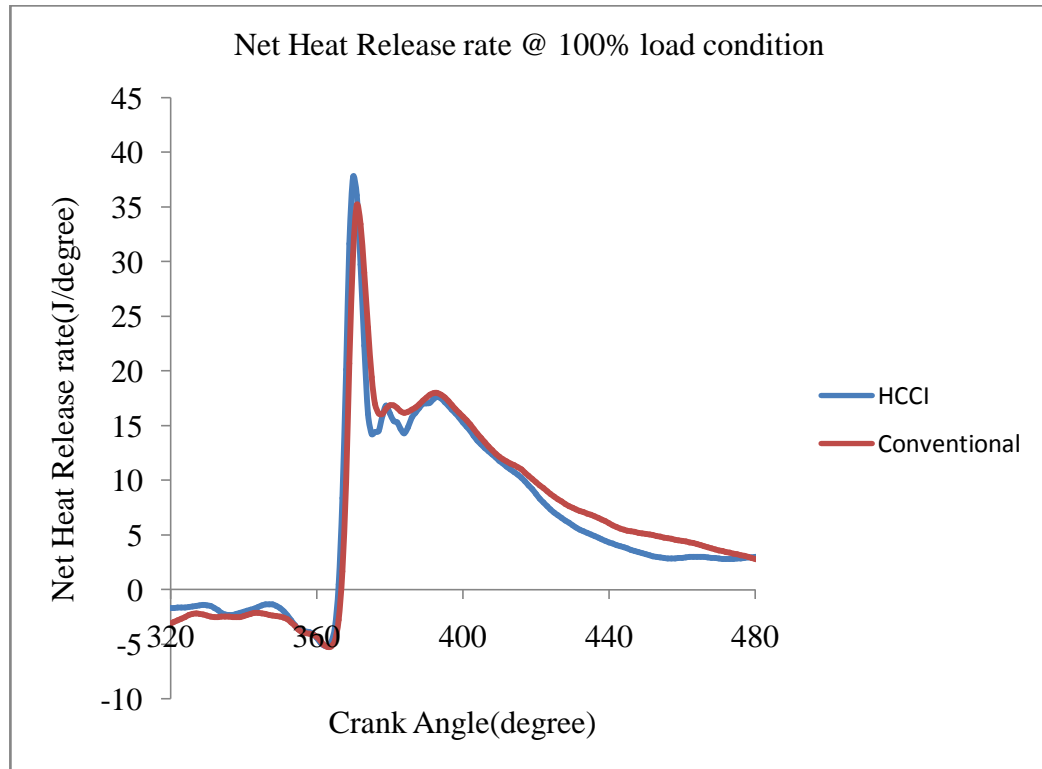


Fig. 5.54 Effect of vapour induction on Net Heat Release rate at 100% load condition

5.1.4 Cumulative Heat Release rate

The variation of cumulative heat release rate with induction of vapour at different load conditions for 200 bar injection pressure and 31.5 deg injection timing are given in Fig. 5.55 to 5.57. The cumulative heat release rate is the aggregate sum of instantaneous heat release rates. It is observed that there is not much difference between CHRR value between conventional mode and HCCI mode. The initial heat release rate is higher for HCCI mode which is an indication of early combustion by supplying homogenous mixture.

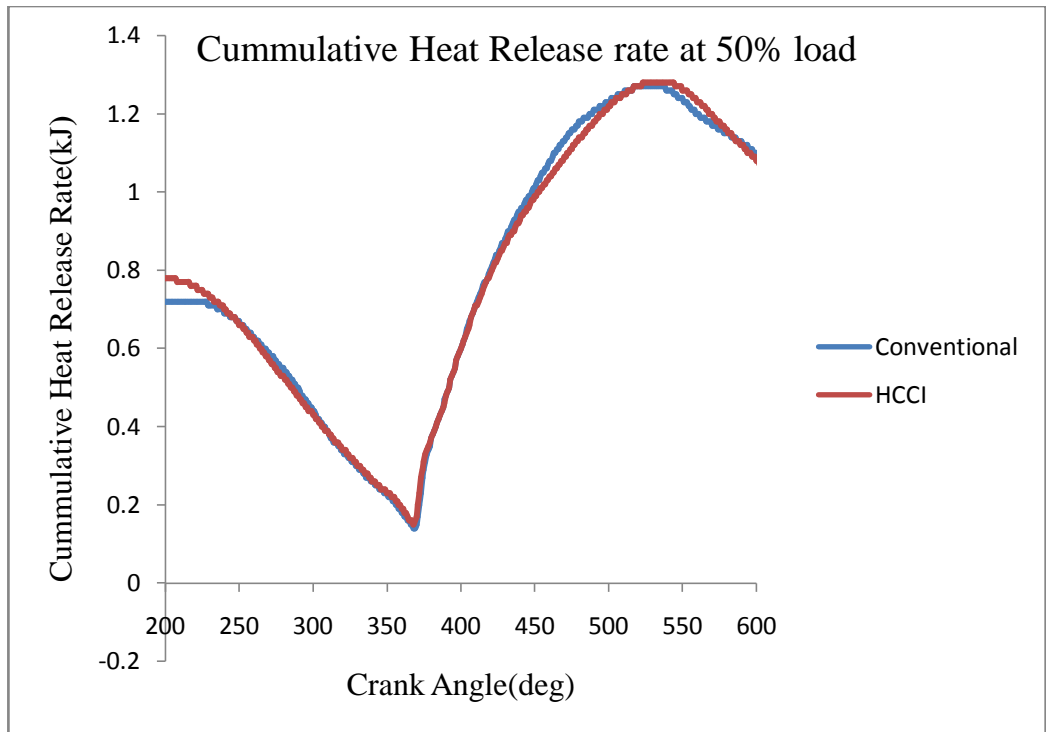


Fig. 5.55 Effect of vapour induction on Cumulative Heat Release rate at 50% load condition

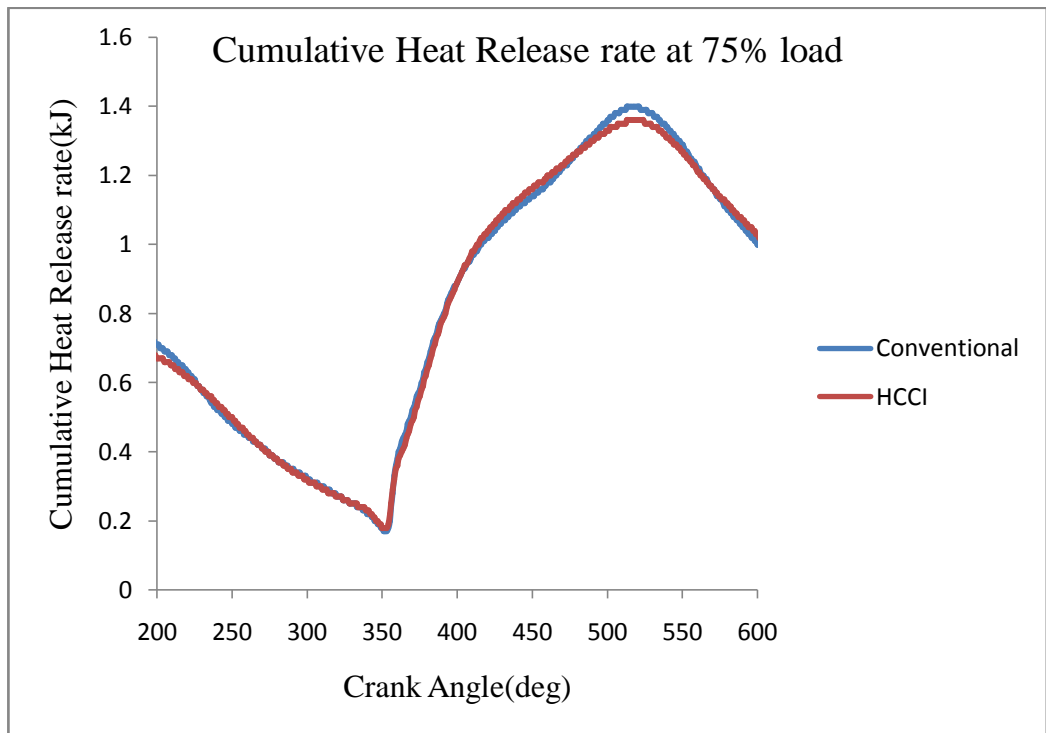


Fig. 5.56 Effect of vapour induction on Cumulative Heat Release rate at 75% load condition

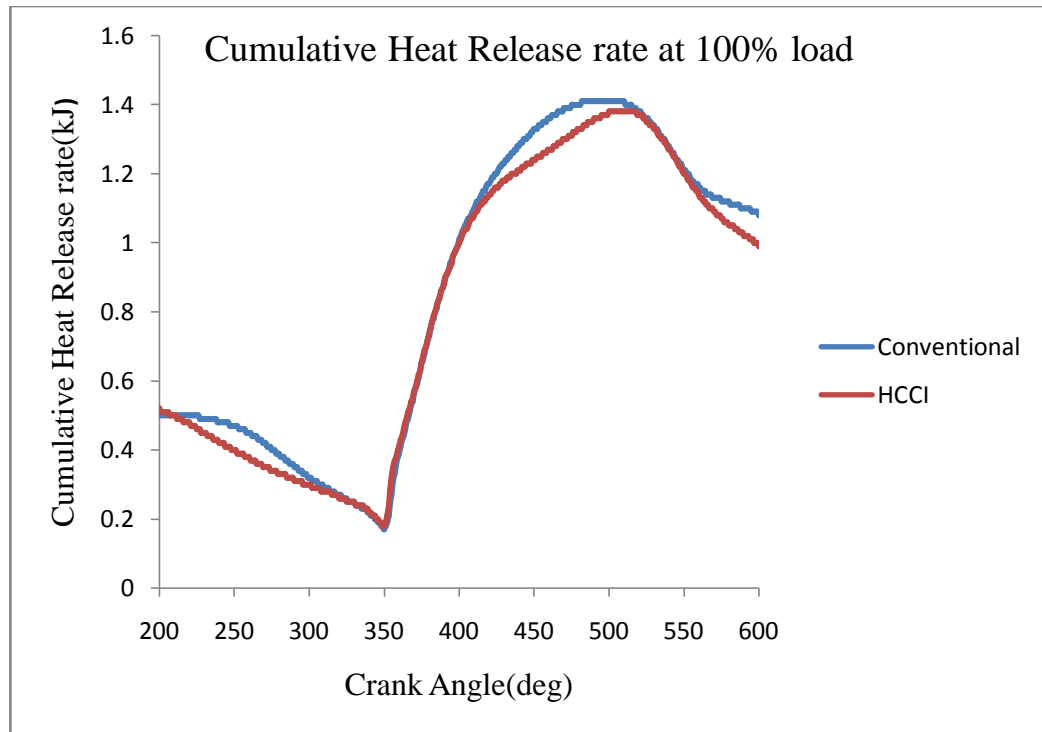


Fig. 5.57 Effect of vapour induction on Cumulative Heat Release rate at 75% load condition

The exhaustive experiments on the engine and the analysis of the results suggest that both NO_x and smoke opacity decrease with vapour induction whereas there is a slight increase in HC and CO emissions. This can be attributed to the decrease in temperature associated with HCCI mode of combustion.

Major outcomes of the phase – 1 of the experimental analysis, along with details as to how to adjust the different parameters to suit vapour induction are given below:

- ✓ The experimental analysis on the engine revealed that a delayed injection timing of **31.5 deg. bTDC and higher injection pressure - 200 bar was the optimum condition for diesel vapour induction.**
- ✓ The increase in vapour mass fraction increased the performance of the engine. This was mainly because the HCCI mode of combustion was approached. At the same time the start of combustion was still governed

by the injection of vapour fuel. This gave a method of control of combustion which is normally absent in HCCI engines.

5.2 EFFECT OF PREHEATING OF AIR ON THE PERFORMANCE AND EMISSION CHARACTERISTICS

The experimental analysis on the engine revealed that a delayed injection timing of 31.5 deg. bTDC and higher injection pressure - 200 bar was the optimum condition for diesel vapour induction. It also shows that if the %vapour induction is increased beyond a certain limit, the brake thermal efficiency is reduced and also CO and HC emissions are increased to a higher level. The main reason behind the limitation of %vapour induction was the condensation of diesel vapour near the intake manifold. This badly affects the preparation of homogenous mixture, thus the performance of the engine. One possible method for preventing the condensation of diesel vapour is increasing the temperature of intake charge. This can be achieved by heating the intake air to possible levels. Air can be heated by using the exhaust gases or by an external source. Here waste flue gases are already used in a heat exchanger for producing diesel vapour; hence an electrical heating coil is used for heating purpose.

This section of the report deals with the analysis of the performance and emission characteristics of the engine working in a dual fuel mode - vapor diesel induction and direct diesel injection. The steady state performance and emission tests were conducted at rated engine speed of 1500 rpm at 200 bar injection pressure and injection timing of 31.5⁰ bTDC. Later the set of experiments were repeated for different load conditions. For each load condition the readings were also taken for different preheating temperatures. The experimental results obtained for conventional direct injection diesel mode were taken as baseline data for comparison.

5.2.1 PERFORMANCE PARAMETERS

The combustion performance of the engine was assessed by calculating and comparing the brake thermal efficiency (BTE), Exhaust gas temperature and percentage vapor

utilization. The variation of exhaust gas temperature with the increasing amount of diesel vapor induction was plotted. The brake thermal efficiency by vapor diesel induction as compared to direct injected diesel is discussed under this section.

5.2.1.1 Effect of preheating on Brake Thermal Efficiency at different load conditions

Preheating can be considered as an effective tool in utilizing more diesel vapor with simultaneous improvement in brake thermal efficiency. The air was preheated using an external heating coil and the temperature was varied from 40 to 55 °C. The preheating temperature was limited to 65 °C as the change in performance and emission parameters were incremental when comparing 60° C and 65° C. Also higher values of intake temperature may increase NO_x emissions.

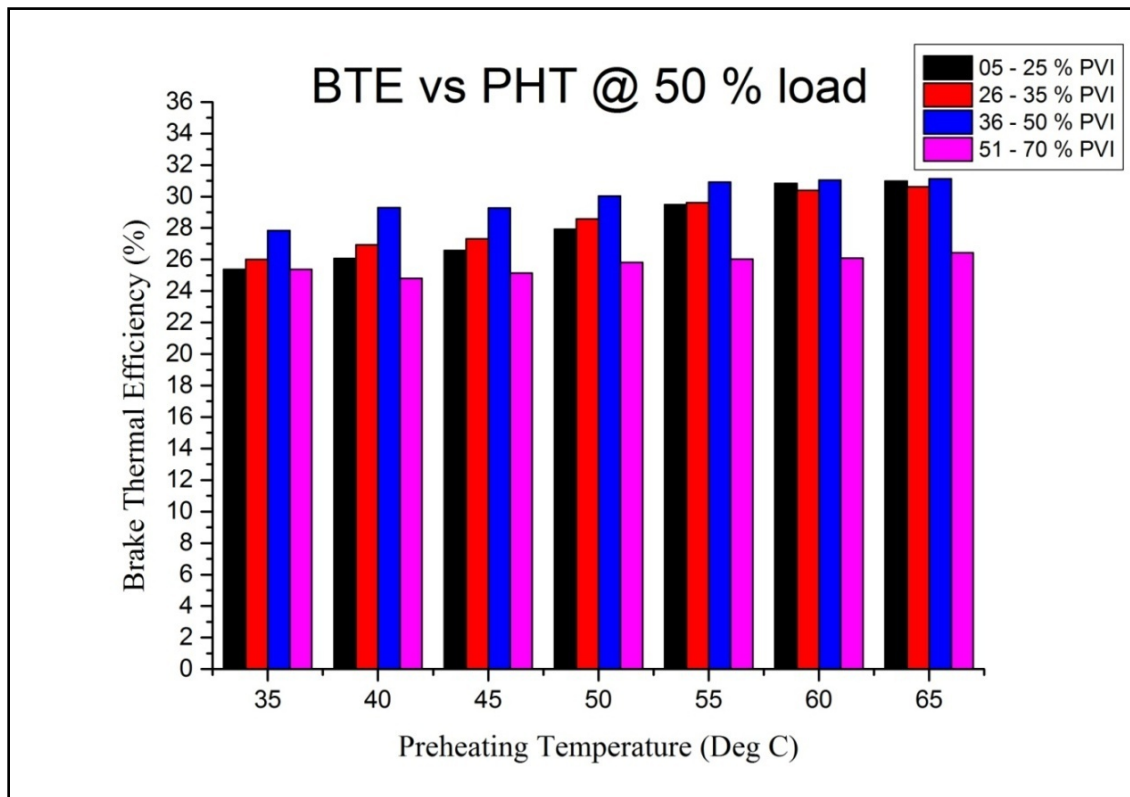


Fig 5.58 Brake thermal Efficiency vs Pre heating temperature for different % vapor induction at 50 % load at 200 bar injection pressure and at injection timing of 31.5° bTDC

The Fig 5.58 shows the variation in Brake thermal efficiency with an increase in the preheating temperature for different amount of vapor inducted. The amount of vapor inducted was increased through 4 trials so as to know the point where the engine knocks. The ranges of % vapour inducted for each trial are given in Fig 5.58. As seen from the Fig 5.58 BTE increases first then comes down with an increase in the vapor flow rate.

This is again clearly evident in Fig 5.58 and the trial 4 indicates the knock limited amount of vapor induction. The initial temperature 35° C indicates the condition without preheating and as the air preheating temperature increases there is an increase in the brake thermal efficiency.

The reason behind this is that the inlet air temperature is an important parameter for creating the homogeneous mixture. An increasing inlet air temperature is used to improve fuel vaporization and create more homogeneity air/fuel charge. A higher temperature of inlet air also reduces the chance of condensation of diesel vapor as both air and vapor mixes near the inlet manifold. Thus higher inlet air temperature promotes more complete combustion.

The maximum Brake thermal efficiency was obtained at 65 °C preheating temperature where the percentage vapor utilization was found to be 50.394 %. The percentage increase in efficiency was found to be 23.315 % when compared to the conventional engine and 11.8 % when compared to that of HCCI mode without preheating.

As observed from the Fig 5.59 and 5.60 a similar trend in brake thermal efficiency was seen with increase in preheating temperature for 75 % and 100 % load. For 75 % load a maximum efficiency of 33.53 % was obtained at a preheating temperature of 55 °C where the percentage vapor utilization was found to be 37.95 %. The percentage increase in efficiency for this condition is 29.50 % when compared to the conventional engine and 7.38 % when compared to that of HCCI mode without preheating.

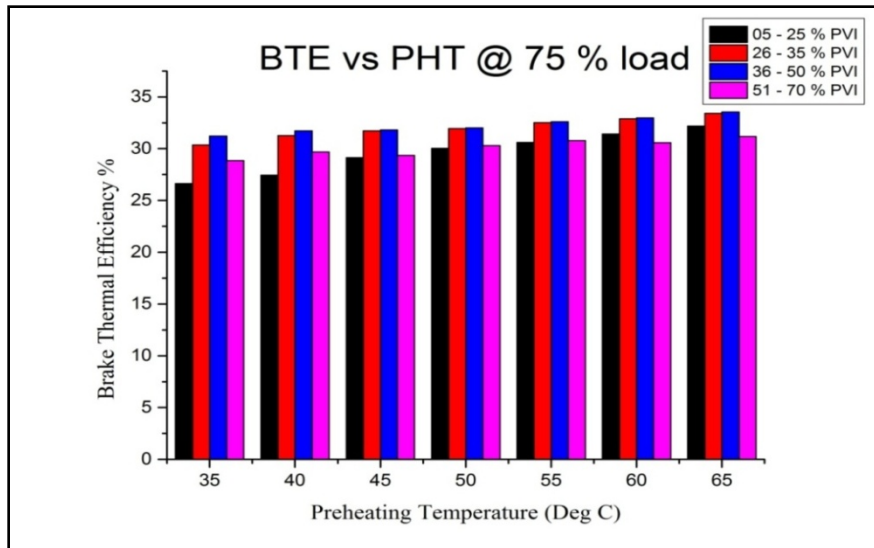


Fig 5.59 Brake thermal Efficiency vs Preheating temperature for different % vapor induction at 75 % load at 200 bar injection pressure and at injection timing of 31.5⁰ bTDC

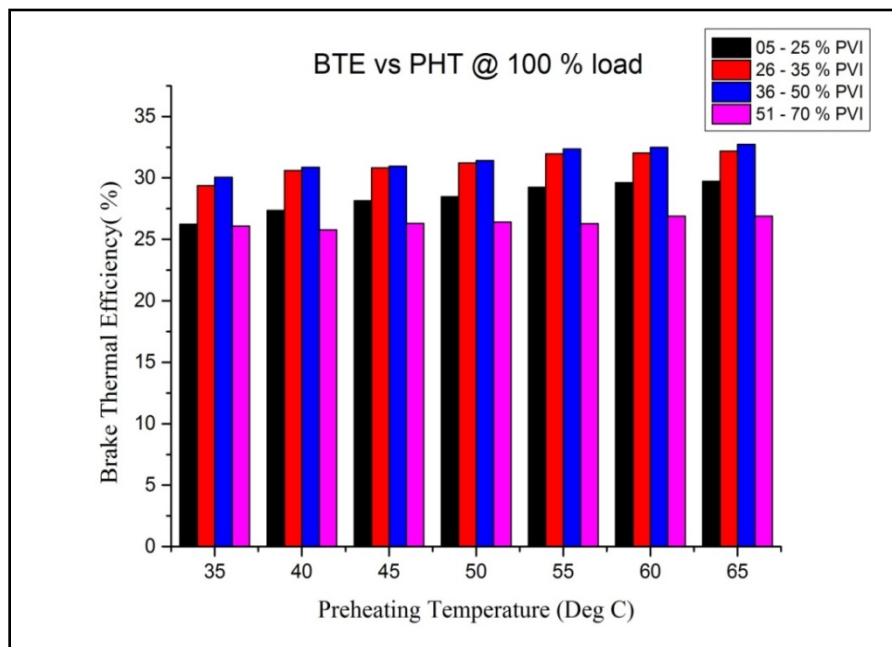


Fig 5.60 Brake thermal Efficiency v/s Preheating temperature for different % vapor induction at 100 % load at 200 bar injection pressure and at injection timing of 31.5⁰ bTDC

As given in Fig. 5.60 for 100 % load the maximum efficiency obtained is 32.73 % at a preheating temperature of 65 °C where the percentage vapor utilization was found to be 41.5 %. The percentage increase in efficiency for this condition is 40.4% when compared to the conventional engine and 8.91 % when compared to that of HCCI mode without preheating.

Table 5.3 shows the change in maximum brake thermal efficiency along with the corresponding percentage vapor utilization when preheating was employed.

Table 5.3 Maximum efficiency at different load conditions

% Maximum Load	Maximum efficiency without preheating (%)	vapour utilization (%)	Maximum efficiency with preheating (%)	vapour utilization (%)
50	27.9	47.8	31.04	49.74
75	31.5	34	33.54	37.95
100	30.05	38.74	32.73	41.60

5.2.1.2 Effect of preheating on Brake Specific Fuel Consumption at different load conditions

In Fig 5.61 each trial indicates an increase in the percentage of vapor inducted with trial 4 being the maximum vapor inducted. The reason for decrease in BSFC with more amount of vapor is the approaching of HCCI mode for the engine as more vapor is inducted. This makes the mixture more homogeneous and brings down the fuel requirement as explained earlier. However for trial 4 at a percentage vapor of 59 % the engine knocks and causes the BSFC to increase. The minimum BSFC is attained at a preheating of 50 °C and at a percentage vapor of 49.74 % where the efficiency is maximum and the value being 0.255 kg/kWhr.

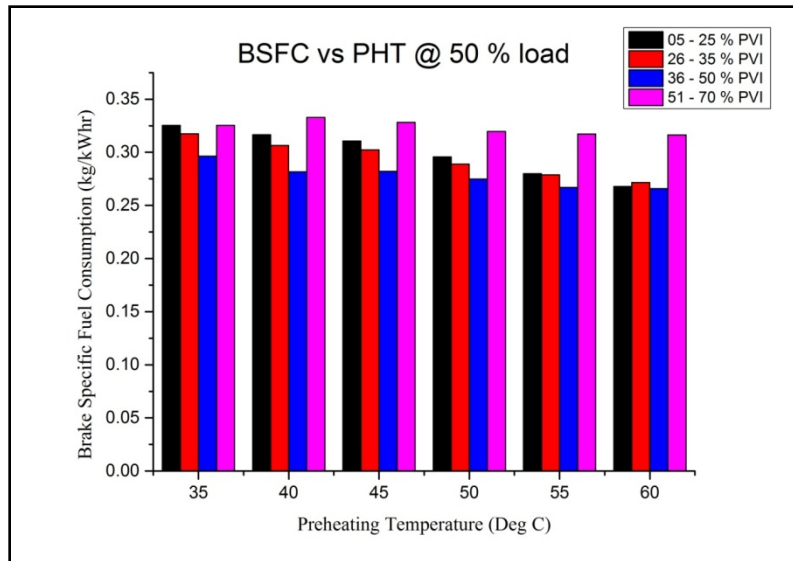


Fig 5.61 Brake Specific Fuel Consumption vs Preheating temperature for different % vapor induction at 50 % load at 200 bar injection pressure and at injection timing of 31.5⁰ bTDC.

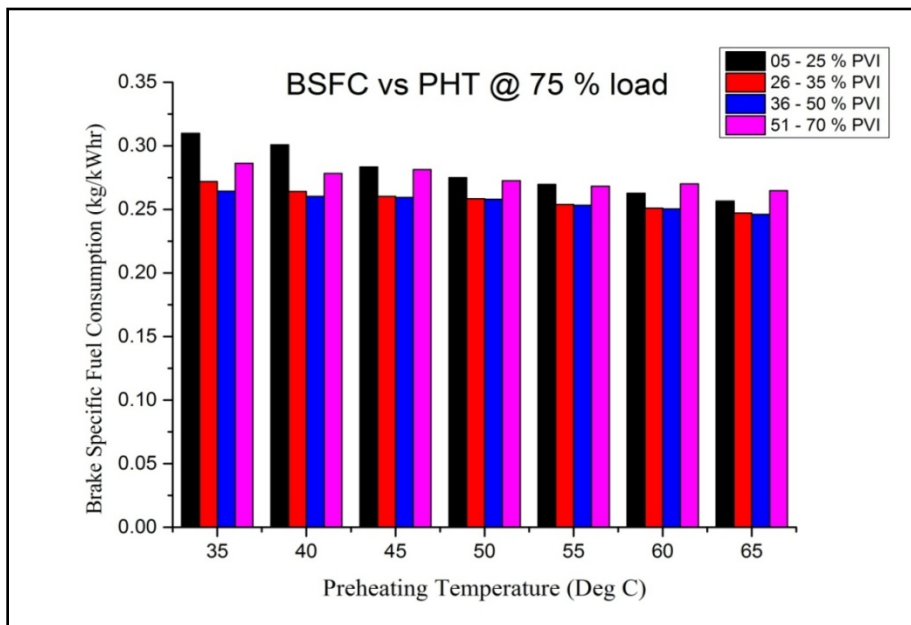


Fig 5.62 Brake Specific Fuel Consumption vs Preheating temperature for different % vapor induction at 75 % load at 200 bar injection pressure and at injection timing of 31.5⁰ bTDC

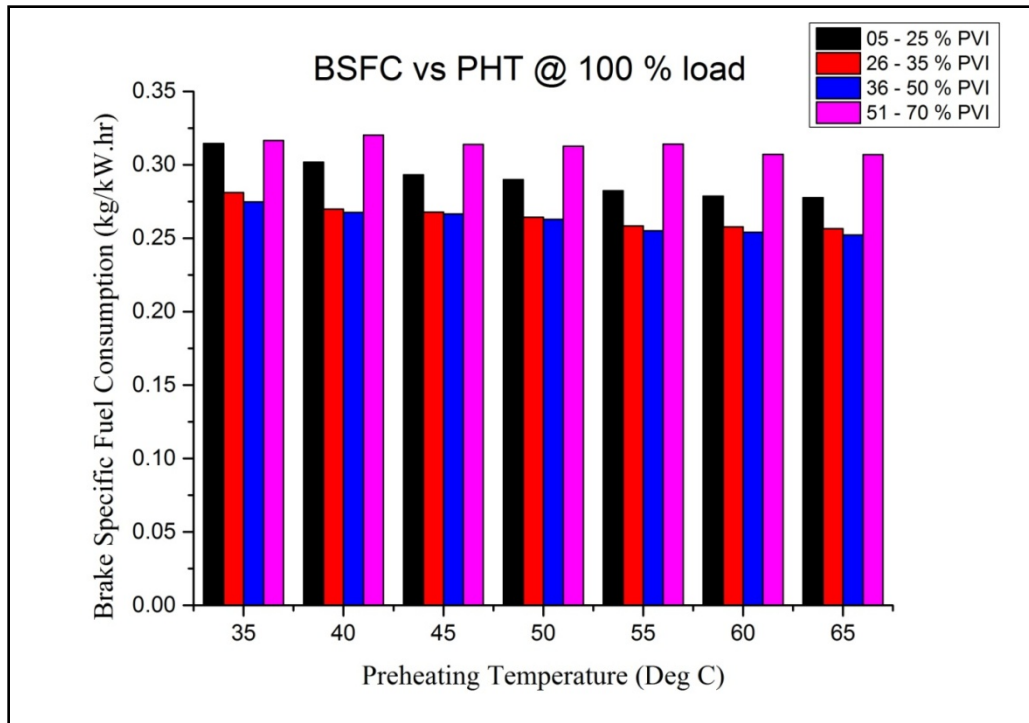


Fig 5.63 Brake Specific Fuel Consumption vs Preheating temperature for different vapor induction at 100 % load at 200 bar injection pressure and at injection timing of 31.5⁰ bTDC

Similar trends can be seen in Fig 5.62 and 5.63 which shows the variation of BSFC with preheating temperature for different amount of vapor for 75 % and 100 % load respectively.

For 75 % load the minimum BSFC is attained at a preheating of 55 °C and at a percentage vapor of 37.95 % where the efficiency is maximum and the value being 0.245 kg/kWhr.

For 100 % load the minimum BSFC is attained at a preheating of 55 °C and at a percentage vapor of 41.5 % where the efficiency is maximum and the value being 0.2522 kg/kWhr.

5.2.1.3 Effect of preheating on Exhaust Gas Temperature at different load conditions

Exhaust gas temperature is one of the most important parameters in the HCCI mode of operation of the engine as it is a direct measure of the in-cylinder temperature at that point of time. The in cylinder temperature is responsible for most of the merits and demerits of the HCCI engine. For example the increase in thermal efficiency of the engine can also be attributed to the comparatively lesser amount of heat that is lost to the engine cooling water. It can also as will be seen later be held responsible for the decrease of NO_x.

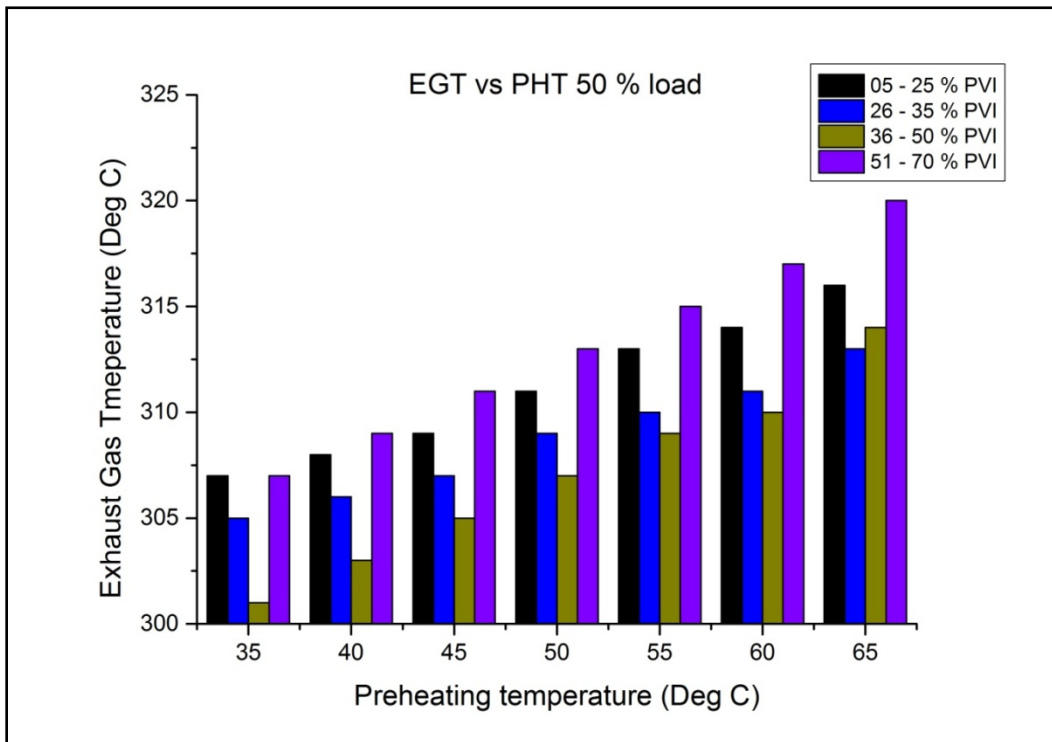


Fig 5.64 Exhaust Gas Temperature vs Preheating temperature for different vapour induction at 50 % load at 200 bar injection pressure and at injection timing of 31.5⁰ bTDC

It can be seen from Fig 5.64 that preheating of air causes an increase in the exhaust gas temperature. With preheating the combustion efficiency increases as seen earlier which

also results in an increase in the in cylinder temperature thereby increasing the exhaust gas temperature. The maximum Exhaust gas temperature was found to be 320 °C at a preheating temperature of 65 °C and a maximum percentage vapour of 71.33%.

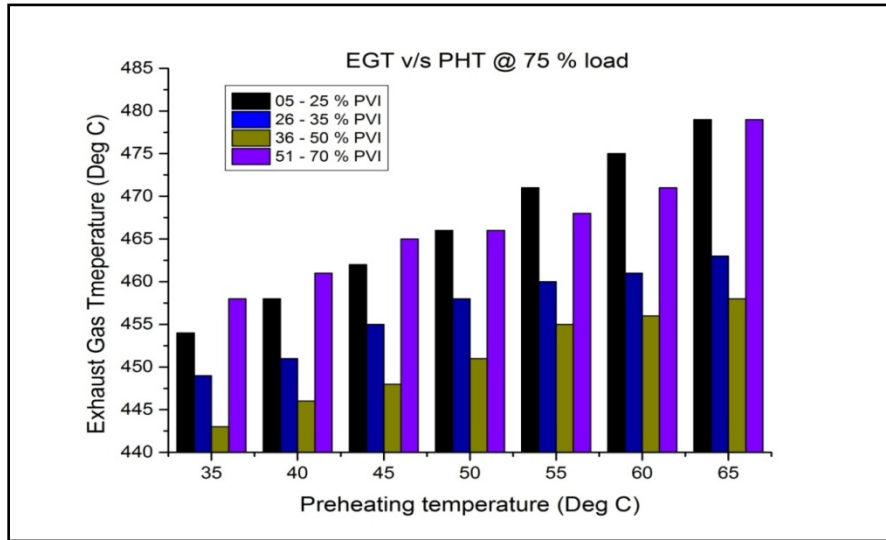


Fig 5.65 Exhaust Gas Temperature vs Preheating temperature for different vapour induction at 75 % load at 200 bar injection pressure and at injection timing of 31.5⁰ bTDC

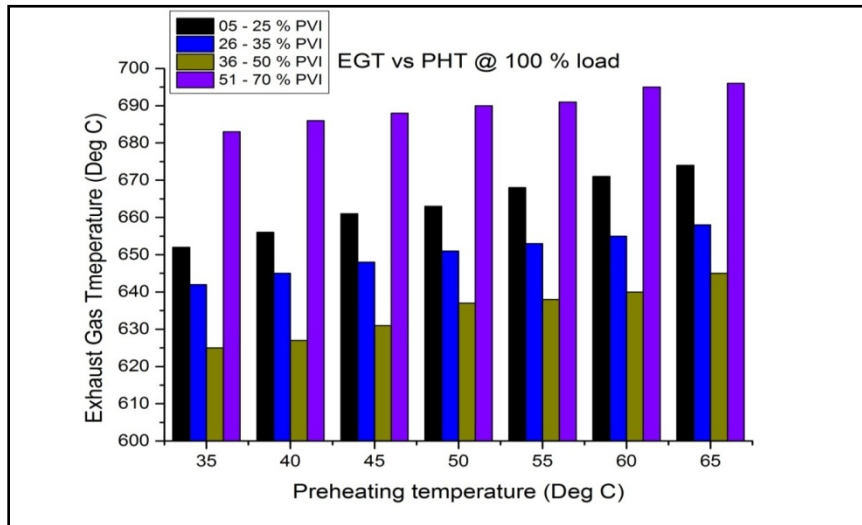


Fig 5.66 Exhaust Gas Temperature vs Preheating temperature for different vapour induction at 100 % load at 200 bar injection pressure and at injection timing of 31.5⁰ bTDC

At higher loads the exhaust gas temperature increases and as seen in Fig 5.65 and 5.66 for 75 % and 100 % load exhaust gas temperature increases with an increase in the preheating temperature. For 75 % load the maximum value of exhaust gas temperature is 479 °C at 65 °C preheating temperature and a maximum percentage vapour of 54.8 %. For 100 % load the maximum value of exhaust gas temperature is 595 °C at 65 °C preheating temperature and a maximum percentage vapour of 58%.

5.2.1.4 Effect of preheating on % Vapour Utilization at different load conditions

Percentage vapour utilization is an important parameter showing the performance of the engine in HCCI mode. It quantifies the utilization of the diesel vapour inducted. More amount of diesel vapour inducted causes the percentage vapour to increase. It can be also understood as a mixing ratio between diesel vapour and diesel fuel injected through a separate tank on a mass basis. An increase in percentage vapour indicates better homogeneity of charge and better combustion. However vapour cannot be inducted beyond a limit due to knocking caused by fuel accumulation and misfiring charge.

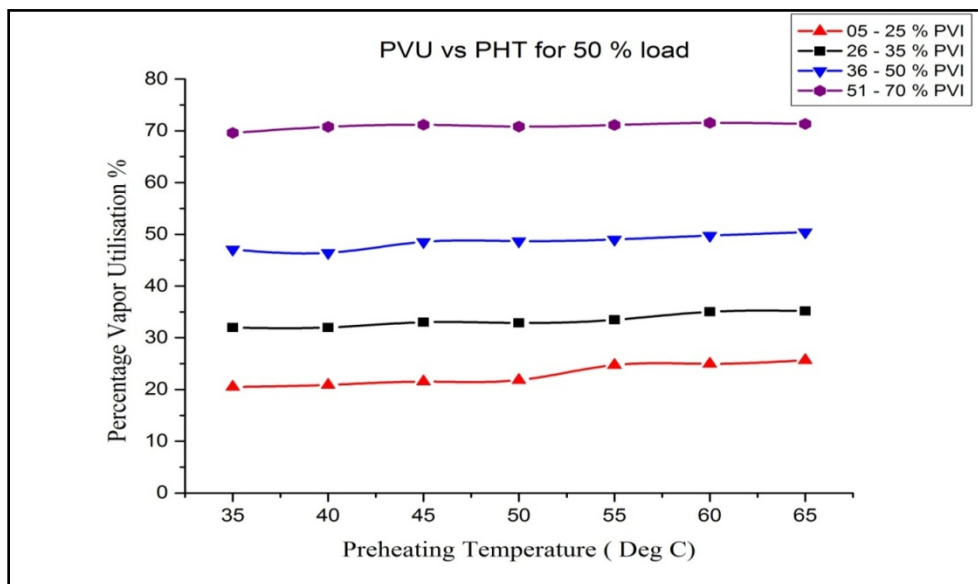


Fig 5.67 Percentage vapour Utilization vs Preheating Temperature for different % vapour induction at 50 % load at 200 bar injection pressure and at injection timing of 31.5⁰ bTDC

In Fig 5.67 each trial indicates an increase in the percentage vapour with trial 4 being the maximum percentage vapour inducted. As seen from the Fig 5.67 for 50 % load an increase in the preheating temperature causes the percentage diesel vapour utilization to increase. Maximum Percentage vapour utilization was found at 65 °C for all the loads. This increase is attributed to better fuel vaporisation and atomization at higher charge temperature which uses the diesel vapour more effectively. Each value indicates different amount of vapour and trial 4 is where the percentage diesel inducted is maximum. For trial 4 without preheating the percentage vapour is 59.5 % and further preheating causes the preheating to reach a maximum of 71.5 %. However this is not advised as it causes abnormal engine combustion resulting in poor efficiency and higher incylinder temperature.

So the better value of percentage vapour to be inducted is 47.05 % for trial 3 and with preheating it can be increased to maximum of 50.394 % at 65 °C.

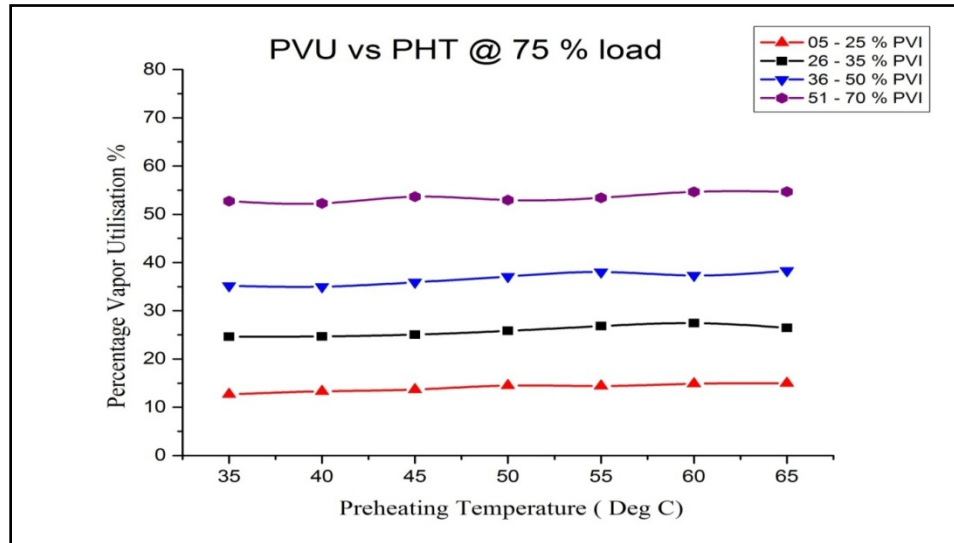


Fig 5.68 Percentage vapour Utilization vs Preheating Temperature for different %vapour induction at 75% load at 200 bar injection pressure and at injection timing of 31.5⁰ bTDC

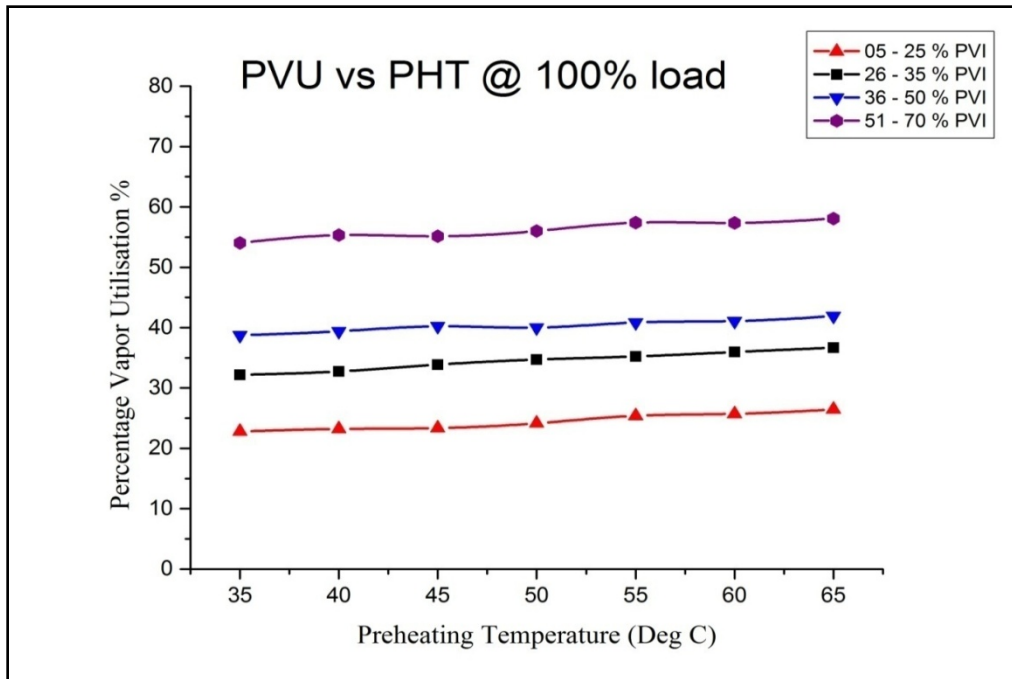


Fig 5.69 Percentage vapourUtilization v/s Preheating Temperature for different %vapour induction at 100 % load at 200 bar injection pressure and at injection timing of 31.5⁰ bTDC

Again for Fig 5.68 and Fig 5.69 at loads 75 % and 100 % the trend observed is same as 50 % load. The explanation given for 50 % load can be again adapted for 75% and 100 % load and the suitable value of percentage vapour can be found out. For 75 % load a suitable percentage vapour of 35.17 % can be obtained for trial 3 which can be further increased to 37.95 % by preheating to 65 °C. For 100 % load a suitable percentage vapour of 38.74 % can be obtained for trial 3 which can be further increased to 41.50 % by preheating to 65 °C.

Table 5.4 gives the maximum % vapour utilisation at different load conditions with and without preheating.

Table 5.4 Maximum percentage vapour possible for different loads

Load %	PVU without preheating	PVU with preheating	Percentage increase in PVU with preheating
50	47.05 %	50.394% at 65 °C	5.92%
75	35.17 %	37.95 % at 65 °C	7.93%
100	38.74 %	41.50 % at 65 °C	7.3 %

5.2.2 EMISSION PARAMETERS

Automobile emissions are dealt with stringent rules nowadays. The newer emission norms demand very less amount of emissions. There are several researches being carried on to develop technologies that would reduce harmful emissions or atleast minimize the need of costlier metals used in after-treatment devices. Here the trend of all the emission parameters at different load and different preheating temperatures for diesel vapor induction are being discussed.

5.2.2.1 Effect of preheating on Carbon Monoxide Emissions (CO)

Carbon monoxide is the toxic byproduct of all hydrocarbon combustion. This is the result of incomplete combustion as enough oxygen would not be present for the carbon monoxide to be converted into carbon dioxide which is harmless.

As seen from the Fig 5.70 the amount of CO decreases with an increase in the preheating temperature. As the preheating temperature increases the in cylinder temperature increases causing better and complete combustion (Zhang et al. 2011). Complete combustion results in more CO₂ emissions subsequently reducing the more harmful CO emissions.

So for 50 % load the minimum amount of CO is obtained at 65 °C preheating temperature and at a percentage vapour of 25.55 %.

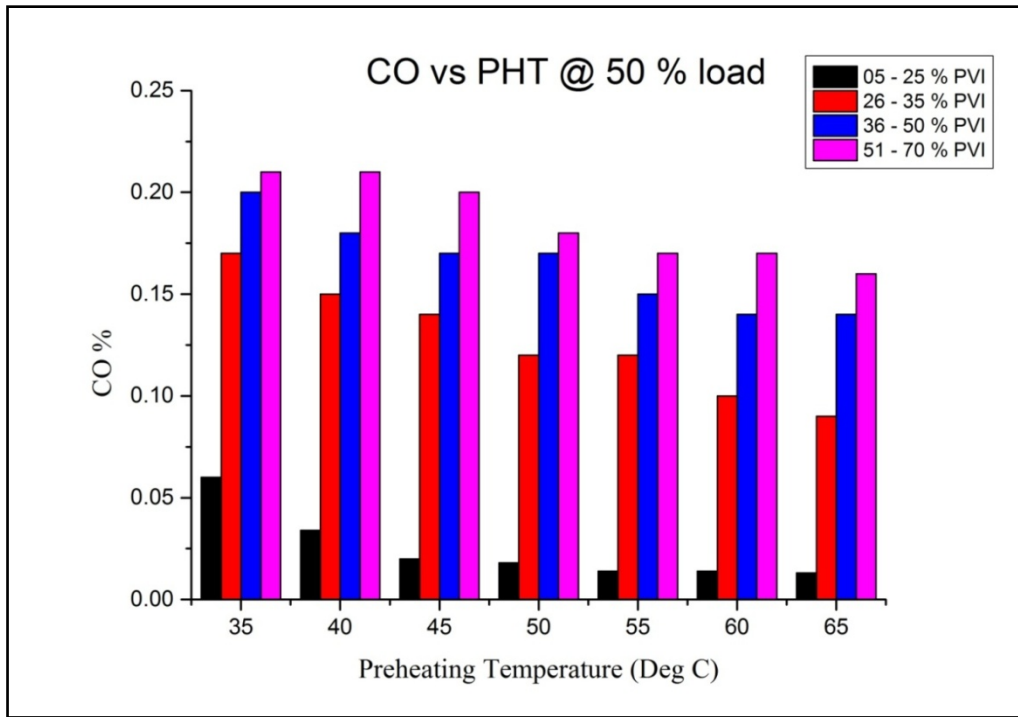


Fig 5.70 Carbon monoxide vs Preheating Temperature for different %vapor induction at 50 % load

Table 5.5 shows the maximum attainable reduction in CO for different percentage vapour at 50 % load. It can be seen from the table that as more vapour is induced the effectiveness of preheating comes down in terms of reduction in CO.

Table 5.5 Maximum reduction in CO for 50 % load

Percentage vapor %	Maximum reduction in CO with preheating at 65 °C
20.49	78.33%
31.98	47.05%
47.05	30 %
59.59	23.80%

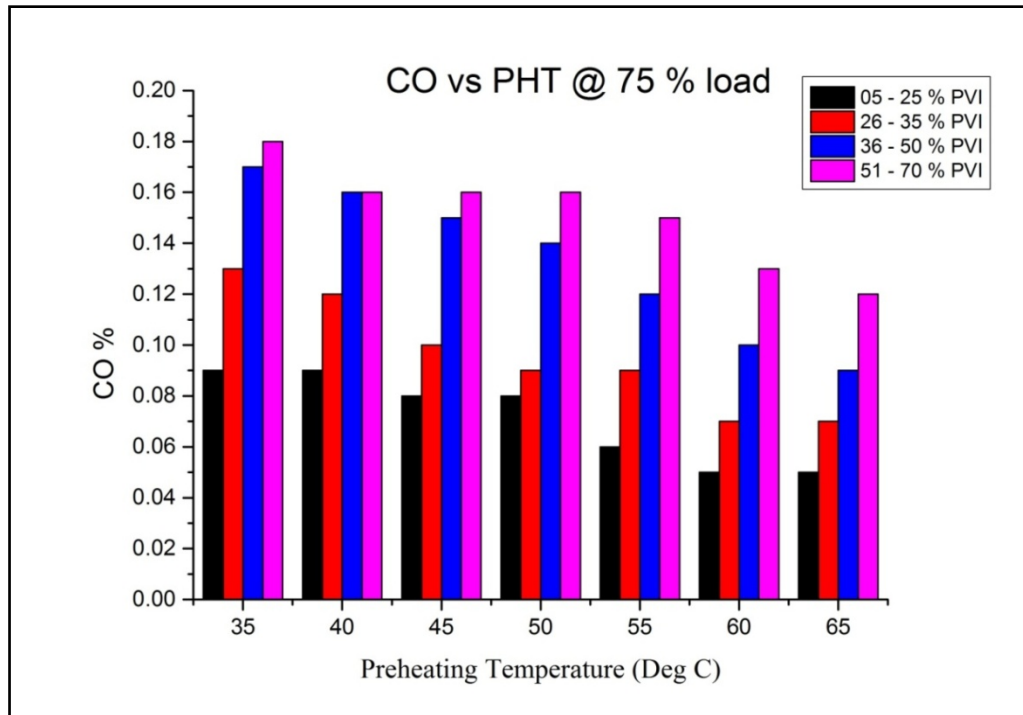


Fig 5.71 Carbon monoxide v/s Preheating Temperature for different vapor induction at 75 % load

As given in Fig. 5.71 for 75 % load the minimum amount of CO is obtained at 55 °C preheating temperature. Table 3.4 shows the maximum attainable reduction in CO for different percentage vapour at 75 % load.

Table 5.6 Maximum reduction in CO for 75 % load

Percentage vapor %	Maximum reduction in CO with preheating
12.53	44.44 %
24.05	45.15 %
35.17	47.05%
52.727	33.33%

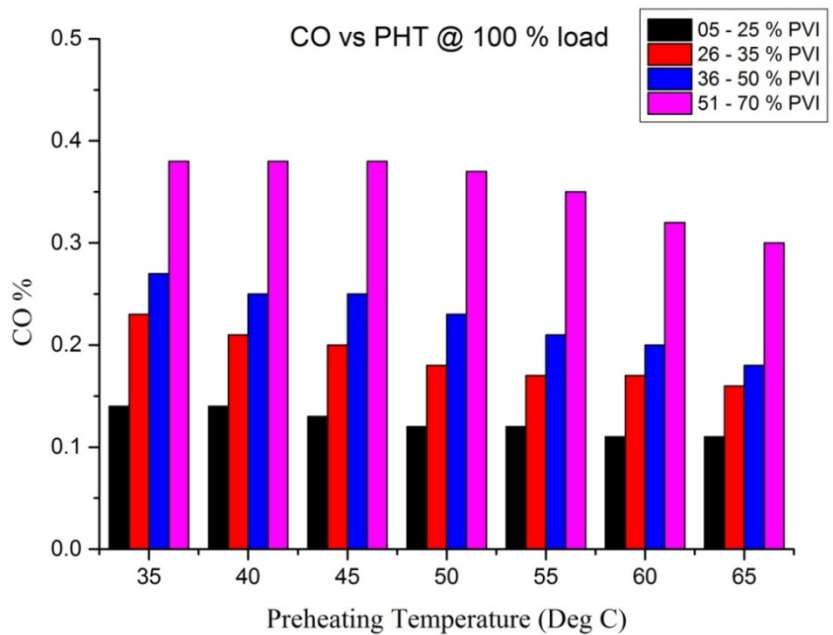


Fig 5.72 Carbon monoxide v/s Preheating Temperature for different % vapor induction at 100 % load

As given in fig. 5.72 for 100 % load the minimum amount of CO is obtained at 65 °C preheating temperature and at a percentage vapour of 25.45%.

Table 5.5 shows the maximum attainable reduction in CO for different percentage vapour at 100 % load

Table 5.7 Maximum reduction in CO for 100 % load

Percentage vapor %	Maximum reduction in CO with preheating
22.794	57.14%
32.18	30.43%
38.74	33.33 %
54.047	21.05%

5.2.2.2 Unburned Hydrocarbons

Different values of PVI in Fig 5.73 indicates an increase in percentage vapour .As seen from the Fig 5.79 for 50 % load with an increase in the preheating temperature there is a decrease in the unburned hydrocarbons. The maximum decrease in ppm of UBHC is obtained at 65 °C at a percentage vapour of 25.55 %. As the preheating temperature increases there is better homogeneity and higher in cylinder temperature. This improves combustion efficiency and results in achieving almost complete combustion. As a result the fraction of unburned hydrocarbons decreases. Even the hydrocarbons trapped in piston rings and crevices take part in combustion due to higher combustion temperature. Thus unburned hydrocarbons reduce to satisfactory levels.

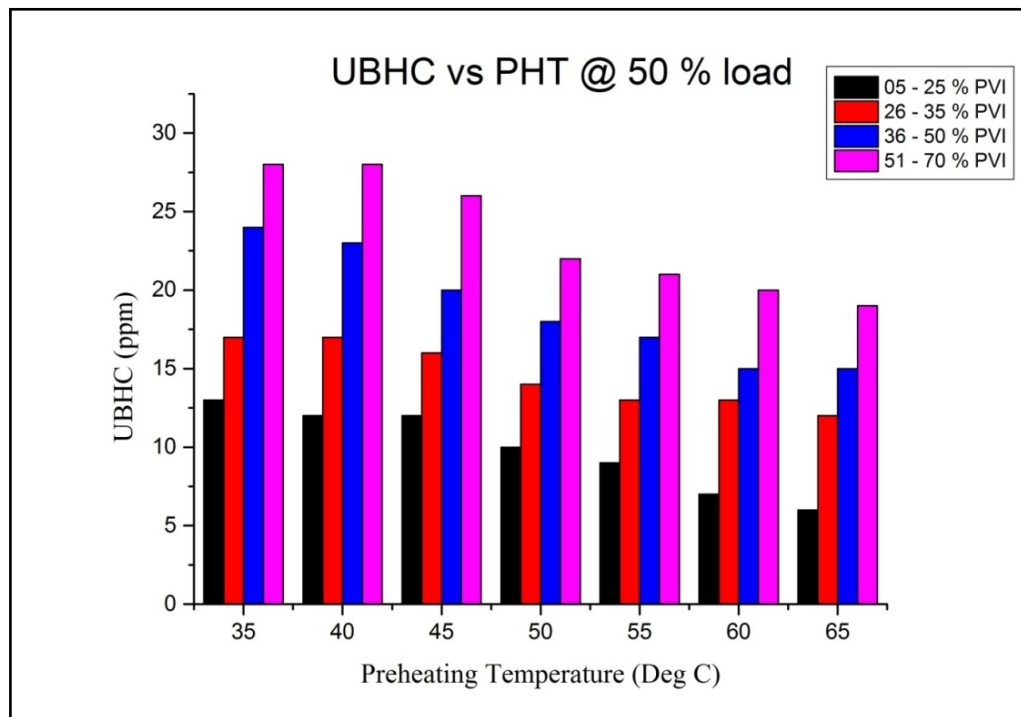


Fig 5.73 Unburned Hydrocarbons vs Preheating Temperature for different vapor induction for 50 % load

Fig 5.74 and 5.75 shows the variation of unburned hydrocarbons with preheating temperature for 75 % and 100 % load respectively. Here also it is clearly evident that the emission of hydrocarbons reduces as the preheating temperature is raised. For 75 % load minimum ppm of unburned hydrocarbons is at 65 °C preheated temperature and at a percentage vapour of 15 %. Whereas for 100 % load the minimum value of unburned hydrocarbons is at 65 °C preheating temperature and at a percentage vapour of 25.45 %

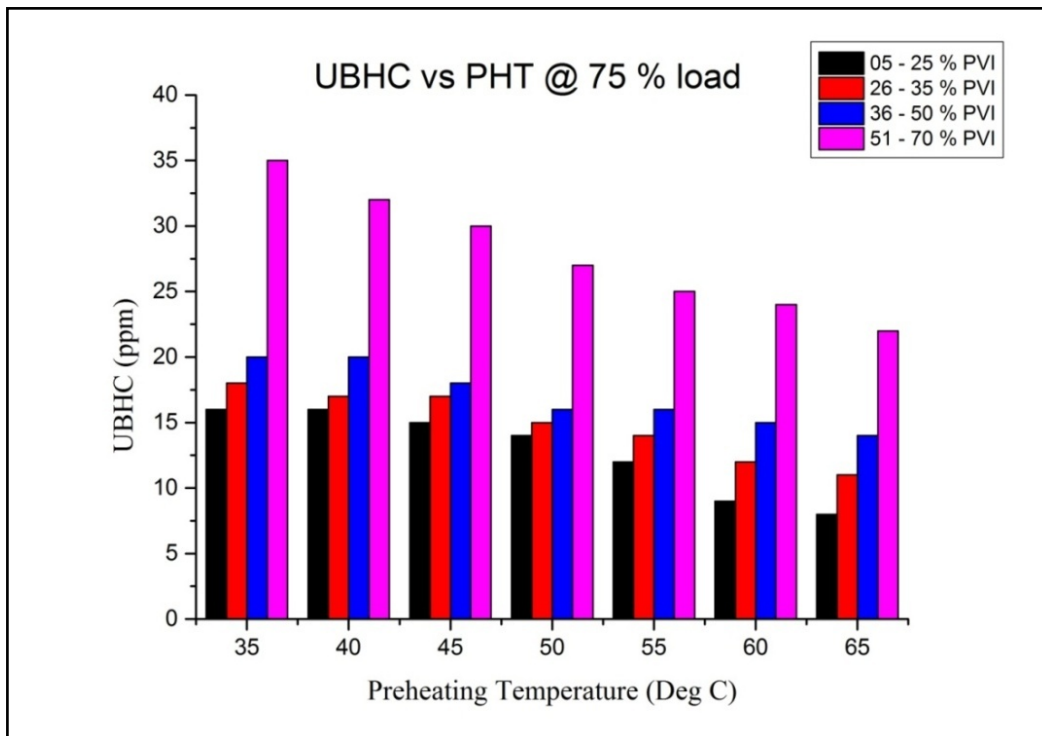


Fig 5.74 Unburned Hydrocarbons vs Preheating Temperature for different % vapor induction for 75 % load

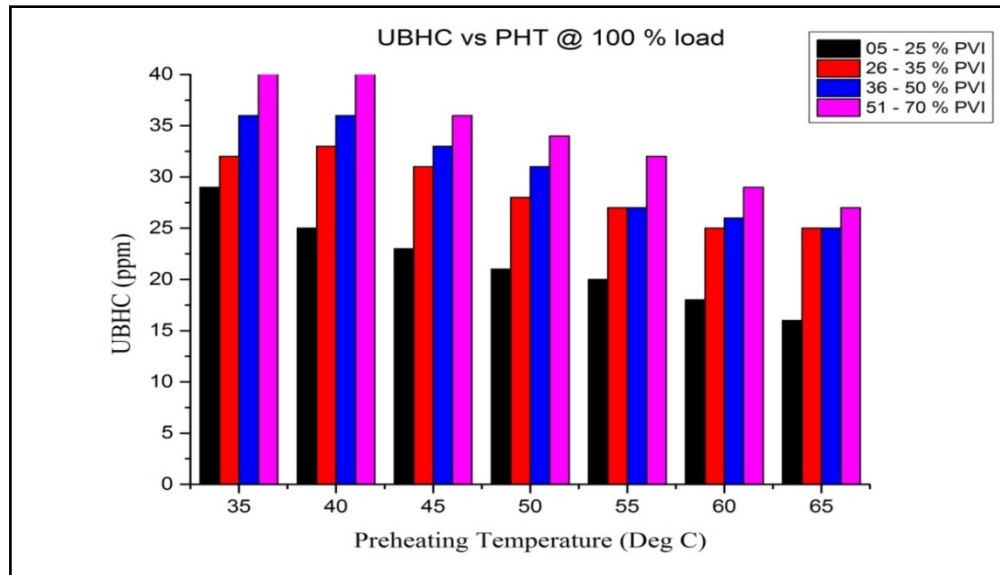


Fig 5.75 Unburned Hydrocarbons vs Preheating Temperature for different %vapor induction for 100 % load

Table 5.8 Operating conditions for minimum UBHC for each load

Load	Minimum UBHC ppm	Percentage vapor %	Maximum percentage decrease %
50	5 at 65 °C	25.55	48.3
75	8 at 65 °C	15	50
100	15 at 65 °C	25.45	44.82

5.2.2.3 Effect of preheating on NO_x emissions

As seen from the Fig 5.76 preheating results in an increase in the NO_xemissions. With increase in the preheating temperature, combustion efficiency increases causing a simultaneous rise in engine cylinder temperature. This causes the NO_x emission to increase. This result can be correlated to section 5.2.1.3 which explains the increase in exhaust gas temperature with preheating.

Again, as given in Fig 5.76 to 5.78 NO_x increased with an increase in the preheating temperature. Maximum NO_x (789 ppm) is seen for 100 % load at a preheating temperature of 65 °C and at a percentage vapour of 58.054 %.

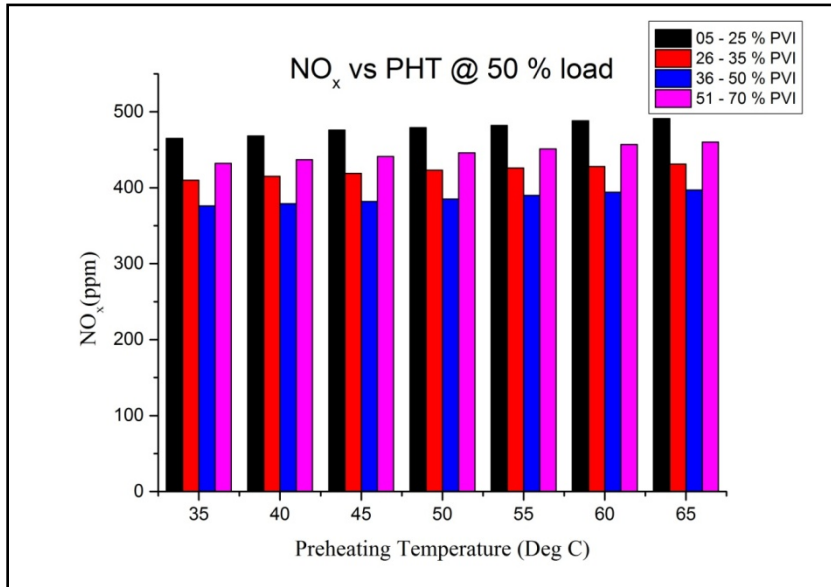


Fig 5.76 NO_x vs Preheating temperature for 50 % load at different %vapor induction

Thus preheating is not advised if reduction in NO_x is the main objective. Table 5.9 shows the maximum increase in NO_x for all loads when preheating was employed.

Table 5.9 Preheating employed for minimum NO_x condition

% Maximum Load	NOx without preheating	NOx with preheating (Maximum)	Percentage increase
50	375	397	5.58%
75	388	411	5.92%
100	585	507	3.5%

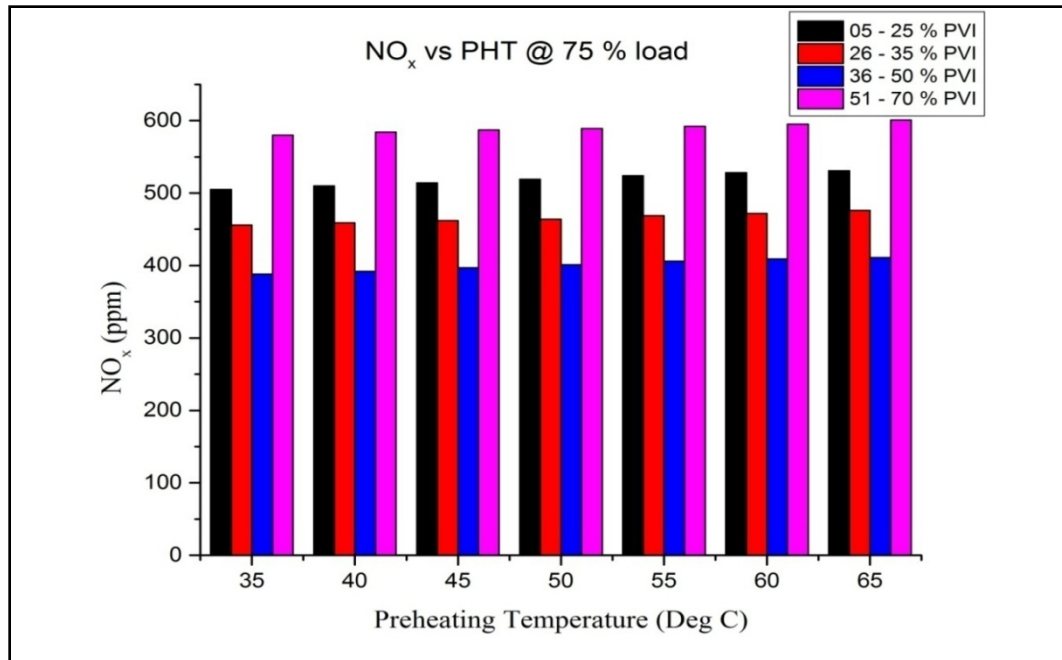


Fig 5.77 NO_x vs Pre-heating temperature for 75 % load at different %vapor induction

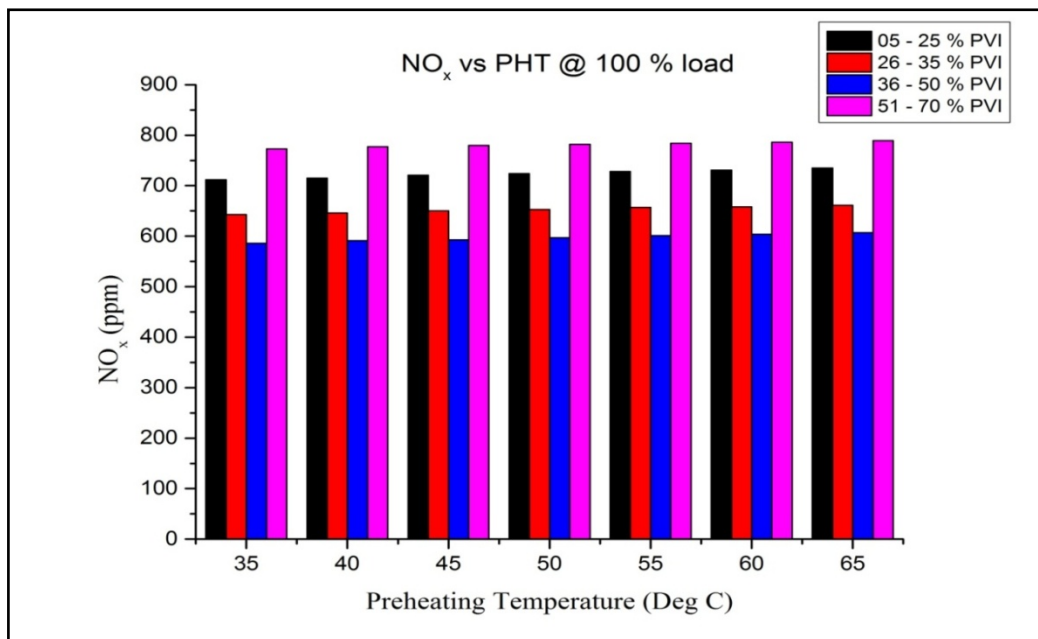


Fig 5.78 NO_x vs Preheating temperature for 100 % load at different %vapor induction

5.2.2.4 Effect of Preheating on smoke opacity

As seen from Fig 5.79, 5.80 and 5.81 smoke emissions decrease with more vapor induction. Also preheating the air reduced the smoke emissions due to better combustion of the charge. As given in Fig 5.80 for 75 % load the minimum smoke is seen at a percentage vapor of 37.95 % and at preheating temperature of 65 °C. When more vapour was inducted smoke started to increase due to abnormal combustion.

As given in fig. 5.81 for 100 % load the minimum value of smoke is 57 % opacity at 65 °C and a percentage vapour of 41.5 %.

The reason for low smoke emission is due to the absence of rich fuel pocket inside the combustion chamber. HCCI engine uses lean air–fuel charge and combustion takes place at multiple points in the combustion chamber at the same time, which eliminates rich fuel region, due to that, HCCI engine has low smoke emissions than the conventional diesel engine.

However for 50 % load smoke was seen increasing with more vapour inducted. This may be due to poor vapor quality and low in cylinder temperature at lower loads.

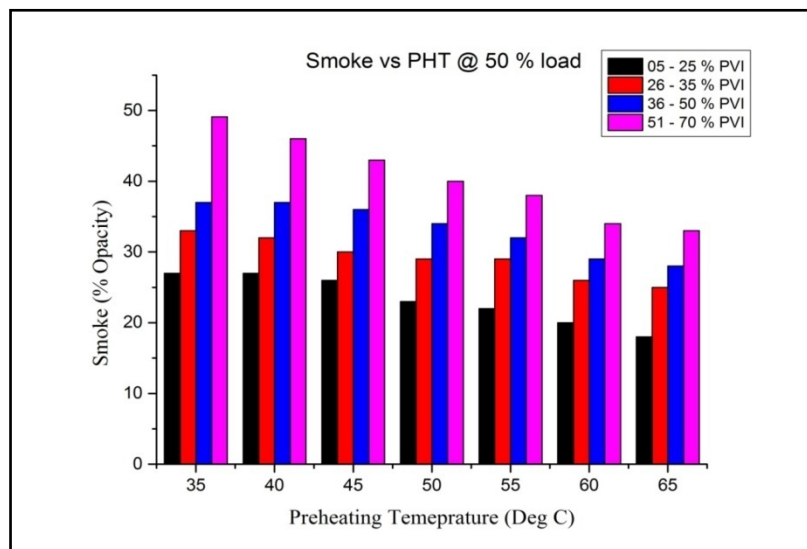


Fig 5.79 Smoke opacity vs preheating temperature for 50 % load for different %vapor induction

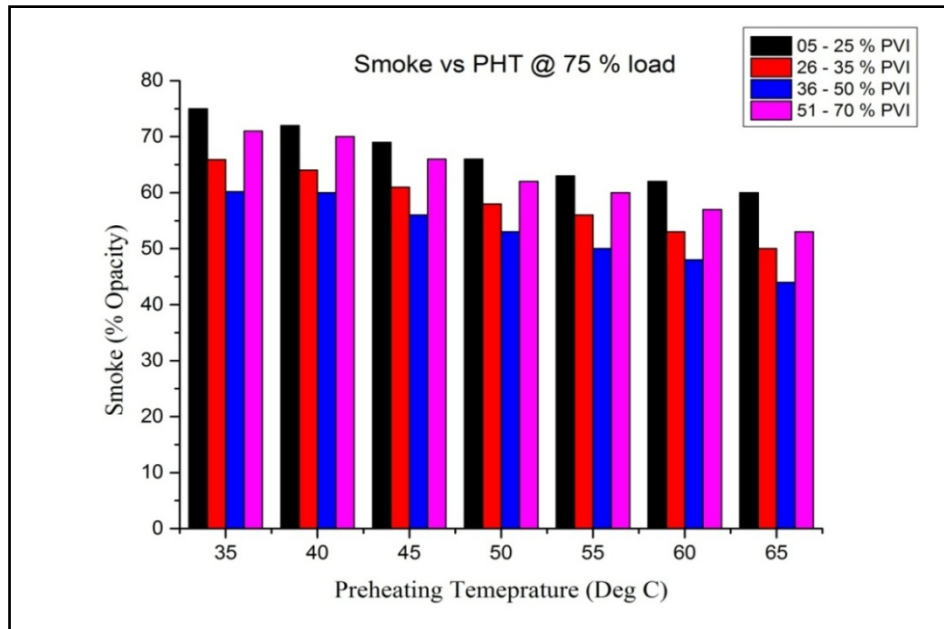


Fig 5.80 Smoke opacity vs preheating temperature for 75 % load for different vapor induction

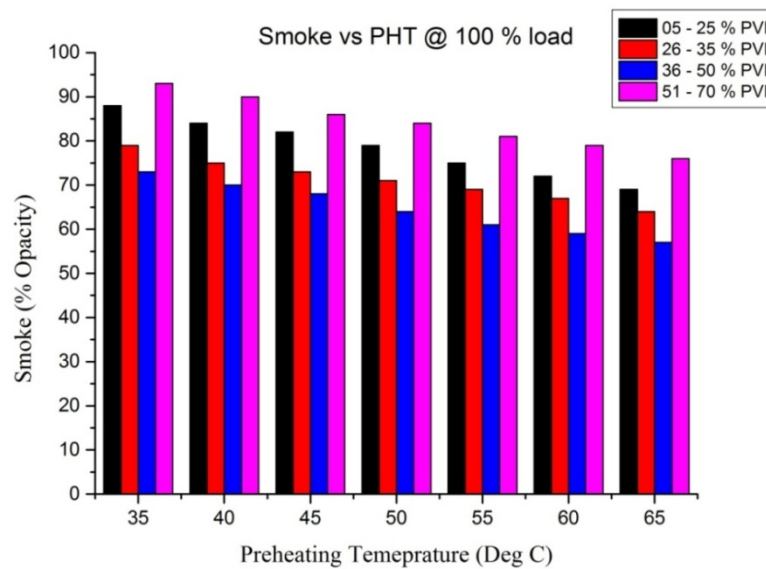


Fig 5.81 Smoke opacity vs preheating temperature for 100 % load for different % vapor induction

5.2.3 Net Heat Release rate

The net heat release trends for various load conditions in conventional mode and HCCI mode with preheating are given in figures 5.82 to 5.84 respectively. Heat release calculations are an attempt to get some information about the combustion process in an engine. The vapour induction and preheating results in the advancement of maximum net heat release rate. This is a clear indication of achieving HCCI mode of combustion by vapour induction. Further by increasing the preheating the temperature the mixture becomes more homogenous and the net heat release rate is decreased.

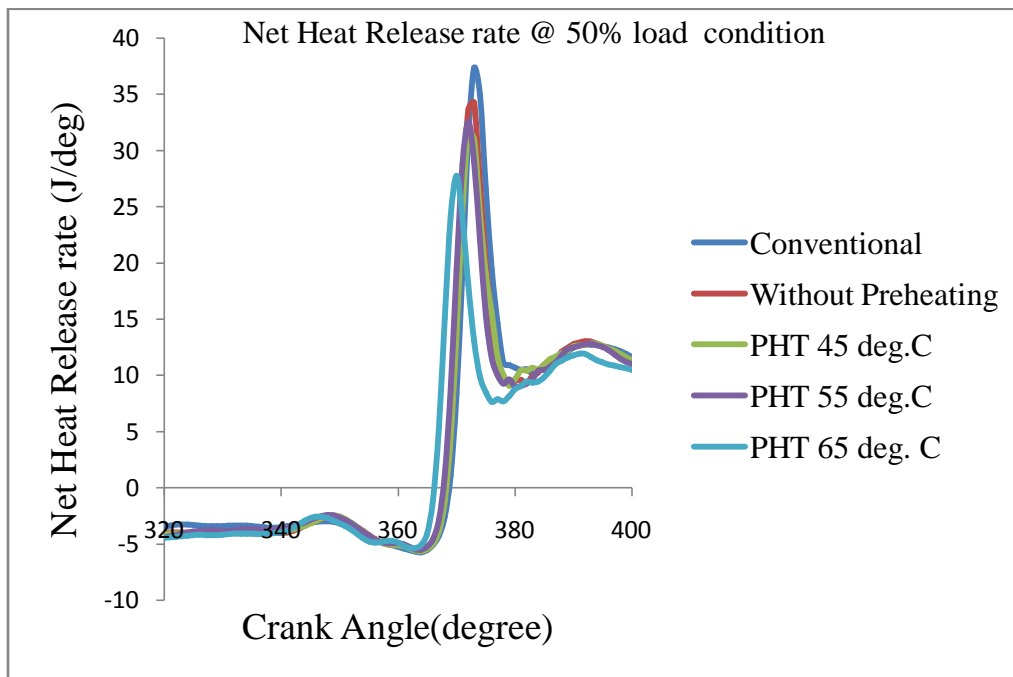


Fig 5.82 Net Heat Release rate at 50% load and different preheating temperatures.

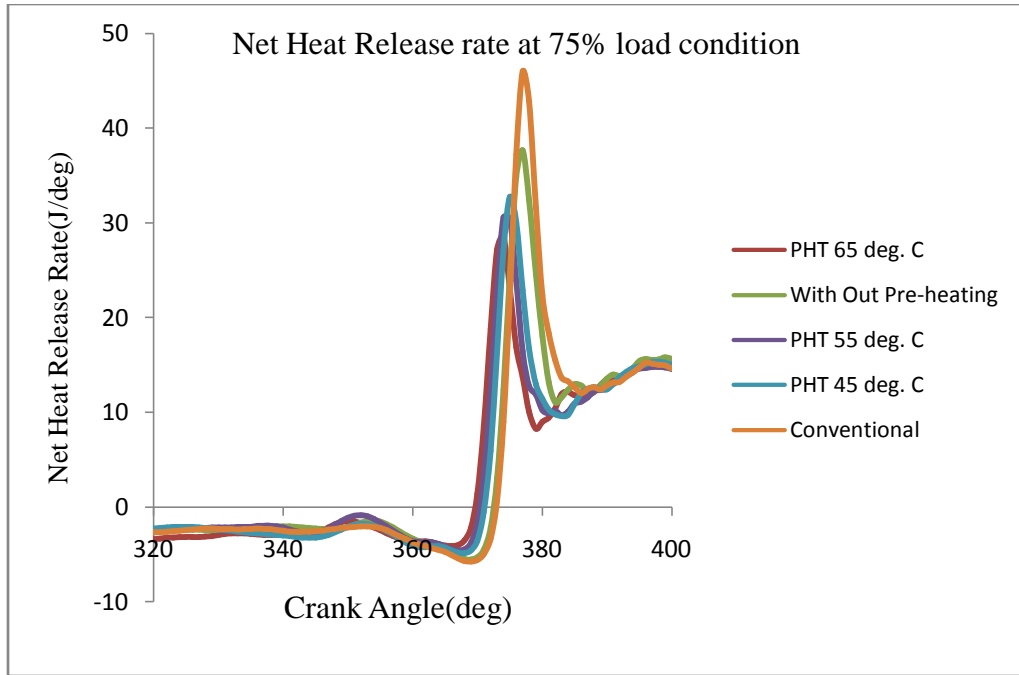


Fig 5.83 Net Heat Release rate at 75% load and different preheating temperatures.

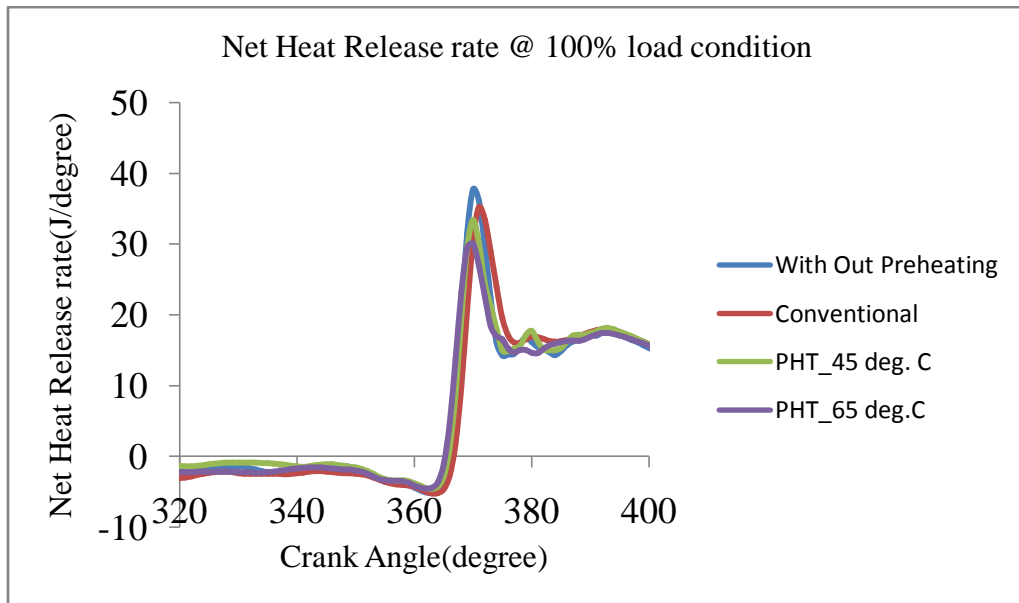


Fig 5.84 Net Heat Release rate at 100% load and different preheating temperatures.

5.2.4 Cumulative Heat Release rate

The cumulative heat release trends for various load conditions in conventional mode and HCCI mode with preheating are given in figures 5.85 to 5.87 respectively. It is found that CHRR decreases by inducing vapour fuel and increasing the air inlet temperature. This is an indication of lean combustion as the mixture becomes more and more homogeneous. The minimum value of CHRR is shortly TDC for all load conditions.

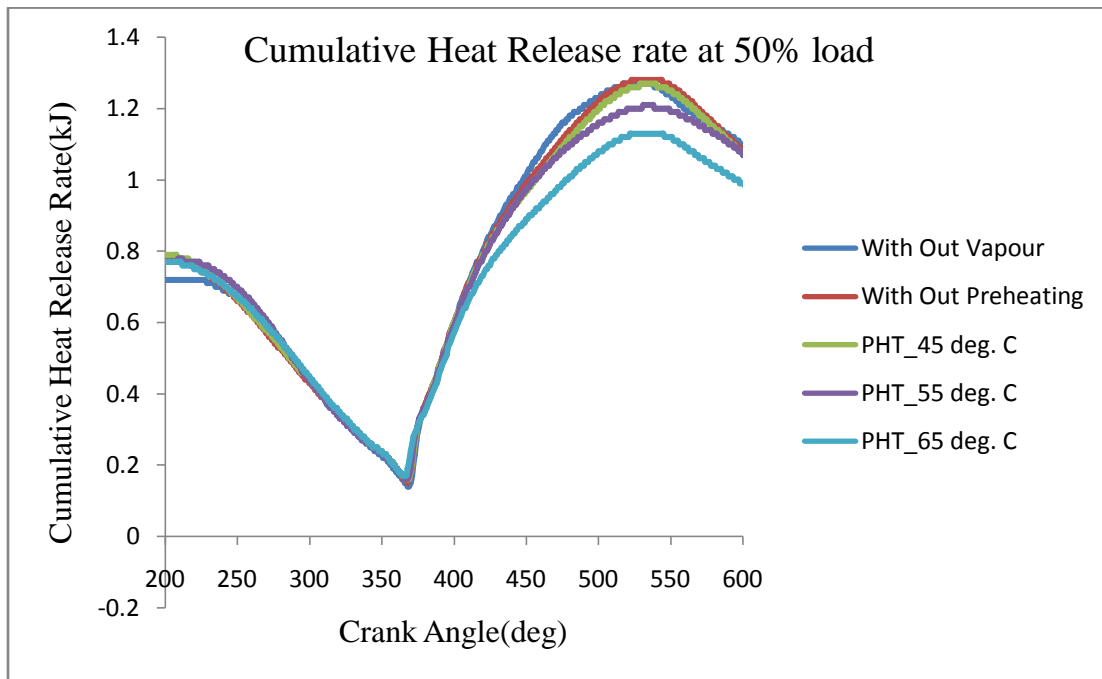


Fig 5.85 Cumulative Heat Release rate at 50% load and different preheating temperatures

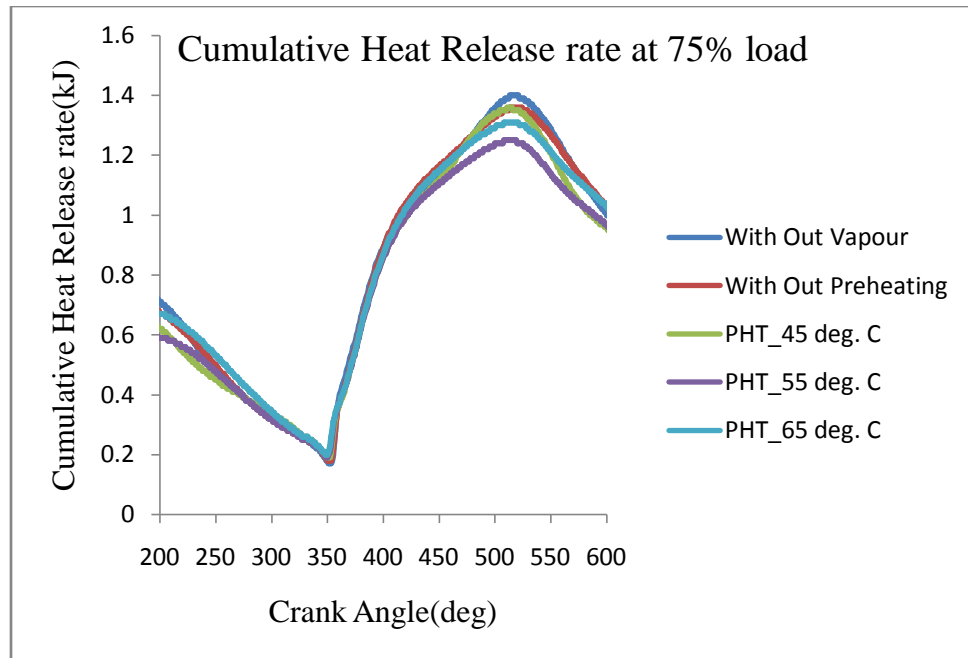


Fig 5.86 Cumulative Heat Release rate at 75% load and different preheating temperatures

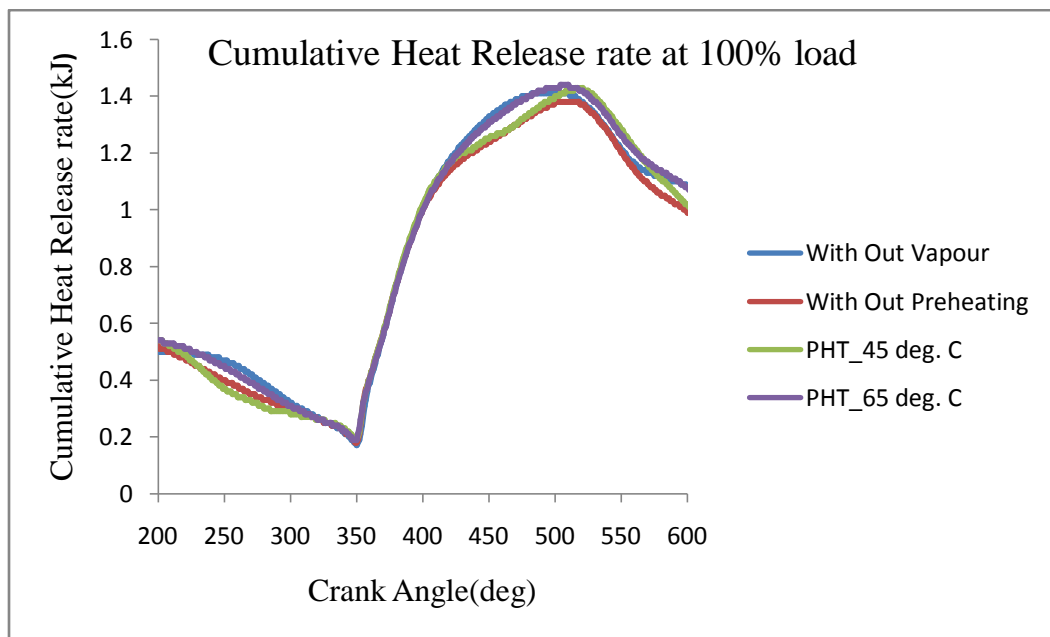


Fig 5.87 Cumulative Heat Release rate at 100% load and different preheating temperatures

[This page is kept intentionally blank]

CHAPTER 6

CONCLUSIONS AND SCOPE FOR FUTURE WORK

The investigation was focused on the effect of diesel vapour induction on the engine performance and to try and achieve HCCI mode of combustion in the engine. The percentage diesel vapour and preheating temperatures were varied and tests were conducted at 50%, 75% and 100% load conditions to find out the optimum conditions for vapour induction. The performance and emission study of the engine was done at each test condition and as described in the previous chapters favorable conditions are found out. It was found that the operation of engine using diesel vapour depends on a variety of parameters. For different load conditions the vapour produced from heat exchanger was successfully utilized for combustion. Major conclusions that are drawn from the experimental analysis, along with details as to how to adjust the different parameters to suit vapour induction, summary and future work to be carried out are discussed in this chapter.

- ✓ Exhaust gas heat from the engine that is normally goes as waste is successfully utilized by using a designed shell and tube heat exchanger.
- ✓ A compact shell and tube type heat exchanger can provide diesel vapour with sufficient degree of superheat (50° C) required to be inducted in combustion chamber.
- ✓ The total amount of diesel being consumed can be decreased with vapour mode of induction of diesel under proper constraints.
- ✓ For every load there is a limit on the maximum amount of vapour that can be fed without compromising on engine performance.
- ✓ The experimental analysis on the engine revealed that a delayed injection timing of 31.5 deg. bTDC and higher injection pressure - 200 bar is the optimum condition for diesel vapour induction.

- ✓ The vapour induction mode gave highest brake thermal efficiency at 31.5 deg. bTDC and 200 bar injection pressure. A maximum of 20.54 % increase in brake thermal efficiency is obtained at 75 % load.
- ✓ Brake specific fuel consumption decreased with increase in vapour induction.
- ✓ NO_x emissions are reduced upto a maximum of around 50% at 31.5 deg. bTDC, 200 bar injection pressure and in vapour induction by 37%. Average reduction in NO_x emissions with increase in vapour induction is 24%.
- ✓ On a whole the work showed that partially vapourising the fuel in CI diesel engine would increase the efficiency and decrease the NO_x emissions and PM at the cost of increase of CO (increased by 31.25%) and HC emissions(increased by 47%).
- ✓ Preheating of vapour increased the brake thermal efficiency and the maximum efficiency is 33. 5% seen at 75% load for 65 °C and at a percentage vapour of 37.95 %.
- ✓ Preheating also improved the percentage vapour utilization .A percentage increase of 5.91 %,7.93 % and 7.3 % in percentage vapour is found for 50 %,75 % and 100 % load for the optimum conditions.
- ✓ CO emission is found to increase with increase in vapour fraction but it is successfully reduced by preheating of air. A maximum reduction of 78.33 %, 45.15 % and 57.14 % in CO emissions is attained by preheating of air at 50, 75 and 100 % load respectively.
- ✓ Unburned hydrocarbon emissions increases with increase in vapour fraction but is successfully reduced by preheating of air. A maximum percentage decrease of 48.3%, 50% and 44.82 % was attained by preheating for loads 50,75 and 100 % respectively.
- ✓ Nitrogen oxides emission is reduced by inducting more vapour fraction, however preheating resulted in an increase in NO_x emissions. Maximum NO_x reduction is attained at a percentage vapour of 47.05%, 35.17 %,38.7 % for

50,75 and 100 % load respectively. The corresponding percentage decrease in NO_x are 20.84 %,24.5 % and 18.51 % respectively.

- ✓ Smoke emissions decreases with increase in vapour fraction at higher loads but at 50 % load, smoke is found to increase with increase in vapour fraction.
- ✓ The vapour induction and preheating results in the advancement of maximum net heat release rate. This is a clear indication of achieving HCCI mode of combustion by vapour induction.
- ✓ The most suitable operating condition for HCCI mode can be identified at 75 % load coupled with 65 °C preheating.
- ✓ The increase in vapour mass fraction increased the performance of the engine. This is mainly because the HCCI mode of combustion is approached. At the same time the start of combustion is still governed by the injection of vapour fuel. This gives a method to control of combustion which is normally absent in HCCI engines.

6.1 SCOPE FOR FUTURE WORK

Following are some of the suggestions for improving the HCCI setup and areas of further research.

- ❖ Modification of the combustion chamber can be done by increasing or decreasing the compression ratio according to the requirement.
- ❖ Tests can be done by using some light fuel blends such as acetyl, cyclohexane, propane, etc. to reduce the boiling temperature and increase the mass flow of vapourised fuel.
- ❖ Stability is an issue with HCCI engines. Different fuels, bio fuels, additives and various substitute fuels as hydrogen, CNG etc., can be tested for their effect on stability.
- ❖ Cooled EGR technique is one of the combustion control method normally used and this can be studied.

- ❖ The effect of cooling water flow can be studied and exploited to use as a combustion control technique.
- ❖ Quick and precise control is required in the HCCI engine. An electronic control system for changing the parameters of the engine would be helpful in future.
- ❖ Additives can be used to improve the auto ignition temperature of the diesel fuel, and thereby controlling the start of ignition with more precision.
- ❖ Thermodynamic analysis of the combustion process with all possibilities of auto ignition can be carried out for further analysis.
- ❖ Ion voltage obtained through “Lab View” can be integrated to the “Engine Soft” so that experimental analysis can be done on the engine without using the piezo transducer.

REFERENCES

- Abdul Khaliq, Shailesh K. Trivedi and Ibrahim Dincer (2011),“Investigation of a wet ethanol operated HCCI engine based on first and second law analyses”, *Applied Thermal Engineering*, 31, 1621-1629.
- Amit Bhawe, Markus Kraft, Luca Montorsi and Fabian Mauss (2007), “Sources of CO emissions in an HCCI engine: A numerical analysis”, *Combustion and Flame*,144, 634–637.
- Anders Hultqvist, Andreas Vressner, Petter Strandh, Per Tunestal and Bengt Johansson (2004), “Multiple point Ion current Diagnostics in an HCCI engine”, *SAE Technical Paper Series*, 2004 – 01 – 0934.
- Andreas Vressner, Anders Hultqvist, Per Tunestal and Bengt Johansson (2005), “Fuel Effects on Ion current in an HCCI Engine”, *SAE Technical Paper Series*, 2005– 01 – 2093.
- Andreas Vressner, Andreas Lundin, Magnus Christensen, Per Tunestal and Bengt Johansson (2003), “Pressure Oscillation during Rapid HCCI Combustion”, *SAE Technical Paper Series*, 2003 – 01 – 3217.
- Annarita Viggiano and Vinicio Magi (2012),“A comprehensive investigation on the emissions of ethanol HCCI engines”, *Applied Energy*, 93, 277–287.
- Anthony Dubreuil, Fabrice Foucher, Christine Mounaim Rousselle, Guillaume Dayma and Philippe Dagaut (2007), “HCCI combustion: Effect of NO in EGR”, *Proceedings of the Combustion Institute*, 31, 2879–2886.
- Bang Quan He, Mao Bin Liua, Hua Zhao (2015), “Comparison of combustion characteristics of n-butanol/ ethanol–gasoline blends in a HCCI engine”, *Energy Conversion and Management*, 95, 101–109.
- Cai Lu Xing, Chen Wei, Huang Zhen (2005). “A fundamental study on the control of HCCI combustion and emissions by fuel design concept combined with controllable EGR”, *Fuel* , 84, 1084-1092.

Can Cinar ,Ozer Can, FatihSahin, SerdarYucesu, H. (2009). “Effects of premixed diethyl ether (DEE) on combustion and exhaust emissions in a HCCI-DI diesel engine” *Applied Thermal Engineering*, 30, 360–365.

Can Cinar, Ahmet Uyumaz, Hamit Solmaz,Tolga Topgul.(2015), “ Effects of valve lift on the combustion and emissions of a HCCI gasoline engine”, *Energy Conversion and Management* ,94, 159–168.

Christensen Magnus and Johansson Bengt (1998),“Influence of Mixture Quality on Homogeneous Charge Compression Ignition” ,*SAE Technical paper series – 1998*.

Chunhua Zhang, Han Wu (2016), “Combustion characteristics and performance of a methanol fueled homogenous charge compression ignition (HCCI) engine”, *Journal of the Energy Institute* ,89, 346-353.

Gajendra Singh, Akhilendra Pratap Singh, Avinash Kumar Agarwal(2014) , “Experimental investigations of combustion, performance and emission characterization of biodiesel fuelled HCCI engine using external mixture formation technique”, *Sustainable Energy Technologies and Assessments* ,6 , 116–128

Ganesh, D., Nagarajan, G. (2010),“ Homogeneous charge compression ignition (HCCI) combustion of diesel fuel with external mixture formation”, *Energy* ,35 , 148–157.

Ganesh, D., Nagarajan, G., Mohamed Ibrahim M. (2008), “Study of performance, combustion and emission characteristics of diesel homogeneous charge compression ignition (HCCI) combustion with external mixture formation”, *Fuel* ,87 , 3497–3503.

Gregory Bogin Jr., Jyh Yuan Chen, Robert W. Dibble (2009),“The effects of intake pressure, fuel concentration and bias voltage on the detection of ions in a Homogeneous Charge Compression Ignition (HCCI) engine”, *Proceedings of the Combustion Institute*, 32, 2877–2884

Gregory Chin, J.Y. Chen (2011), “Modeling of emissions from HCCI engines using a consistent 3-zone model with applications to validation of reduced chemistry”, *Proceedings of the Combustion Institute* ,33 , 3073–3079.

Haifeng Liu , Peng Zhang , Zheming Li , Jing Luo, ZunqingZheng , Mingfa Yao (2011), “Effects of temperature in homogeneities on the HCCI combustion in an optical engine” *Applied Thermal Engineering* ,1-7.

Haruyuki Yokota, Yugo kudo, Hiroshi Nakajima, Toshiaki Kakegawa and Takashi Suzuki (1997), “A new concept of low emission diesel combustion”,*Society of Automobile Engineers*

Hatim Machrafi, Simeon Cavadias, Jacques Amouroux (2008), “A parametric study on the emissions from an HCCI alternative combustion engine resulting from the auto-ignition of primary reference fuels”, *Applied Energy*, 85, 755–764.

Hatim Machrafi, Simeon Cavadias, Jacques Amouroux (2009), “Influence of fuel type, dilution and equivalence ratio on the emission reduction from the auto-ignition in an Homogeneous Charge Compression Ignition engine”, *Energy*, 35, 1829–1838.

Hatim Machrafi, Simeon Cavadias, Philippe Guibert (2007), “An experimental and numerical investigation on the influence of external gas recirculation on the HCCI autoignition process in an engine: Thermal, diluting, and chemical effects” *Combustion and Flame*, 155, 476–489.

Hui Xie , Le Li, Tao Chen, Hua Zhao(2014), “ Investigation on gasoline homogeneous charge compression ignition (HCCI) combustion implemented by residual gas trapping combined with intake preheating through waste heat recovery”, *Energy Conversion and Management* ,86, 8–19.

Hyung Jun Kim , Kwan Soo Lee , Chang Sik Lee (2011), “A study on the reduction of exhaust emissions through HCCI combustion by using a narrow spray angle and advanced injection timing in a DME engine”, *Fuel Processing Technology* ,92, 1756–1763.

Iván D. Bedoya, Samveg Saxena, Francisco J. Cadavid, Robert W. Dibble, Martin Wissink (2012), “Experimental study of biogas combustion in an HCCI engine for power generation with high indicated efficiency and ultra-low NO_x emissions”,*Energy Conversion and Management* ,53, 154–162

Jacek Hunicz (2014), “An experimental study of negative valve overlap injection effects and their impact on combustion in a gasoline HCCI engine”, *Fuel* ,117, 236–250.

Javad Rezaei, Mahdi Shahbakhti , Bahram Bahri , Azhar Abdul Aziz(2015), “ Performance prediction of HCCI engines with oxygenated fuels using artificial neural networks”, *Applied Energy* ,138, 460–473.

John E. Dec (2009). “Advanced compression-ignition engines understanding the in-cylinder processes”, *Proceedings of the Combustion Institute*, 32, 2727–2742.

John H Mack, Bruce A Buchholz, Daniel L Flowers, Robert W Dibble (2005), “The effect of the di-tertiary butyl peroxide additive on HCCI combustion of fuel blends of ethanol and diethyl ether” *SAE international paper* , 2005-01-2135

Junjun Ma, Xingcai Lu, Libin Ji, Zhen Huang (2008), “An experimental study of HCCI-DI combustion and emissions in a diesel engine with dual fuel”, *International Journal of Thermal Sciences* ,47, 1235–1242

Junnian Zheng, Jerald A. Caton (2012) ,“Effects of operating parameters on nitrogen oxides emissions for a natural gas fueled homogeneous charged compression ignition engine (HCCI): Results from a thermodynamic model with detailed chemistry”, *Applied Energy* ,92, 386–394.

Khandala, S.V., Banapurmath, N.R., Giaconda, V.N. , Hiremath, S.S. (2017), “Paradigm shift from mechanical direct injection diesel engines to advanced injection strategies of diesel homogeneous charge compression ignition (HCCI) engines- A comprehensive review”, *Renewable and Sustainable Energy Reviews* ,70, 369–384.

Komninos, N.P. (2009), “Investigating the importance of mass transfer on the formation of HCCI engine emissions using a multi-zone model”, *Applied Energy* ,86, 1335–1343.

Kyeonghyeon Lee, Seokwon Cho, Namho Kim, Kyoungdoug Min(2015), “ A study on combustion control and operating range expansion of gasoline HCCI”, *Energy* ,91, 1038-1048.

Lijima, A., Yoshida, K., Shoji, H., and Lee, J. T. (2007). “Analysis of HCCI combustion Characteristics based on experimentation and simulation- influence of fuel octane number

and internal EGR on combustion” *International journal of Automotive Technology*, 8 , 137-147.

Lu Xing cai , Hou Yuchun, Zu Linlin, Huang Zhen(2006),“Experimental study on the auto-ignition and combustion characteristics in the homogeneous charge compression ignition (HCCI) combustion operation with ethanol/n-heptane blend fuels by port injection”, *Fuel* ,85, 2622–2631.

Ma Junjun, Lu Xing Cai, Ji Libin(2008), “ An experimental study of HCCI-DI combustion emissions in a diesel engine with dual fuel”, *International Journal for Thermal sciences* ,47 ,1235-1242.

Magnus Sjoberg , John E. Dec (2007), “Comparing late-cycle auto ignition stability for single-and two-stage ignition fuels in HCCI engines” ,*Proceedings of the Combustion Institute* ,31 ,2895–2902.

Magnus Sjoberg, John E. Dec (2011), “ Effects of EGR and its constituents on HCCI auto ignition of ethanol”, *Proceedings of the Combustion Institute* ,33, 3031–3038.

Mahrous,A.F.M.,Potrzebowski,A., Wyszynski,M.L., Xu,H.M., Tsolakis,A. and Luszcz, P. (2009), “A modelling study into the effects of variable valve timing on the gas exchange process and performance of a 4-valve DI homogeneous charge compression ignition (HCCI) engine”, *Energy Conversion and Management*, 50, 393–398.

Mathivanan, K., Mallikarjuna, J. M., Ramesh A.(2016), “ Influence of multiple fuel injection strategies on performance and combustion characteristics of a diesel fuelled HCCI engine – An experimental investigation”,*Experimental Thermal and Fluid Science* ,77, 337–346.

Mehresh, P., Souder, J., Flowers, D., Riedel, U., Dibble, R.W. (2005), “Combustion timing in HCCI engines determined by ion-sensor: experimental and kinetic modeling”, *Proceedings of the Combustion Institute*, 30, 2701–2709.

Miguel Torres Garci, Francisco Jose, Jimenez Espadafor Aguilar,Tomas Sanchez Lencero (2009),“Experimental study of the performances of a modified diesel engine operating in homogeneous charge compression ignition (HCCI) combustion mode versus the original diesel combustion mode” *Energy*, 34, 159–171.

Miguel Torres Garcia, Francisco, J., Jiménez Espadafor Aguilar, José A. Becerra Villanueva, Elisa Carvajal Trujillo (2011), “Analysis of a new analytical law of heat release rate (HRR) for homogenous charge compression ignition (HCCI) combustion mode versus analytical parameters”, *Applied Thermal Engineering* ,31, 458 – 466.

Ming Jia , Maozhao Xie , Tianyou Wang , Zhijun Peng(2011) ,“The effect of injection timing and intake valve close timing on performance and emissions of diesel PCCI engine with a full engine cycle CFD simulation”, *Applied Energy* ,88 , 2967–2975.

Mingfa Yao, Zhaolei Zheng, Haifeng Liu (2009), “Progress and recent trends in homogeneous charge compression ignition (HCCI) engines” ,*Progress in Energy and Combustion Science* ,35, 398–437.

Morteza Fathi, Khosh bakhti Saray, R., David Checkel,M.(2010). “Detailed approach for apparent heat release analysis in HCCI engines”, *Fuel* , 89 , 2323–2330.

Morteza Fathi, Omid Jahanian,Mahdi Shahbakhti(2017), “ Modeling and controller design architecture for cycle-by-cycle combustion control of homogeneous charge compression ignition (HCCI) engines – A comprehensive review”, *Energy Conversion and Management* ,139, 1–19.

Mustafa Canakci (2008), “An experimental study for the effects of boost pressure on the performance and exhaust emissions of a DI-HCCI gasoline engine”, *Fuel* , 87, 1503–1514.

Mustafa Canakci (2012), “Combustion characteristics of a DI-HCCI gasoline engine running at different boost pressures”, *Fuel* , 96, 546 – 555.

Myung Yoon Kim, Chang Sik Lee(2007), “Effect of a narrow fuel spray angle and a dual injection configuration on the improvement of exhaust emissions in a HCCI diesel engine”, *Fuel* ,86, 2871 – 2880.

Onishi, S., Jo, S.H., Shoda, K., Jo, P.D., and Kato, S. (1979), “Active Thermo-Atmosphere Combustion (ATAC) – A new Combustion Process for internal combustion engines”, *SAE Paper*, 790501.

Pandiyarajan, V., Chinna Pandian, M. E., Velraj, R., Seeniraj, R.V. (2011), "Experimental investigation on heat recovery from diesel engine exhaust using finned shell and tube heat exchanger and thermal storage system", *Applied Energy*, 88, 77–87.

Pranab Das, Subbarao, P.M.V., Subrahmanyam, J.P. (2015), "Effect of main injection timing for controlling the combustion phasing of a homogeneous charge compression ignition engine using a new dual injection strategy", *Energy Conversion and Management*, 95, 248–258.

Pravin Kumar, Rehman, A., (2016), "Bio-diesel in homogeneous charge compression ignition (HCCI) combustion", *Renewable and Sustainable Energy Reviews*, 56, 536–550.

Qian Zuo qin, Lu Xing cai (2006), "Characteristics of HCCI engine operation for additives, EGR, and intake charge temperature while using iso-octane as a fuel", *Zhejiang Univ SCIENCE*, 252-258.

Qiang Fang, Junhua Fang, Jian Zhuang, Zhen Huang (2012) "Influences of pilot injection and exhaust gas recirculation (EGR) on combustion and emissions in a HCCI-DI combustion engine", *Applied Thermal Engineering*, 48, 97 – 104.

Rakesh Kumar Maurya, Dev Datt Pal, Avinash Kumar Agarwal (2011), "Digital signal processing of cylinder pressure data for combustion diagnostics of HCCI engine", *Mechanical Systems and Signal Processing*, 10, 108 – 115.

Rakesh Kumar Maurya, Avinash Kumar Agarwal (2010), "Experimental investigation on the effect of intake air temperature and air–fuel ratio on cycle-to-cycle variations of HCCI combustion and performance parameters", *Applied Energy*, 88, 1153–1163.

Rakesh Kumar Maurya, Avinash Kumar Agarwal (2012), "Investigations on the effect of measurement errors on estimated combustion and performance parameters in HCCI combustion engine", *Measurement*, 86, 123-128.

Rakesh Kumar Maurya, Avinash Kumar Agarwal (2011), "Experimental study of combustion and emission characteristics of ethanol fuelled port injected homogeneous charge compression ignition (HCCI) combustion engine", *Applied Energy*, 88, 1169–1180.

Rakesh Kumar Maurya, Avinash Kumar Agarwal(2014), “ Experimental investigations of performance, combustion and emission characteristics of ethanol and methanol fueled HCCI engine”, *Fuel Processing Technology* ,126, 30–48.

Rakesh Kumar Maurya, Nekkanti Akhil(2016), “ Numerical investigation of ethanol fuelled HCCI engine using stochastic reactor model. Part 2: Parametric study of performance and emissions characteristics using new reduced ethanol oxidation mechanism”, *Energy Conversion and Management*, 121, 55–70.

Saxena, S., Chen, J. Y., Dibble, R.W.(2011), “Increasing the signal-to-noise ratio of sparkplug ion sensors through the addition of a potassium acetate fuel additive” , *Proceedings of the Combustion Institute* ,33 , 3081–3088.

Shi Lei, Yi Cui, Deng Kangyao, Peng Haiyong, Chen Yuanyuan (2006), “ Study of low emission homogeneous charge compression ignition (HCCI) engine using combined internal and external exhaust gas recirculation (EGR)”, *Energy*, 31 ,2665-2676.

Shingeru Onishi, Souk Hong Jo, Kastuji Shoda, Pan Do Jo, Satoshi Kato(1979), “ Active Thermo-Atmosphere Combustion(ATAC) - New combustion process for internal combustion engines”, *SAE Technical Paper* ,790 – 501.

Shuaiqing Xu , Yang Wang, Tao Zhu, Tao Xu, Chengjun Tao(2011), “ Numerical analysis of two-stroke free piston engine operating on HCCI combustion”, *Applied Energy* ,88, 3712–3725.

Starck, L., Lecoite, B., Forti, L., Jeuland N.(2010) ,“Impact of fuel characteristics on HCCI combustion: Performances and emissions”, *Fuel* ,89 , 3069–3077.

Stuart Daw, C., Robert M. Wagner, Dean Edwards K., Johny B. Green Jr (2007), “ Understanding the transition between conventional spark-ignited combustion and HCCI in a gasoline engine”, *Proceedings of the Combustion Institute* ,31, 2887–2894.

Su, W. H., Lin, T. J.,Zaho, H., Pei, Y. Q. (2005), “Research and development of an advanced combustion system for direct injection diesel engine”, *Journal of Automobile engineering* , 12,219-221.

Sunmeet Singh Kalsi, Subramanian, K.A. (2017), “Effect of simulated biogas on performance, combustion and emissions characteristics of a bio-diesel fueled diesel engine”, *Renewable Energy* ,106 , 78-90.

Suyin Gan, Hoon Kiat Nig , Kar Mun Pang(2011), “Homogeneous Charge Compression Ignition (HCCI) combustion:Implementation and effects on pollutants in direct injection diesel engines”, *Applied Energy* ,88 , 559–567.

Tao Chen, Hui Xie, Le Li, Lianfang Zhang, Xinyan Wang, Hua Zhao(2014), “ Methods to achieve HCCI/CAI combustion at idle operation in a 4VVAS gasoline engine”, *Applied Energy* ,116, 41–51.

Toshio Shudo, Yosuke Shima, Tatsuya Fujii(2009), “Production of dimethyl ether and hydrogen by methanol reforming for an HCCI engine system with waste heat recovery – Continuous control of fuel ignitability and utilization of exhaust gas heat”, *International Journal of Hydrogen Energy* ,34, 7638 – 7647.

Wang Pan,Chunde Yao,Guopeng Han,Hongyuan Wei,Quangang Wang(2015), “ The impact of intake air temperature on performance and exhaust emissions of a diesel methanol dual fuel engine”, *Fuel* ,162, 101–110.

Wang Ying, He Li, Zhou Jie, Zhou Longbao (2009) ,“Study of HCCI-DI combustion and emissions in a DME engine”, *Fuel* 88 , 2255–2261.

Wang Ying, Li Wei, Zhou Longbao (2010), “Advanced combustion operation in a single-cylinder engine”, *International Journal of Thermal Sciences* ,49 , 1303 – 1308.

Wen Zenga, Maozhao Xie(2008), “A novel approach to reduce hydrocarbon emissions from the HCCI engine”, *Chemical Engineering Journal* ,139, 380–389.

Xing Cai Lu, Dong Han, Zhen Huang (2011), “Fuel design and management for the control of advanced compression-ignition combustion modes”, *Progress in Energy and Combustion Science* ,37 , 741 – 783.

Xing Cai Lu, Wei Chen, Zhen Huang (2005), “A fundamental study on the control of the HCCI combustion and emissions by fuel design concept combined with controllable EGR.Part 1. The basic characteristics of HCCI combustion”, *Fuel*, 84, 1074–1083.

Xing Cai Lu, Wei Chen, Zhen Huang (2005), “A fundamental study on the control of the HCCI combustion and emissions by fuel design concept combined with controllable EGR. Part 2. Effect of operating conditions and EGR on HCCI combustion”, *Fuel* ,84, 1084–1092.

Yaopeng Li, Ming Jia , Yaodong Liu, Maozhao Xie(2013), “ Numerical study on the combustion and emission characteristics of a methanol/diesel reactivity controlled compression ignition (RCCI) engine”, *Applied Energy* ,106, 184–197.

Yap, D., Peucheret, S.M., Megaritis, A., Wyszynski, M.L., Xu H.,(2006), “ Natural gas HCCI engine operation with exhaust gas fuel reforming”, *International Journal of Hydrogen Energy*, 31, 587 – 595.

Zhang Chunhua, Pan Jiangru, Ton Juanjuan, Li Jing (2011), “Effects of Intake Temperature and Excessive Air Coefficient on Combustion Characteristics and Emissions of HCCI Combustion”, *Procedia Environmental Sciences*, 11, 1119 – 1127.

Zhaolei Zheng, Mingfa Yao (2009), “Charge stratification to control HCCI: Experiments and CFD modeling with n-heptane as fuel”, *Fuel*, 88, 354–365.

Zhi Wang , Shi Jin Shuai, Jian Xin Wang, Guo Hong Tian (2006),“A computational study of direct injection gasoline HCCI engine with secondary injection” ,*Fuel* ,85,1831–1841.

Zhongquan Gao, Xiaomin Wu, Chao Man, Xiangwen Meng, Zuohua Huang(2012), “The relationship between ion current and temperature at the electrode gap”, *Applied Thermal Engineering* ,33,15 – 23.

Text books:

Ludwig Fahrmeir, Thomas Kneib, Stefan Lang and Brian Marx (2013), “Regression: Models, Methods and applications”, *Berlin Heidelberg: Springer-Verlag*.

APPENDIX I

DESIGN OF SHELL AND TUBE HEAT EXCHANGER

Basic considerations

The engine exhaust gas is passed through the shell side and liquid diesel is passed through the tube side of the heat exchanger. The diameter and length of the tube are determined by applying the LMTD method of heat exchanger design. The properties of exhaust gases and diesel fuel are used for the calculations. The design calculations are given below:

Properties of exhaust gas:

Inlet temperature of exhaust gas, $T_{in} = 480^{\circ} \text{C}$

Outlet temperature of exhaust gas, $T_{out} = 250^{\circ} \text{C}$

All physical properties taken at bulk mean temperature $T_m = ((480+250)/2) = 365^{\circ} \text{C}$

$(C_p)_{average} = 1.05 \text{ kJ/kg K}$

$K = 0.04908 \text{ W/mK}$

$Pr = 0.676$

$\mu = 31.38 \times 10^{-6} \text{ Ns/m}^2$

$\nu = 55.46 \times 10^{-6} \text{ m}^2/\text{s}$

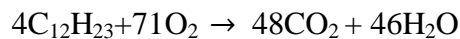
$\alpha = 81.861 \times 10^{-6} \text{ m}^2/\text{s}$

Properties of Diesel:

Diesel is a mixture of hydrocarbons where Carbon vary from 12 to 15.

Average constituent of Hydro carbon is $\text{C}_{12}\text{H}_{23}$.

Chemical reaction:



Specific gravity of diesel = 0.81

Mass flow rate = $810 \text{ kg/m}^3 \times 0.54 \text{ cc/sec}$
 $= 4.374 \times 10^{-4} \text{ kg/sec}$

$$M_{\text{diesel}} = 12 \times 12 + 23 = 167 \text{ gm/mol}$$

$$\begin{aligned} \text{No. of moles of Diesel} &= \frac{4.374 \times 10^{-4}}{167 \times 10^{-3}} \\ &= 2.619 \times 10^{-3} \text{ mole} \end{aligned}$$

$$\begin{aligned} \text{Moles of O}_2 \text{ required} &= 2.619 \times 10^{-3} \times \frac{71}{4} \\ &= 0.0465 \text{ mole} \end{aligned}$$

$$\text{Mass} = 1.49 \text{ gram}$$

$$\frac{\text{Mass of O}_2}{\text{Mass of Dry air}} = 23.1\%$$

$$\text{Mass of air} = \frac{1.49 \times 100}{23.1} = 6.45 \text{ gram}$$

Now taking 15% more air at full load

$$\begin{aligned} \text{Total Air intake} &= 6.45 + 6.45 \times \frac{15}{100} \\ &= 7.85 \text{ gram} \end{aligned}$$

Properties of cold fluid(Diesel):

$$t_{\text{inlet}} = 30^\circ\text{C}$$

$$t_{\text{outlet}} = 100^\circ\text{C}$$

$$\text{Properties at } T_{\text{avg}} = \frac{100+30}{2} = 65^\circ\text{C}$$

$$\rho = 790 \text{ kg/m}^3$$

$$C_p = 2.2 \text{ kJ/kg}^\circ\text{C}$$

$$\mu = 2.7 \times 10^{-3} \text{ N.s/m}^2$$

$$K = 0.1768 \text{ W/m.k}$$

$$\begin{aligned} \text{Total Heat required} &= m.C_p.\Delta T + mL \\ &= 0.54 \times 10^{-2} \times 790 \times 2.1 \times 70 + 0.54 \times 10^{-6} \times 790 \times 326 = 0.204 \text{ kJ/sec} \\ &\approx 0.25 \text{ kJ/sec} \end{aligned}$$

$$\text{Heat lost by exhaust gases} = m \times C_p \times \Delta T$$

$$\begin{aligned}
 &= 7.85 \times 10^{-3} \times 1.05 \times (480-250) \\
 &= 1.896 \text{ KJ/s}
 \end{aligned}$$

We can see that exhaust gas heat is sufficient to vaporize diesel.

For counter flow:

$$\text{LMTD } \Delta T = \frac{\Delta T_1 - \Delta T_2}{\ln \frac{\Delta T_1}{\Delta T_2}}$$

$$\Delta T_1 = 480 - 100 = 380 \text{ K}$$

$$\Delta T_2 = 250 - 30 = 220 \text{ K}$$

$$\text{LMTD} = \frac{380 - 220}{\ln \frac{380}{220}} = 292.75 \text{ K}$$

$$Q = U \times A \times \Delta T \times f \quad (\text{neglecting 'f' initially})$$

Now assuming $U = 200 \text{ W/m}^2\text{k}$

$$\Rightarrow 1.896 \times 10^3 = 200 \times A \times 292.75 \quad (\text{assuming } U=200\text{W/m}^2\text{-K})$$

$$\Rightarrow A = 0.0324 \text{ m}^2 = 324 \text{ cm}^2$$

Considering pipe flow:

$$\Pi \times d \times l = 0.0324 \text{ m}^2$$

Taking standard diameter of tube $d_o = 6 \text{ mm}$

$$\Pi \times 6 \times 10^{-3} \times L = 0.0324 \text{ m}^2$$

$$L = 1.72 \text{ m}$$

Tube side calculations:

$$\text{Mass flux rate of fuel } G_f = \frac{W}{A_t} = \frac{4.374 \times 10^{-4}}{\frac{3.14}{4} \times 4.8^2 \times 10^{-6}} = 24.172 \text{ kg/m}^2\text{s}$$

$$\text{Re} = \frac{G_s D}{\mu} = \frac{24.172 \times 4.8 \times 10^{-3}}{2.7 \times 10^{-3}} = 42.97$$

Hence flow is laminar then for constant heat flux appropriate correlation used

$$N_u = 4.36$$

For constant heat flux:

$$h_i = \frac{N_u K}{D} = \frac{4.36 \times 0.1768}{4.8 \times 10^{-3}} = 160.6 \text{ W/m}^2\text{K}$$

Shell side calculation:

For pipe : $d_o = 6$ mm, $d_i = 4.8$ mm, $t = 0.6$ mm

Pitch $P_t = 18$ mm

$$\text{Equivalent diameter : } d_e = \frac{\sqrt{12}P_t^2 - \pi d_o^2}{\pi d_o} = \frac{\sqrt{12} \times 18^2 - \pi \times 6^2}{\pi \times 6} = 53.54 \text{ mm}$$

$$A_s = \frac{d_s C B}{144 P_t} = \frac{6 \times 10^{-2} \times 12 \times 10^{-2} \times 6 \times 10^{-2}}{144 \times 18 \times 10^{-3}} = 1.667 \times 10^{-4} \text{ m}^2$$

Where d_s = shell diameter, C = clearance,

B = baffle plate spacing

G_s = Mass flux rate of Exhaust gas

$$G_s = \frac{W_s}{A_s} = \frac{7.85 \times 10^{-3}}{1.667 \times 10^{-4}} = 47.091 \text{ kg/m}^2 \text{ s}$$

$$Re = \frac{G_s d_e}{\mu} = \frac{47.091 \times 53.54 \times 10^{-3}}{31.38 \times 10^{-6}} = 80.34 \times 10^4$$

Flow is Turbulent.

$$Pr = \frac{\mu C_p}{k} = \frac{31.38 \times 10^{-6} \times 1005}{0.04908} = 0.6425$$

$$Nu_u = 0.36 Re^{0.55} Pr^{0.333} = 0.36(80 \times 10^4)^{0.55} 0.6425^{0.333} = 154.9$$

$$h_0 = \frac{Nu_u \times k}{d_e} = \frac{154.9 \times 0.04908}{53.54 \times 10^{-3}} = 141.99$$

So, $h_i = 160.6$, $h_0 = 154.9$, $t = 6$ mm, $k = 386$

$$\frac{1}{U} = \frac{1}{h_i} + \frac{1}{h_0} + \frac{t}{k}$$

Where t is the thickness of tube and K is the thermal conductivity of copper tube

$K = 386$ W/mk

$$= \frac{1}{160.6} + \frac{1}{141.99} + \frac{0.006}{386} \Rightarrow U = 75.3$$

$$A = \frac{1.896 \times 10^3}{75.3 \times 292.75} = 0.086 \text{ m}^2$$

$$L = \frac{0.086}{6 \times 10^{-3} \times \pi} = 4.56 \text{ m}$$

Next iteration

Assuming a suitable length between 1.8 and 4.56

$L = 2.5 \text{ m}$

For pipe: $d_o = 6 \text{ mm}$, $d_i = 4.8 \text{ mm}$, $t = 0.6 \text{ mm}$

$P_t = 12 \text{ mm}$

Equivalent diameter: $d_e = \frac{\sqrt{12}P_t^2 - \Pi d_o^2}{\Pi d_o} = \frac{\sqrt{12} \times 12^2 - \Pi \times 6^2}{\Pi \times 6} = 20.46 \text{ mm}$

$$A_s = \frac{d_s C B}{144 P_t} = \frac{6 \times 10^{-2} \times 6 \times 10^{-2} \times 6 \times 10^{-2}}{144 \times 12 \times 10^{-3}} = 1.25 \times 10^{-5}$$

Where d_s = shell diameter, C = clearance,

B = baffle plate spacing

$$G_s = \frac{W_s}{A_s} = \frac{7.85 \times 10^{-3}}{1.25 \times 10^{-5}} = 628$$

$$\text{Re} = \frac{G_s d_e}{\mu} = \frac{628 \times 20.46 \times 10^{-3}}{31.38 \times 10^{-6}} = 40.94 \times 10^4$$

$$\text{Pr} = \frac{\mu C_p}{k} = \frac{31.38 \times 10^{-6} \times 1005}{0.04908} = 0.6425$$

$$N_u = 0.36 \text{Re}^{0.55} \text{Pr}^{0.333} = 0.36(40.94 \times 10^4)^{0.55} 0.6425^{0.333} = 379.31$$

$$h_o = \frac{N_u \times k}{d_e} = \frac{379.31 \times 0.04908}{20.46 \times 10^{-3}} = 909.89$$

So, $h_i = 160.6$, $h_o = 909.89$, $t = 6 \text{ mm}$, $k = 386$

$$\frac{1}{U} = \frac{1}{h_i} + \frac{1}{h_o} + \frac{t}{k} = \frac{1}{160.6} + \frac{1}{909.89} + \frac{0.006}{386} \Rightarrow U = 136.21 \text{ W/m}^2 \text{ K}$$

$$A = \frac{1.896 \times 10^3}{136.21 \times 292.75} = 0.04754 \text{ m}^2$$

$$L = \frac{0.04754}{6 \times 10^{-3} \times \Pi} = 2.52 \text{ m}$$

So got approximately same length. Hence assumption are correct.

Number of baffle plates: $N_B = \frac{50}{6} - 1 = 8.33 - 1 = 7.33 \sim 7$

The detailed specification of the Heat Exchanger is given in Table 4.2

APPENDIX II

Development of a correlation between Ion voltage and cylinder Pressure

Regression is the most popular and commonly used statistical methodology for analyzing empirical problems in social sciences, engineering, economics, and life sciences (Fahrmeir 2013). There exist a large variety of models and inferential tools, ranging from conventional linear models to modern non/semi-parametric regression. Sir Francis Galton (1822–1911) was a diverse researcher, who did pioneering work in many disciplines. Galton is viewed as a pioneer of regression analysis, because of his regression analytic study of heredity. His successors like Karl Pearson (1857–1936), Francis Ysidro Edgeworth (1845–1926), and George Udny Yule (1871–1951) formalized his work. The first step when conducting a regression analysis is to get an overview of the variables in the data set. We in general follow the corresponding goals for the initial and following analysis:

- a) Summary and exploration of the distribution of the variables.
- b) The pattern of the distribution.
- c) The viability of the parameters and the study of parametrical distribution to the response.
- d) Establishment of the correlation with the required mathematical computations.

Linear regression requires linear parameters while nonlinear does not. Nonlinear regression is used instead of ordinary least squares regression when you cannot adequately model the relationship with linear parameters. Nonlinear equation can take many different forms. In fact there are infinite number of possibilities you must specify the expectation function used to perform nonlinear regression. The choice for the expectation function often depends on prior knowledge about the response curve's shape or the behavior of physical and chemical properties in the system. Potential nonlinear shapes include Gaussian, concave, convex, exponential growth or decay, sigmoidal and asymptotic curves. The relation between crank angle with ion voltage; and crank angle with pressure follows a Gaussian\Lorentz distribution. Two correlations for crank angle vs ion voltage; and crank angle vs pressure are developed using nonlinear regression by Levenberg Marquardt iteration algorithm using Origin lab software. The coefficients of determination obtained for each equation are 97.6% and 99.5% respectively. These two equations are coupled together to obtain the correlation between ion voltage and cylindrical pressure. Detailed reports for both regression equations are obtained.

Nonlinear Curve Fit (Gauss) Notes Crank Angle vs Ion Voltage

Description	Nonlinear Curve Fit
User Name	Sumanlal
Operation Time	
Iteration Algorithm	Levenberg Marquardt
Model	Gauss
Number of Parameters	4
Number of Derived Parameters	3
Number of Datasets	1
Equation	$y=y_0 + (A/(w*\sqrt{PI/2}))*\exp(-2*((x-c)/w)^2)$
Report Status	New Analysis Report
Special Input Handling	

Input Data

		Dep/Indep	Data	Range	Weight Type
Ion Voltage	x	Indep	[Book]Sheet !A"Crank angle"	[1*:168*]	No Weighting
	y	Dep	[Book]Sheet !B"Ion Voltage"	[1*:168*]	No Weighting

Parameters

		Value	Standard Error
Ion Voltage	v0	-0.3680773689	0.0036349187
	xc	380.0911841101	0.3563910368
	w	48.4391493228	0.7831415767
	A	46.5957769098	0.7561286469
	sigma	24.2195746614	0.3915707884
	FWHM	57.0327398948	0.9220787415
	Height	0.7675207248	0.0101130255

Statistics

	Ion Voltage
Number of Points	168
Degrees of Freedom	164
Reduced Chi-Sqr	0.001368933
Residual Sum of Squares	0.2245050165
Adj. R-Square	0.9762796972
Fit Status	Succeeded (100)

	y0		xc		w		A		si	FWHM	Height	Statistics	
	Value	Standard Error	Value	Standard Error	Value	Standard Error	Value	Standard Error	Value			Reduced Chi-Sqr	Adj. R-Square
Ion Voltage	-0.3680773689	0.0036349187	380.0911841101	0.3563910368	48.4391493228	0.7831415767	46.5957769098	0.7561286469	24.2195746614	57.0327398948	0.7675207248	0.001368933	0.9762796972

Nonlinear Curve Fit (Lorentz) Notes Crank angle vs Pressure

Description	Nonlinear Curve Fit
User Name	Sumanlal
Operation Time	
Iteration Algorithm	Levenberg Marquardt
Model	Lorentz
Number of Parameters	4
Number of Derived Parameters	1
Number of Datasets	1
Equation	$y = y_0 + (2 * A / \pi) * (w / (4 * (x - x_c)^2 + w^2))$
Report Status	New Analysis Report
Special Input Handling	

Input Data

		Dep/Indep	Data	Range	Weight Type
Cylinder pressure	x	Indep	[Book]Sheet !A"Crank angle"	[1*:168*]	No Weighting
	y	Dep	[Book]Sheet !B"Cylinder pressure"	[1*:168*]	No Weighting

Parameters

		Value	Standard Error
Cylinder pressure	y0	0.9547485392	0.126788159
	xc	368.657519139	0.1327907309
	w	42.5949687584	0.4682221834
	A	3998.410242499	38.0542372131
	H	59.7598047988	0.3749470784

Statistics

	Cylinder pressure
Number of Points	168
Degrees of Freedom	164
Reduced Chi-Sqr	1.1610601299
Residual Sum of Squares	190.413861309
Adj. R-Square	0.9951240243
Fit Status	Succeeded (100)

	y0		xc		w		A		H	Statistics	
	Value	Standard Error	Value	Standard Error	Value	Standard Error	Value	Standard Error	Value	Reduced Chi-Sqr	Adj. R-Square
Cylinder pressure	0.9547485392	0.126788159	368.657519139	0.1327907309	42.5949687584	0.4682221834	3998.410242499	38.0542372131	59.7598047988	1.1610601299	0.9951240243

List of Publications based on PhD Research Work

Sl. No.	Title of the paper	Authors (in the same order as in the paper. Underline the Research Scholar's name)	Name of the Journal/ Conference, Vol., No., Pages	Month, Year of Publication	Category *
1.	Experimental Investigation of a Single Cylinder CI engine achieving HCCI mode of combustion	<u>Sumanlal, M.R.</u> , Jithin Gopintha and Mohanan P.	Proc. of International conference on Alternate fuels for IC Engines, MNIT Jaipur, Paper code IC051, 101-105	February 5 -7, 2013	3
2.	An approach towards HCCI Engine by using Diesel Vapour Induction on a DI Diesel Engine and finding the effect of it on the Performance and Emission Characteristics	<u>Sumanlal M.R.</u> , Bhaskara and Mohanan P	Proceedings of 24 th National Conference on IC Engines and Combustion., UPES, Dehradun, 85-91	October 31 to November 2 2015,	3
3.	The Effect of Air Preheating on the performance and emission characteristics of a DI Diesel Engine achieving HCCI mode of combustion	<u>Sumanlal, M.R.</u> , Sreeram Nanadakumar and Mohanan P.	International Journal of Theoretical and Applied Mechanics. ISSN 0973-6085 Volume 12 pp. 411-421	April 2017	1
4.	Part Load Characterestics of a DI diesel engine achieving HCCI mode of Combustion with air preheating	<u>Sumanlal, M.R.</u> , Sreeram Nanadakumar and Mohanan P.	International Journal of Mechanical Engineering and Technology Volume 8, Issue 4 , pp. 337-350	April 2017	1
5.	Effect of Diesel Vapour Induction and Air Preheating on the Exhaust Gas Temperature of a DI Diesel Engine Achieving HCCI Mode of Combustion	<u>Sumanlal, M.R.</u> , Sreeram Nanadakumar and Mohanan P.	25 th National Conference on IC Engines and Combustion., NITK, Surthakal	December 2017	4

*Category: 1: Journal paper, full paper reviewed

2: Journal paper, Abstract reviews

3: Conference/Symposium paper, full paper reviewed

4: Conference/Symposium paper, abstract reviewed 5: others (including papers in Workshops, NITK Research Bulletins, Short notes etc.)

BIO –DATA

SUMANLAL M. R.

Assistant Professor (Senior Grade),

Department of Mechancial Engineering,

Federal Institute of Science and Technology, Angamaly, Kerala

Home Town: Perumbavoor, Kerala

Contact Numbers : 09947442092, 08281071550

E-Mail ID : sumanlalmr@gmail.com

Residential Address : Manjackal(H), Aruvappara(P.O), Kuruppampady(Via),
Ernakulam – Kerala, PIN – 683545.

Educational Qualification :

- Post Graduate (2007) M.Tech in Heat Power Engineering from National Institute of Technology Karanataka, Surathkal.
- Graduate in Mechanical Engineering (2000) from M A College of Engineering, Kothamangalam, Kerala.

Teaching Experience : 15 Years

Number of Publications : 4